4. Catalytic aptitude of –OH functionalized catalysts

Developing dynamic, selective and energy lucrative heterogeneous catalytic processes are enormously essential to an inexhaustible future as heterogeneous catalysis is at the heart of the chemicals and pharmaceutical industries. The formation and execution of selective heterogeneous catalytic processes could have a stunning encouraging impact on the orb because it may perform the catalytic reaction at a lower temperature, pressure and/or in less time and as a result wealth can be saved in up-scale reactions. Contrarily, catalyst deactivation is notably the subject of great seriousness[1], which is the key barricade to research, design and advancing sustainable catalysts. That's why it is necessary to be aware of the reason and remedy for catalytic deactivation. Since last three decades the dimension of the research focuses particularly on deactivation of catalyst has been expanding progressively across-the-board[2-15]. Deactivation broadly categorized into three types, for instance, chemical, mechanical and thermal which includes metal poisoning, foiling, thermal degradation, leaching, solid-solid interactions and mainly support[16-18]. However, it can be minimized by heedful control of process conditions and vigilant choice of support materials.

In accordance with the archaic apophthegm "prevention is better than cure", we have to be more cautious in selecting the support. As described in chapter 1, amongst the available heaps of supports, the carbonaceous materials and particularly graphite has emerged as attracting and captivating support due to its unique properties[19-22]. It is well known that GO possesses various functional groups on its surface and basal plane, for instance, hydroxyl and epoxy groups on its surface while carboxyl groups on the edges. Theses functional groups make the functionalization process smoothen. This covalently modified material is lasting and fastens a metal in such a manner as to achieve a desired result. These covalently grafted transition metal on GO nanosheet are believed to be a proficient move towards the the remedy of shortcomings of homogeneous catalysis[23-25].

In this chapter, catalytic aptitude of the catalysts synthesized by selective modification of hydroxyl groups of GO by APTMS followed by grafting of transition metal complex via ligand spacer is demonstrated. The as-prepared heterogeneous catalysts [$M(L)_n$-*f*-GO] were weigh up against the

selective catalytic oxidation reactions, for instance, oxidation of benzyl alcohol, epoxidation of styrene, epoxidation of norbornene and oxidation of glucose (Scheme 4.1).

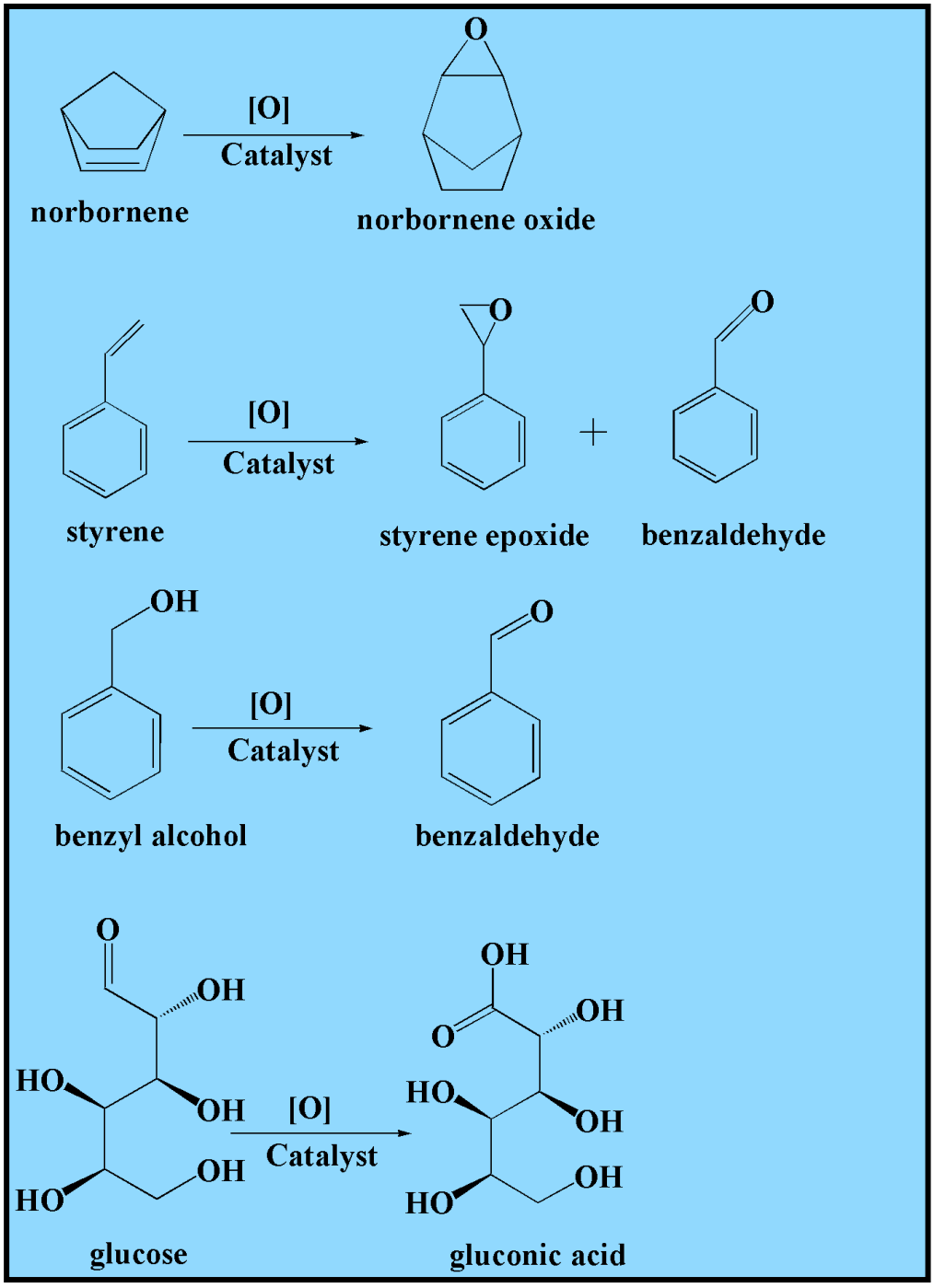

Scheme 4.1. Catalytic olefinic oxidation reactions with their probable products.

4.1. Selective oxidation of benzyl alcohol

It is a very demanding to identify and separate out the key intermediates from the reaction mixture and platform chemicals with the utmost potential for use as value-added chemicals[26,27]. Kinds of literature related to manufacture and transformation of these intermediate chemicals were seen to be extensively augmented for widespread reactions, for instance, reduction, dehydration and especially oxidation of alcohols which plays a vital role in their development[28].

Conversely, selective oxidation of alcohols to aldehydes, ketones and/or carboxylic acids governs by strict control is a crucial tasks of these most significant transformations in organic production[29]. Predominantly, aldehydes and ketones are precious organic intermediates/ products in dyes, perfumeries and agro-chemicals industries[30]. Over the years, the use of harmful oxidants and toxic heavy metals has been made for conventional oxidation of alcohols[31], however, these oxidants and heavy metals are carcinogenic and adverse to the surroundings also. As an antidote of these unaccepted circumstances, this era moved ahead with aqueous hydrogen peroxide (H_2O_2), a distinctly eye-catching oxidant owing to a gentle, inexpensive and environmentally friendly and gladden reagent with active oxygen to a great extent and solely water as the by-product. A long-established method to yield benzaldehyde (BzH) is the hydrolysis of benzal chloride and formation of BzH by this way the product is contaminable with chlorine. However, other method is oxidation of toluene which necessitates environmentally adverse organic solvents[27]. To acquire BzH not contaminated with noxious substances, catalytic liquid phase selective oxidation of benzyl alcohol (BzA) has chiefly been adopted.

Hence, the catalytic aptitude of the as-prepared catalysts was assessed by the selective oxidation of BzA using 30% H_2O_2 as an environmentally benign oxidant with the assistance of ethylene glycol as a product selective solvent. It is extremely difficult to control this oxidation reaction in the intermediary step of formation of BzH and for this rationale, diverse parameters have been optimized, for instance, mole ratio, temperature, amount of catalyst, solvent effect, solvent amount, oxidant and grade of raw material etc.

In a typical reaction condition, a catalyst was dispersed in a solvent and stirred for 10 min. followed by addition of reactant molecule in this mixture and stirred again for 10 min. for absolute activation of the substrate. After activating the substrate, oxidant was added bit by bit for successful oxidation and the final mixture was stirred for experimentally pre-decided time to get higher conversion and yield.

For this transformation, 40 mmol BzA, 40 mmol 30% H_2O_2, solvent (5 mL, ethylene glycol) and 50 mg of catalyst are feed to 50 mL three-neck round bottom flask and equilibrated at 90 ºC for 3 h. The reaction progress was analyzed by GC by ejecting aliquots at different time interval viz. 5, 10, 20, 25, 30, 60 and 180 min.

In all the catalytic reactions discussed in this thesis, the product selectivity up to 10% conversion is not considered as such conversion is regarded as GC error.

4.1.1. Impact of catalysts

Table 4.1 demonstrates the assessment of diverse heterogeneous catalysts driven catalytic fabrication of BzH. Amongst all these catalysts, little or no conversion is examined with pristine graphite, GO and A-*f*-GO substantiating the significance of the catalysts. Looking to the outcome of catalysts, CoL-*f*-GO offers 10.07% BzA conversion with 98.8% BzH selectivity; however, VOL-*f*-GO exhibits 49.03% conversion with 65.22% selectivity. The highest catalytic conversion of BzA (99.26%) is attained with CuL-*f*-GO catalyst with 99.66% selectivity of BzH. For this reason, CuL-*f*-GO is chosen as the preferred catalyst for further investigation of the impact of other experimental variables.

Table 4.1

Impact of varying catalysts on oxidation of BzA.

Systems	BzA Conversion (%)	BzH Selectivity (%)	Other Selectivity (%)	TOF[a] (h^{-1})
Graphite	0.65	-	-	-
GO	2.3	-	-	-
A-*f*-GO	5.1	-	-	-
CoL-*f*-GO	10.07	98.8	1.2	106.55
VOL-*f*-GO	49.03	65.22	34.78	28.95
CuL-*f*-GO	99.53	99.67	0.34	1570.97

Reaction condition: BzA (40 mmol), 30% H_2O_2 (40 mmol), catalysts (50 mg), 90 °C, ethylene glycol (5 mL), 3 h.

[a]TOF: Moles of benzyl alcohol converted per mole of metal per hour.

4.1.2. Impact of mole ratio

To determine the impact of varying mole ratios of a substrate to the oxidant on BzA conversion and BzH product selectivity over the catalyst CuL-*f*-GO, four diverse mole ratios (1:1, 1:1.5, 1:2, 1:2.5) are employed by keeping all other parameters fixed (Fig. 4.1). As shown in Fig. 4.1, it is observed that H_2O_2 plays a vital role in the degradation of BzA; low concentration of H_2O_2 to the substrate (1:1) exhibits 99.53% conversion of BzA with 99.67% selectivity of BzH. Further rise in the concentration of H_2O_2 to 1:1.5 results in rather similar conversion to 1:1 ratio but the selectivity is drop-downed noticeably to 90.67%. However, 1:2 mole ratio exhibits slight increase in the conversion of BzA (99.4%) but the selectivity of BzH again experiences reverse trend and decreased to 83.70%. The absolute conversion of 100% is achieved with higher concentration of H_2O_2 (1:2.5) but the selectivity to BzH, however, diminished further with increasing mole ratio. The justification for this decreasing selectivity with increasing mole ratio of BzA to 30% H_2O_2 might be higher amount of oxidant further oxidize the aldehyde to acid and ester up to some extent. Here, conversion increases with increasing mole ratio are not so high but the selectivity lessened significantly. So in an attempt to

obtain higher yields with a higher rate of conversion we have chosen the mole ratio 1:1 to inspect the impact of other parameters.

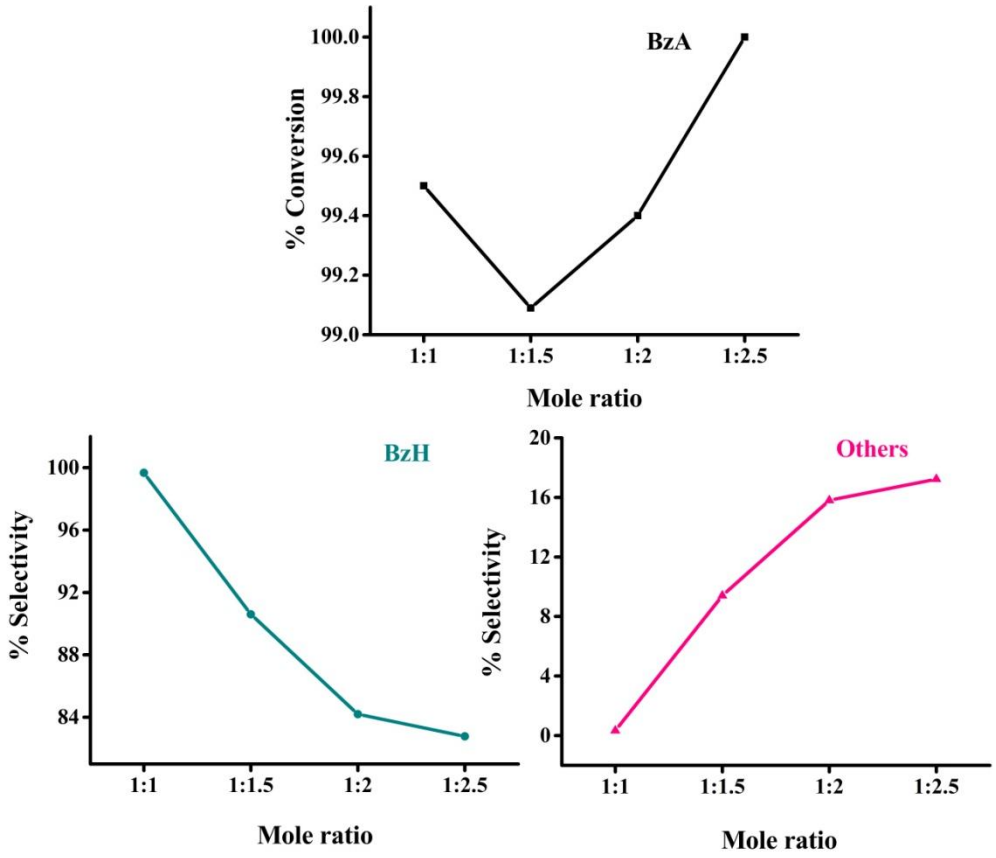

Fig. 4.1. Impact of varying mole ratio on the oxidation of BzA.
Reaction condition: BzA (40 mmol), 30% H_2O_2 (mmol) CuL-*f*-GO (50 mg), 90 °C, ethylene glycol (5 mL), 3 h.

4.1.3. Impact of amount of catalyst

Catalyst amount is imperative factor for any heterogenized catalytic reaction. In this selective oxidation reaction of BzA, we have inspected other two different amount of catalyst like 40 and 10 mg besides 50 mg (Fig. 4.2). After getting the desired conversion of BzA with 50 mg of catalyst, we have inspected the decreased amount of catalyst (eg. 40 mg) on this transformation. We have observed the similar conversion as of 50 mg but the selectivity of BzH is seen to be decreased slightly (98.05%). On further changing the catalyst amount to 10 mg, absolute conversion is examined; however, the selectivity is influenced extensively (97.92%). Highest selectivity of BzH (99.97%) is achieved with 50 mg of catalyst. Selectivity is mainly affiliated

with the reaction mechanism and the active sites involved in terms of metal loading. There is intrinsic mechanism between substrates, catalyst and products and hence, so as to control the selectivity, we need to improve the steadiness of the intermediary product for desired reaction route and to establish the equilibrium between catalyst-intermediate, catalyst-product and catalyst-by-product interactions. Consequently, by increasing the amount of catalyst, the metal concentration is also increased and attains the sufficient for the potent interaction between the catalyst-substrate and catalyst-intermediate. Consequently, in order to achieve the higher conversion of BzA and higher selectivity of BzH, we have chosen 50 mg catalyst for further investigation of other parameters.

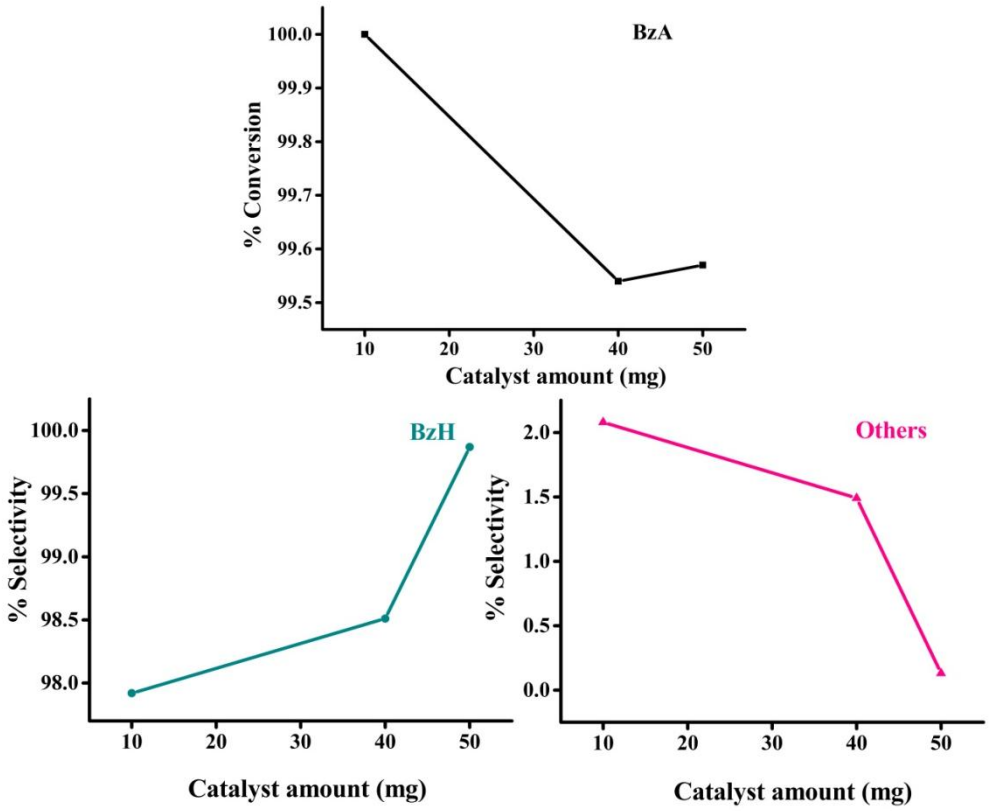

Fig. 4.2. Impact of varying amount of catalyst on the oxidation of BzA. Reaction condition: BzA (40 mmol), 30% H_2O_2 (40 mmol), CuL-*f*-GO (mg), 90 °C, ethylene glycol (5 mL), 3 h.

4.1.4. Impact of time

For this typical selective oxidation reaction of BzA, it is quite crucial to finish this reaction at the accurate time to succeed in attaining selected yield (BzH) as well as higher selectivity of BzH. For this aim, we have carried out this reaction at different time intervals, viz. 5, 10, 20, 25, 30, 60 and 180 min (Fig. 4.3). 99.53% conversion of BzA is achieved in first 5 min but the selectivity for BzH is found to be 94.3%. On further continuing the reaction to 10 min no change in the conversion (99.50%) is observed, however, the selectivity for BzH shows slight increase (96.12%). After the examination of the reaction mixture drawn at 15 min, it is noticed that conversion increased to 99.71% with 96.4% selectivity of BzH. Maximum selectivity of 99.97% is seen at 20 min of time with 99.53% of the BzA conversion. On further continuing the reaction for 25, 30, 60 and 180 min, the conversion obtained is 99.50, 99.53, 99.40 and 99.53%, respectively, and the selectivity exhibited is 99.53, 99.40, 99.20 and 99.67%, respectively. Hence, it is noticed that the conversion and selectivity both increased with time and attained maximum at 20 min. However, no significant change in the conversion of BzA is observed if the reaction prolonged up to 180 min, but the selectivity of BzH is fallen extremely, which might be due to over oxidation of this intermediary product to the acid. However, the benzoic acid formed during reaction intereacts immediately with BzA, forming benzyl benzoate and therefore, number of moles of BzA consumed during the catalytic oxidation reaction and it is seen as the effect of a reduction in the selectivity of BzH. For this reason, we have decided to set the reaction time 20 min for further explorations.

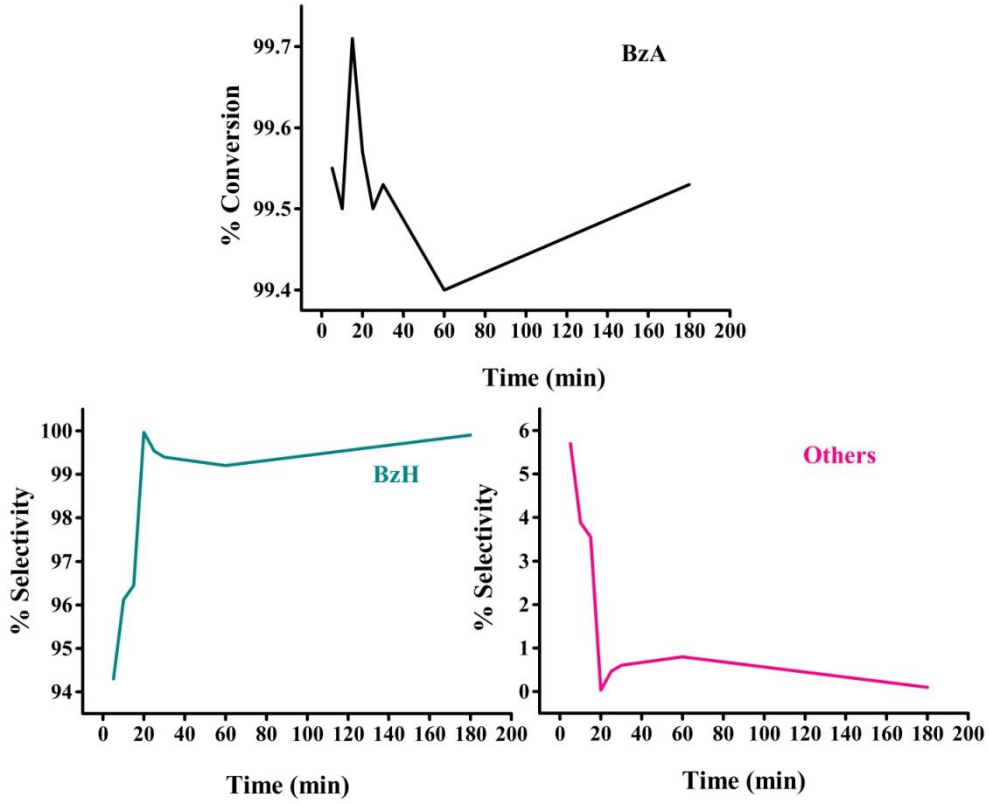

Fig. 4.3. Impact of varying time on the oxidation of BzA.

Reaction condition: BzA (40 mmol), 30% H_2O_2 (40 mmol), CuL-*f*-GO (50 mg), 90 °C, ethylene glycol (5 mL), time (min.).

4.1.5. Impact of solvent

The rate of reaction, selectivity, stability of the desired product, catalytic activity and almost entire process of the reaction would be affected by the choice of solvent[32]. However, as we know, there is no common model for prophesying the effect of solvent on the reactions. For that, a researcher has to pay ample amount of time by putting various solvents into practice to optimize a reaction. This study also intended to evaluate the practicability of solvent effect on the selectivity of BzH and hence, the study of effect of diverse solvents like methanol, acetonitrile, N,N- dimethylformamide (DMF), 1,4-dioxane, toluene, and ethylene glycol is scheduled. As shown in Fig. 4.4, methanol gives 8.03% conversion, while very petite conversion of 3.44% of BzA is observed with toluene. Acetonitrile is able to convert 7.19% of BzA; however, DMF offeres 5.19% conversion of BzA. On the other hand, 1,4-dioxane exhibits 6.81% conversion of BzA. All these solvents, except ethylene glycol, are proved to be substandard for the anticipatory conversion of BzA

and selectivity of BzH. With the immense endeavour, ethylene glycol is found to be the choice of solvent with BzA conversion of 99.53% and BzH selectivity of 99.67%. We might acquire more conversion with other solvents by increasing the time but still the selectivity of BzH is very less as they favour the further oxidation of the intermediary product. However, ethylene glycol produces cyclic acetal with BzH which deny further oxidation as shown inFig. 4.5. As a result, ethylene glycol is chosen as the preferred solvent for this transformation.

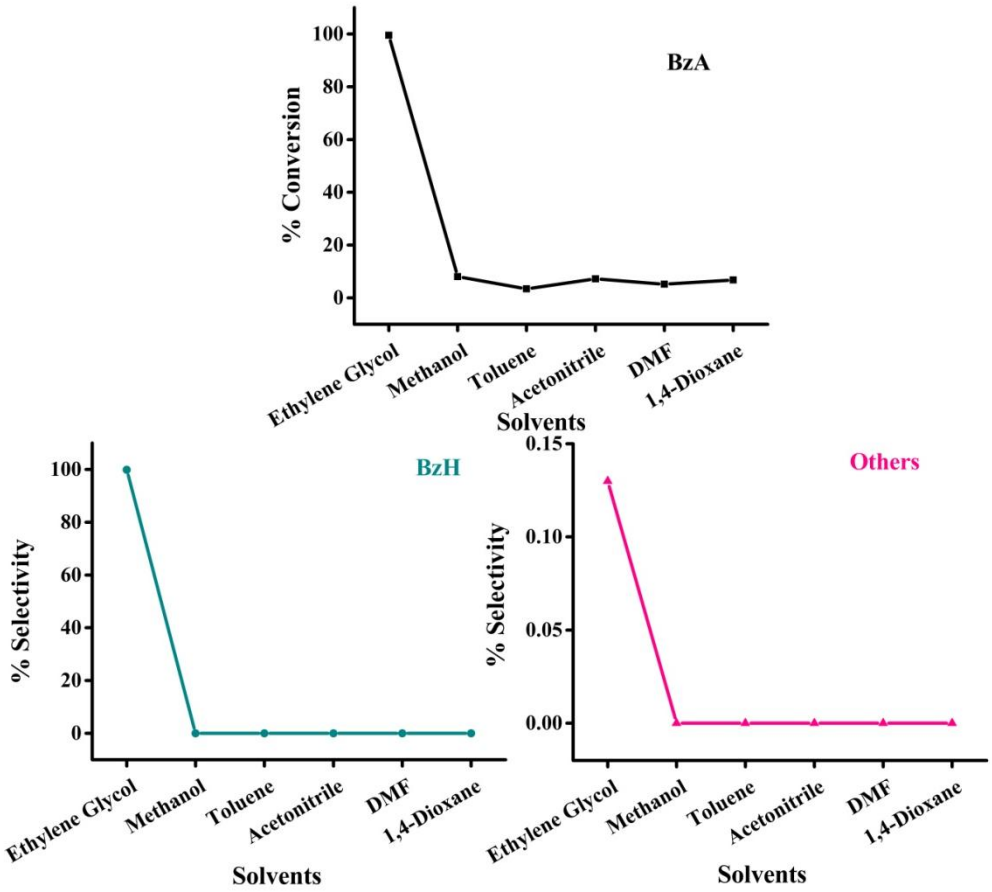

Fig. 4.4. Impact of varying solvents on the oxidation of BzA.

Reaction condition: BzA (40 mmol), 30% H_2O_2 (40 mmol), CuL-*f*-GO (50 mg), 90 °C, solvent (5 mL), 20 min.

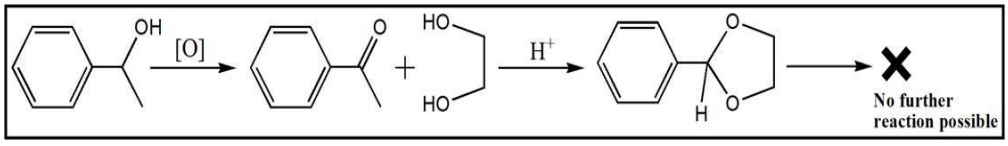

Fig. 4.5. Formation of cyclic acetal with ethylene glycol.

4.1.6. Impact of solvent amount

Excellent results of all these experimentations become a driving force for the optimization of another parameter, solvent amount. We have executed the reaction by varying the amount of solvent (viz. 2, 5 and 10 mL) to obtain the perception of solvent amount on this transformation. As shown in Fig. 4.6, with 2 mL amunt of solvent 99.56% conversion of BzA with 89.27% BzH selectivity is observed. On increase in the amount of ethylene glycol from 2 to 5 mL, conversion of BzA remains same (99.53%) however; the selectivity of BzH is increased considerably from 89.96 to 99.67%. On further increasing the amount of ethylene glycol (10 mL) conversion of BzA (99.26%) and selectivity of BzH (98.93%) is decreased to a small degree. The explanation for this reduction is given in terms of the concentration of the reaction mixture, which might be diluted than the required concentration for the desired outcomes and therefore it decreases the conversion and selectivity[33]. As a result, we have chosen 5 mL of solvent amount for further optimizations.

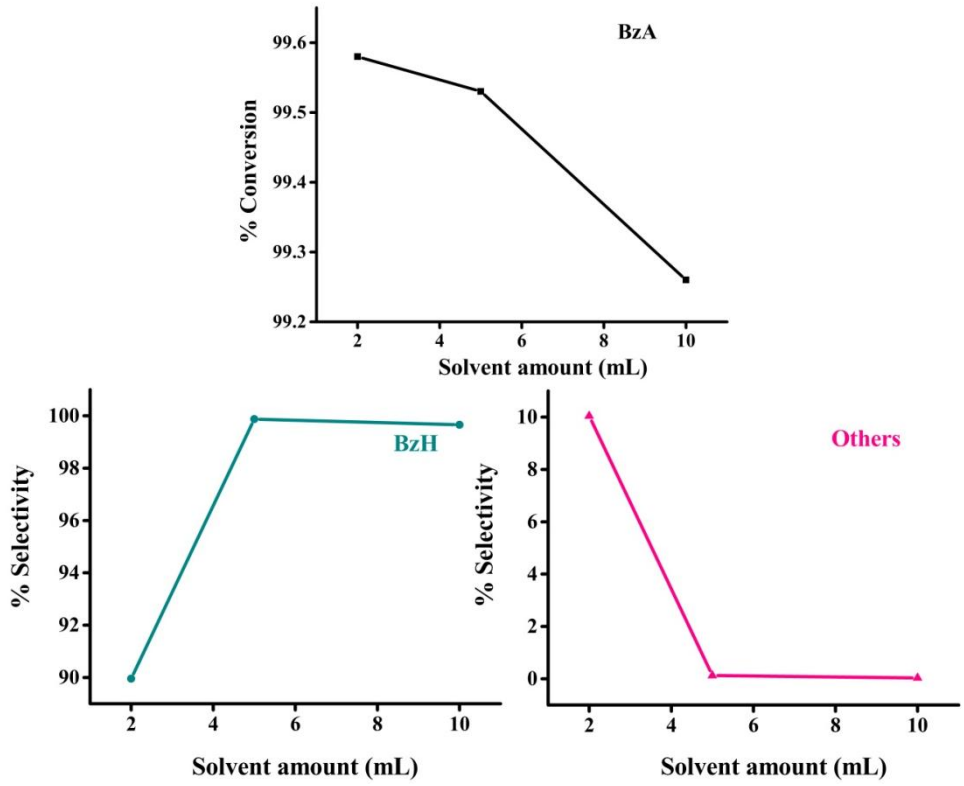

Fig. 4.6. Impact of varying amount of solvent on the oxidation of BzA. Reaction condition: BzA (40 mmol), 30% H_2O_2 (40 mmol), CuL-*f*-GO (50 mg), 90 °C, ethylene glycol (mL), 20 min.

4.1.7. Impact of oxidant

The effect of different oxidants such as 70% TBHP and 30% H_2O_2 on the oxidation of BzA is inspected by choosing an experimentally obtained reaction parameters as shown in Fig. 4.7. The data reveals that the use of 30% H_2O_2 as an oxidant provides a higher conversion of BzA (99.53%) along with higher selectivity of BzH (99.67%) than 70%TBHP which gives only 17.83 % conversion of BzA and 27.43% selectivity of BzH. In addition, 30% H_2O_2 is a greener oxidant, often more efficient, fairly inexpensive, easy to handle and yield only water as the by-product. Subsequently, 30% H_2O_2 is chosen as an oxidant throughout for further the catalytic study.

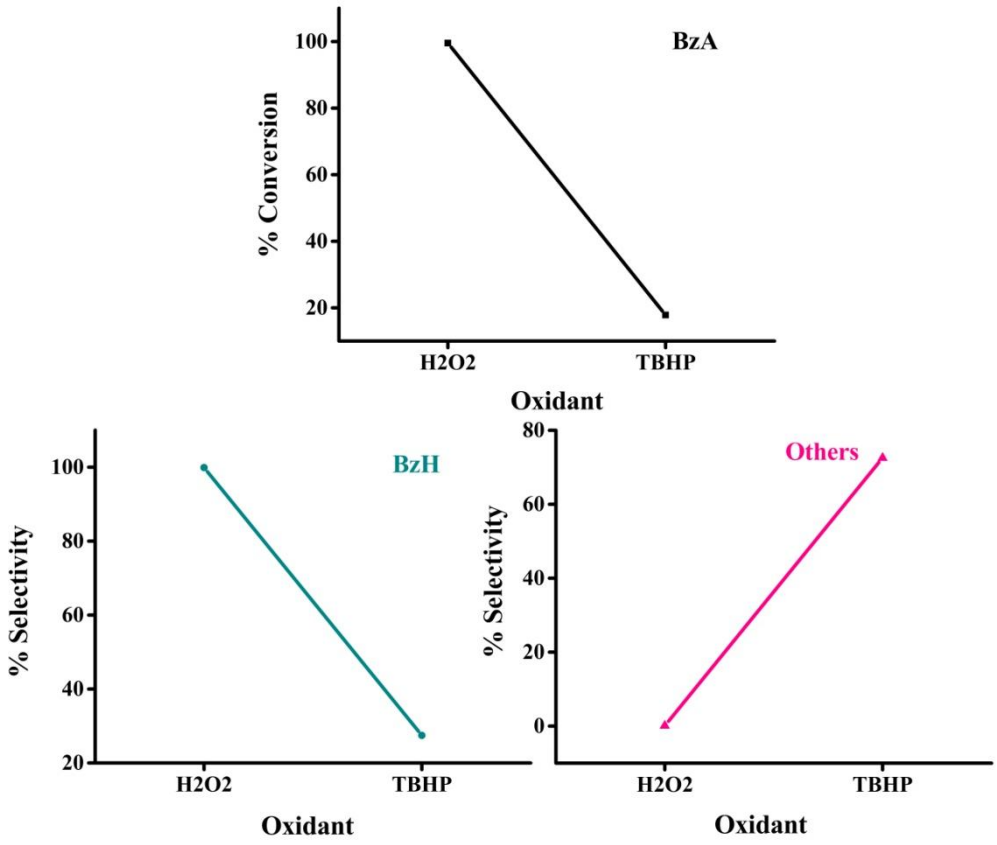

Fig. 4.7. Impact of oxidants on the oxidation of BzA.

Reaction condition: BzA (40 mmol), oxidant (40 mmol) CuL-*f*-GO (50 mg), 90 °C, ethylene glycol (5 mL), 20 min.

4.1.8. Impact of temperature

Effect of four different reaction temperatures such as 70, 80, 90 and 100 °C on the oxidation of BzA is illustrated in Fig. 4.8. It is visible from the

figure that 7.13% conversion of BzA is achieved at 70 °C. On rising the temperature to 80 °C, conversion also increased to 12.22% with 88.58% BzH selectivity. Moreover, maximum conversion of 99.53% of BzA is observed with 99.67% BzH selectivity at 90 °C. However, further increase in the temperature (100 °C) extremely decreases the conversion to 5.08%. This decrease might be due to bulk degradation of H_2O_2 at higher temperature. Subsequently, 90 °C is chosen as representative temperature.

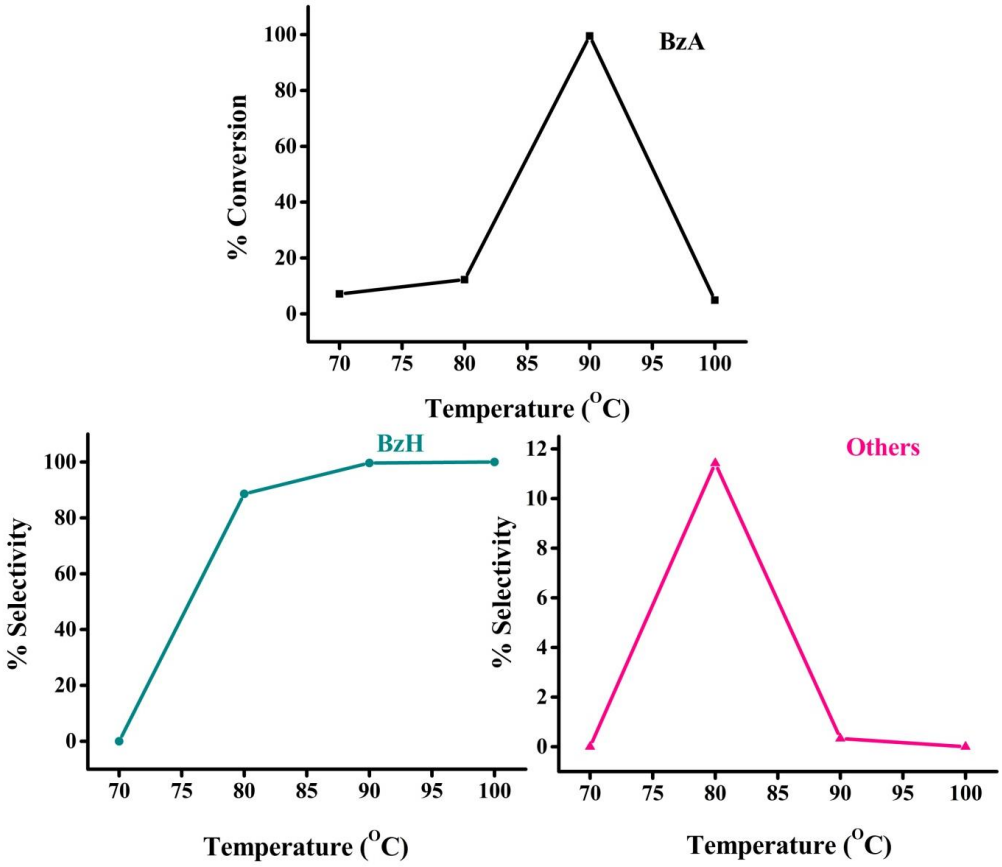

Fig. 4.8. Impact of varying temperature on the oxidation of BzA.
Reaction condition: BzA (40 mmol), 30% H_2O_2 (40 mmol) CuL-*f*-GO (50 mg), temperature (°C), ethylene glycol (5 mL), 20 min.

4.1.9. Recyclability test

For any heterogeneous catalytic system reusability of the catalyst is of enormous significance. To inspect the recyclability of the as-prepared heterogeneous catalyst for this transformation, the catalyst is recovered by filtration from the reaction mixture and washed with solvent followed by oven drying prior to employing for further catalytic test. The reaction mixture of

each catalytic experiment is analyzed by GC under the same conditions as employed for the previous catalytic experiments for determining the optimized reaction parameters. Data screening the results of each recycle tests are depicted in Fig. 4.9 and no significant loss of activity is observed up to four times. The conversion in the frist to fourth recycle is 99.2%, 98.8%, 97.67%, 95.99% and selectivity is 99.1%, 98.2%, 97.1% and 944%, respectively. These experiments proved the truly heterogeneous nature of CuL-*f*-GO catalyst. This truly heterogeneous nature of the catalyst is supposed to be due to reciprocal action of metal-support interaction and we can further provide evidence for the significance of the support.

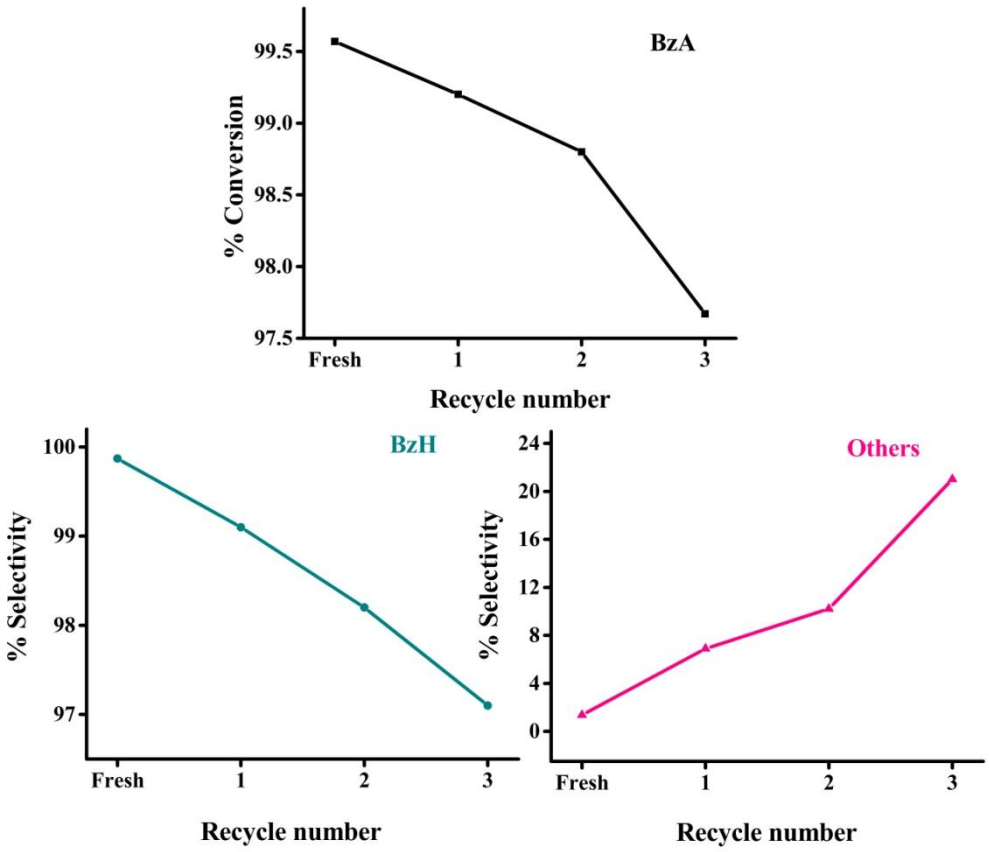

Fig. 4.9. Recyclability test on the oxidation of BzA.

Reaction condition: BzA (40 mmol), 30% H_2O_2 (40 mmol), CuL-*f*-GO (50 mg), 90 °C, ethylene glycol (5 mL), 20 min.

4.1.10. Impact of source of raw material

Inspiring from these explorations, we thought to test one more imperative aspect i.e. mesh size of graphite flakes and grade of the raw

material used for the fabrication of these catalysts. To check and validate the impact of less mesh size of quality of raw material, we purchased low-grade graphite flakes of 60 mesh size from local market and synthesized GO, A-*f*-GO, and CuL-*f*-GO which is then analyzed by assorted physicochemical techniques like FTIR, BET, RAMAN and XRD followed by comparing it with GO, A-*f*-GO and CuL-*f*-GO prepared from high-grade graphite flakes (325 mesh size) from Sigma Aldrich. FTIR spectrum of the GO, A-*f*-GO, and CuL-*f*-GO (prepared from the low-grade graphite flakes) is shown in Fig. 4.10. We can confirm the low degree of oxidation with the peak intensity of all the oxidative groups which is diminished. Apparently, it is anticipated that if the primary oxidation is not adequate then the fabrication of the final catalyst by modifying this oxidative functional groups would not be as good as of high-grade.

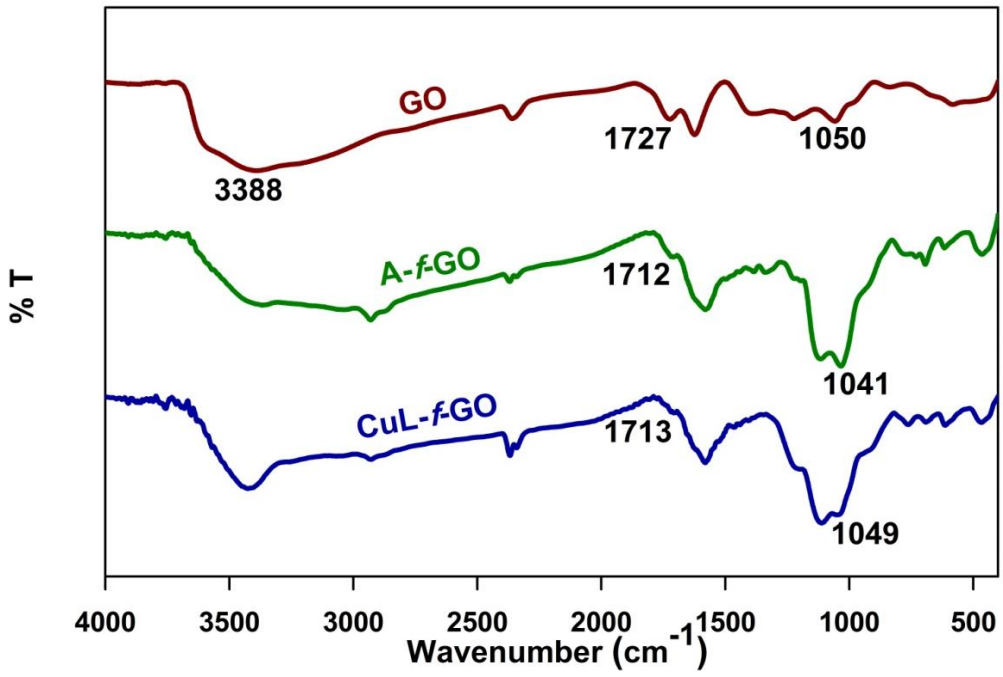

Fig. 4.10. FTIR spectra of GO, A-*f*-GO, and CuL-*f*-GO prepared from low-grade graphite flakes.

XRD pattern also supports this hypothesis (Fig. 4.11). The peak observed at 10.9º in high grade GO is shifted to 12.6º in the XRD pattern of catalyst prepared from low-grade graphite flakes. The calculated interlayer

distance for this low-grade GO is 7.01 Å, less than that of high grade GO demonstrating lesser amount of oxidative functionalities inserted between the layers of graphite which is caused by the low degree of oxidation[34]. From Fig. 4.11, it is seen that in the XRD pattern of catalyst prepared from low-grade graphite flakes, an intensity of the peak at 26.3º is enhanced slightly during the synthesis of the final catalyst which shows that lower grade GO might experience the reduction up to some extent. However, peak observed at 42.2º attributed to the defects caused by the presence of residual trace MnO_2 is also lessened in the XRD pattern of lower grade GO, which further confirms the low degree of oxidation.

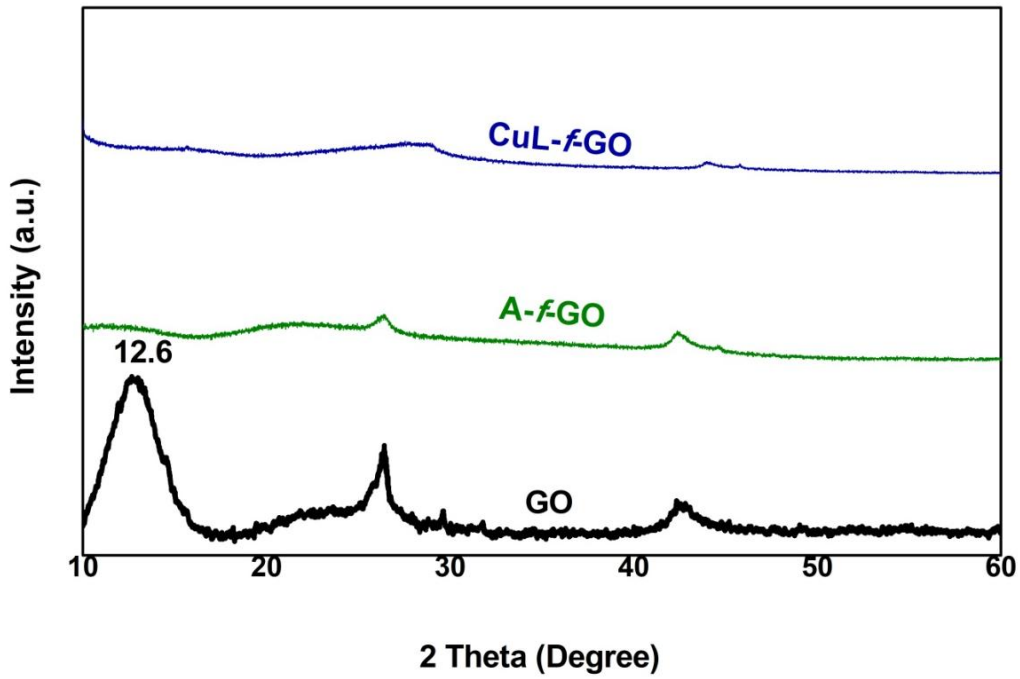

Fig. 4.11. XRD pattern of GO, A-*f*-GO, and CuL-*f*-GO prepared from low-grade graphite flakes.

In the Raman spectra of catalyst prepared from low-grade graphite flakes (Fig. 4.12), ID/IG ratio for GO is 0.81 which is slightly lower than that of high-grade graphite products. However, for metal immobilized GO, ID/IG ratio is 0.94 considerably lower than that of high-grade graphite formation; this reflects low degree of oxidation because the defects build upon the surface of GO is very less. BET results of catalyst prepared from low-grade graphite flakes are also varying from high-grade graphite products. BET surface area observed for the GO prepared from low-grade graphite was 41.6 m^2/g

however, in the final catalyst, the surface area left is just 0.5 m^2/g with a pore volume of 0.004346 cm^3/g. This is extremely fewer for catalytic transformation and the larger pore diameter may also affect desorption of the yield which may reflect in lower catalytic results. For the selective transformation of BzA to BzH, we observed very poor results with the catalyst prepared from low-grade graphite flakes. Maximum conversion of BzA achieved was 49% and selectivity is also very poor.

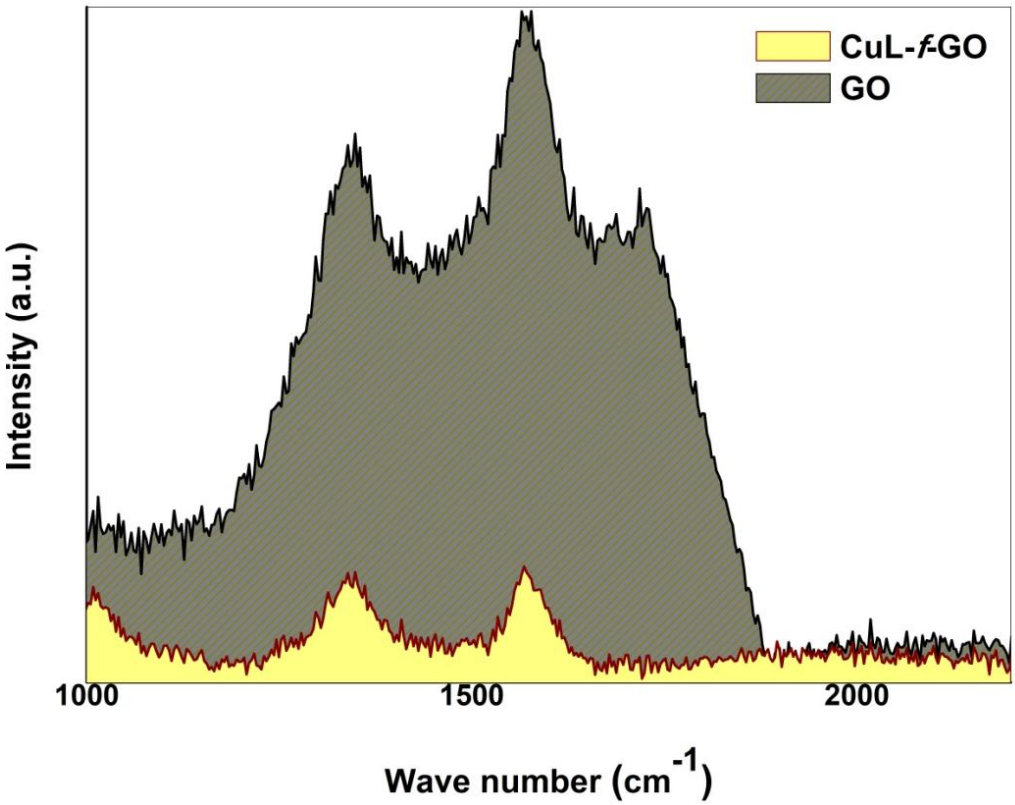

Fig. 4.12. Raman spectra of GO and CuL-*f*-GO prepared from low-grade graphite flakes.

4.1.11. Conclusion

In concluding remarks, catalysts are the fundamentally essential remedy for selective transformation that favors one precise reaction over another, thus again making the process more efficient and cost-effective. This sub-chapter executed the functionalization on the surface hydroxyl groups of GO explored the catalytic aptitude of the composite catalysts. Among them, CuL-*f*-GO is found to be highly effective and best suited catalyst for this

selective oxidation of benzyl alcohol with 99.53% conversion and 99.67% BzH selectivity. This catalyst can be recycled six times and this excellent performance is might be due to the GO support and dynamic immobilization tactic. The influences of distinct parameters like temperature, time, catalyst amount, solvents, amount of solvent and catalytic support have also been studied and observed that support, raw material and especially solvent plays crucial role in this catalytic transformation.

4.2. Selective epoxidation of styrene

Catalytic oxidation of hydrocarbons is "nitty-gritty" for the industrial fabrication of chemicals. In particular, catalytic epoxidation of olefins is of extreme eminence, chiefly in pharmaceuticals and fine chemical industries. Epoxides, the oxidized product of olefins, are regarded as the most versatile raw material in myriad organic synthesis[35] due to its readily accessible partly positive carbon and Lewis-basic oxygen atom in a three-member cyclic ring system. As such inborn polarity unites with ring traction makes the epoxides susceptible to an ample variety of reagents. Epoxidation of styrene is commercially valuable reaction for the synthesis of vital organic intermediate, styrene oxide (SO), which covers a broad range of applications such as stabilizer for high polymers and solvents, an ultraviolet ray absorber, a starting material in pharmaceutical industry, fine chemicals and fabrication of synthetic perfume and a sweetening material[36]. Benzaldehyde (BzH), another oxidized product of styrene epoxidation, is a key intermediate widely used in dyes, resin, food and in pharmaceutical industries which requires high purity[37]. Both of these were conventionally synthesized by epoxidation of styrene using a stoichiometric amount of organic peracids.

However, this method was not endorsed to be adopted pleasingly owing to some detrimental aspects discussed here. These organic peracids generate radical on decomposition which interacts with styrene and lowers the selectivity of SO. Moreover, introduction of peracids leading to the cleavage of SO resulted in ester formation. Hence, it becomes essential to be vigilant during operation so as to evade the risk involved in the use of peracids[38]. Additionally, peracids are pricey, corrosive in nature and also create plenty of waste. This traditional process for the industrial production of SO is known as

the chlorohydrin process or Halcon process which is deleterious to the atmosphere and devastate for catalyst recovery and reusability[39,40]. An oxidant exercised for this transformation was greener and not easily provoked such as molecular oxygen[41], air[42,43], hydrogen peroxide (H_2O_2)[44,45], tert-butyl hydroperoxide (TBHP)[46,47] and urea hydrogen peroxide (UHP)[48] as the relative reactivity of styrene is sluggish rather than other olefins. However, molecular oxygen with triplet ground state does not be in favour of reaction with a molecule in the singlet state[49].

In spite of the numerous benefits over hydrogen peroxide, TBHP is also being suffered from explosive nature at high concentration and relatively high cost[50]. UHP is a source of anhydrous hydrogen peroxide. Although more or less all these oxidants are quite active, by keeping the environmental and financial viability in mind, it is advisable to make use of H_2O_2. It is a meaningful oxidizing agent having promptly accessible and being cheaper as well. Aqueous H_2O_2 has a significant effect on the epoxidation of styrene as well. Epoxidation has resulted in high conversion, albeit with poor selectivity for SO. Ergo, it was being a driving force for the discovery of a catalyst that proves itself more powerful than aforesaid shortcomings. Transition metal ions are recognized as one of the best selective oxidation catalysts and as promising catalyst support also[51-54]. Nur et al.[55] have synthesized a new heterogeneous phase-boundary catalytic system, partially alkylsilylated titanium-loaded zeolite, for the epoxidation of alkene using an aqueous H_2O_2. However, TiO_2 and TiO_2/SiO_2 were employed as catalysts in the oxidation of styrene by Nie et al.[52]. Polymer formation was observed at 100 °C and 10 atm O_2 pressure with no use of catalyst however, use of catalyst selectively promotes the yield of benzaldehyde. Salavati et al.[56] have prepared PVMo catalyst consist of vanadium substituted heteropolymolybdate supported between silicate layers of bentonite and applied for epoxidation of alkenes using 30% H_2O_2 as an oxidant. The transformation resulted in high yields and selectivity of corresponding epoxides.

Here, in this sub-chapter, we evaluate the catalytic aptitude of the as-synthesized catalysts over the selective peroxidative epoxidation of styrene using 30% H_2O_2 as a greener oxidant. We have also shown how the reaction proceed though precise reaction mechanism for this transformation with the

assistance of DFT studies, for example, whether it proceeds via linkage of H_2O_2 with metal species or substrate molecule. According to theoretical computations, the bonding of H_2O_2 with the metal species is more favourable rather than the substrate. Peroxo complexes have been known to exist since primitive time and it is well known that they can be separated from reactions between transition metals and hydrogen peroxide. For this epoxidation of styrene, metal-peroxo species has been isolated the from the reaction mixture and identified by resonance Raman, UV/Vis and FTIR analysis. Based on theoretical and spectroscopic recognition of metal-peroxo species, we have proposed a precise catalytic reaction mechanism through which this transformation proceeds.

The catalytic epoxidation of styrene over the as-synthesized catalysts is carried out in a 50 mL two-necked round-bottom-flask furnished with water condenser in an oil bath with a magnetic stirrer. In a standard reaction condition for determining the best-suited catalyst for the epoxidation styrene, a typical reaction is carried out by taking catalyst arbitrarily (10 mg), temperature (80°C), methanol as a solvent and 30% H_2O_2 as an oxidant for 3 h. A series of experiments is performed in which Impact of the various mole ratio, temperature, oxidants, catalytic amount, solvent, solvent amount and time are examined so as to obtain the optimized reaction condition.

First, the catalyst was dispersed in methanol and stirred for 10 min followed by the addition of substrate molecule. After 10 min of stirring, oxidant is added drop wise in order to avoid the bulk decomposition of H_2O_2. The final reaction mixture was then stirred for an experimentally pre-decided time to obtain the maximum conversion and selectivity. The product formation was confirmed by GC analysis by taking aliquots of the reaction mixture at different time intervals. For the pilot reaction, 40 mmol of styrene, 40 mmol of 30% H_2O_2, 5 mL methanol as a solvent and 10 mg of catalyst (graphite, GO, A-*f*-GO, CuL-*f*-GO, CoL-*f*-GO and VOL-*f*-GO) are feed to a reaction vessel and equilibrated at 80 °C for 3 h. As a result of heterogeneous peroxidative epoxidation of styrene, in addition to the formation of key products SO and BzH, by-products like benzoic acid (BA) and phenylacetaldehyde (PAC) are also identified in little amount.

4.2.1. Impact of catalysts

The evaluation of various heterogeneous catalysts driven catalytic epoxidation of styrene and their effect on styrene conversion and distinct product selectivity are tabulated in Table 4.2. The result reveals that under the identical conditions, little or no conversion is achieved with pristine graphite, GO and A-*f*-GO corroborating the significance of the catalysts and on shifting from CoL-*f*-GO to VOL-*f*-GO, 28.97% conversion of styrene with 20.59% SO selectivity is achieved with CoL-*f*-GO; while CuL-*f*-GO offers 69.15% conversion of styrene with 24.83% SO selectivity. However, maximum conversion of styrene 83.17% with 28.18% SO selectivity is obtained with VO-*f*-GO. Contrarily, with the increasing conversion, the selectivity of SO and BzH have exhibited the conflicting trend to each other. However, the selectivity of key product SO is also seemed to flow in increasing trend, but the reverse trend is found for the selectivity of BzH at the same time. Additionally, the selectivity of other products is also increased. VOL-*f*-GO exhibits the maximum selectivity of 28.18% for SO with 61.63% selectivity for by-products in methanol solvent. Hence, VOL-*f*-GO is chosen as the preferred catalyst for further investigation of other experimental variables.

Table 4.2

Impact of varying catalysts on the epoxidation of styrene.

Systems	Styrene Conversion (%)	SO Selectivity (%)	BzH Selectivity (%)	Others Selectivity (%)	TOF[a] (h^{-1})
Graphite	0	0	0	0	-
GO	0.3	0	0	0	-
A-*f*-GO	0.5	0	0	0	-
CoL-*f*-GO	28.97	20.59	26.47	44.12	510.86
CuL-*f*-GO	69.15	24.83	15.17	59.99	545.72
VOL-*f*-GO	83.17	28.18	10.18	61.63	245.51

Reaction condition: styrene (40 mmol), 30% H_2O_2 (40 mmol), catalyst (10 mg), 80 °C, methanol (5 mL), 3 h.

[a]TOF: Moles of styrene converted per mole of metal per hour.

4.2.2. Impact of solvent

As our centre of attention is mainly on commercially viable products, we have conducted this experiment to inspect the effect of assorted solvents such as toluene, DMF, acetonitrile, 1,4-dioxane, methanol and ethylene glycol on the epoxidation of styrene. The study of effect of different solvents on the epoxidation of styrene is meant to lessen the by-product formation and to boost the key product. By using toluene as a solvent very little conversion (1.77%) is observed, however, DMF and acetonitrile have also exhibited 2.2% and 6.03% conversion of styrene (Fig. 4.13). While employing 1,4-dioxane, the conversion shows slight rise to 12.51% however, interestingly 100% selectivity for SO is observed. Here, as a key product, selectivity for SO is absolute but the concern point is plenary exploitation of styrene molecule which is not as per expectation. Hence, in order to increase % conversion, we thought of using methanol as a solvent. Our belief of using methanol as a solvent is based on two fundamental aspects, one is, being alcohol it may prove to be a good solvent for styrene and another foremost imperative subject of concern is generation of water during the reaction by the decomposition of H_2O_2 employed as an oxidant. The existence of water adversely affects the styrene conversion and product selectivity. To abstain the styrene conversion away from this undesirable cause, it is being necessitat to constantly remove the water produced during the reaction or to make use of other alternative that soak up the water promptly as produced. Methanol is very useful hygroscopic agent[57] too and we got the advantage of this remunerative property of methanol by achieving higher conversion of 83.17% for styrene.

In spite of achieving a high conversion with methanol, the selectivity for key products is very fewer, merely 28.18% for SO and 10.18% for BzH. The selectivity of by-products produced during this reaction is very high (53.88%) believed to be due to over oxidation of the aldehyde. Once being successful in attaining a high conversion, one should focus on the prevention of by-product formation together with more styrene conversion. From our experience of selective oxidation of BzA, we thought of employing ethylene glycol as a solvent for this transformation to prevent acid formation. In addition, to keep the catalyst away from the deactivation by the water

generated, owing to high boiling point and strong affinity to water, ethylene glycol is also useful as a potent desiccant. With the aim of taking more advantage of this astonishing characteristic of ethylene glycol, strategically we injected H_2O_2 at much lower rate so that the produced water promptly get absorb by ethylene glycol. Furthermore, it potently favours the epoxide formation owing to having a high dielectric constant value of 41.4[58]. As per our expectation, it prevents further oxidation of BzH leading to highest styrene conversion of 99.22% with 97.88% selectivity for SO. Therefore, we have chosen ethylene glycol as the preferred solvent for further investigation of other experimental variables.

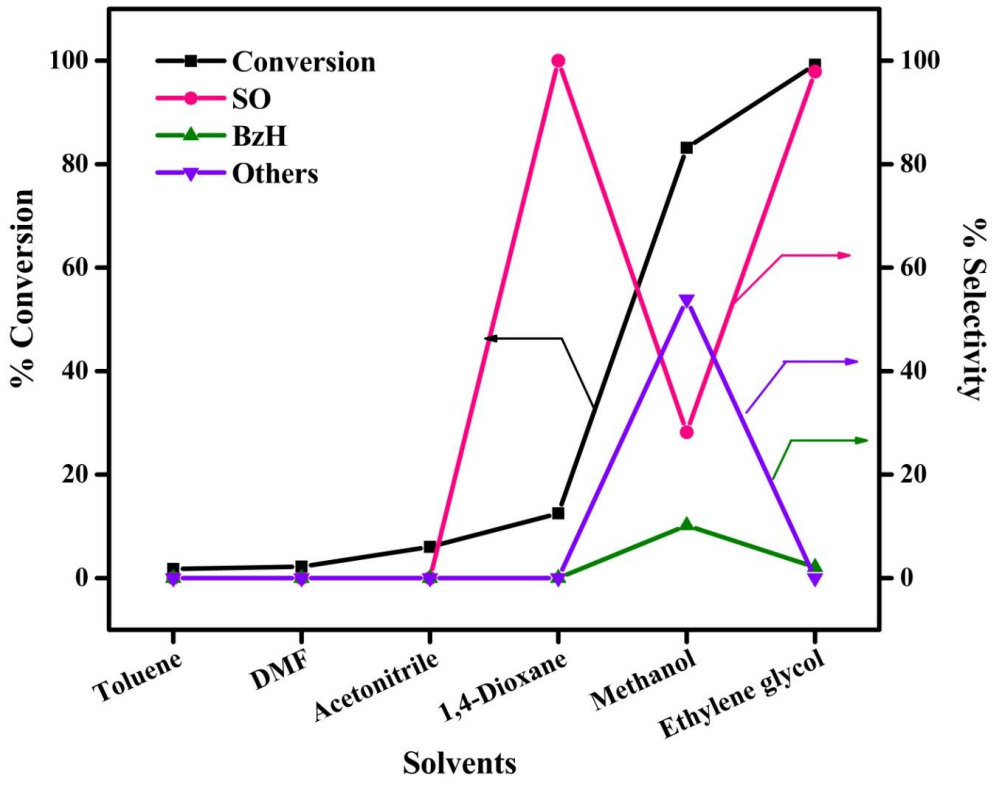

Fig. 4.13. Impact of varying solvents on the epoxidation of styrene.
Reaction condition: styrene (40 mmol), 30% H_2O_2 (40 mmol), VOL-*f*-GO (10 mg), 80 °C, solvent (5 mL), 3 h.

4.2.3. Impact of mole ratio

Data screening the impact of mole ratio of styrene to H_2O_2 on the styrene conversion, product distribution and selectivity over the catalyst VOL-*f*-GO is depicted in Fig. 4.14. Low concentration of H_2O_2 to substrate (1:1) gives 99.22% conversion of styrene with 97.88% SO selectivity. On increasing the mole ratio from 1:1 to 1:1.5, styrene conversion is also exhibited increasing trend and achieved the maximum (100%), however, selectivity of SO decreases to 93.26%. Further rise in mole ratio (1:2 and 1:2.5) has no noteworthy effect on styrene conversion but the selectivity of SO shows reverse trend and lessened to 96.64% and 77.12%, respectively. It is noticed that the product selectivity is greatly affected by high ratio of styrene to H_2O_2. With 1:1 mole ratio, highest selectivity of the key product SO is achieved, but with increasing mole ratio, massive reduction is observed in the selectivity of SO. On the other hand, major yield of BzH is also seen to be affected by higher mole ratio. With 1:1 mole ratio, we obtained BzH as another key product but with increasing mole ratio from (1:1 to 1:2.5), the BzH selectivity is found to be decreased and the selectivity of other products such as BA and PAC is increased noticeably. The justification for this higher selectivity on higher mole ratio may be given as secondary reaction of BzH. Therefore, we have chosen 1:1 as a preferred mole ratio for further investigation of the impact of other experimental variables.

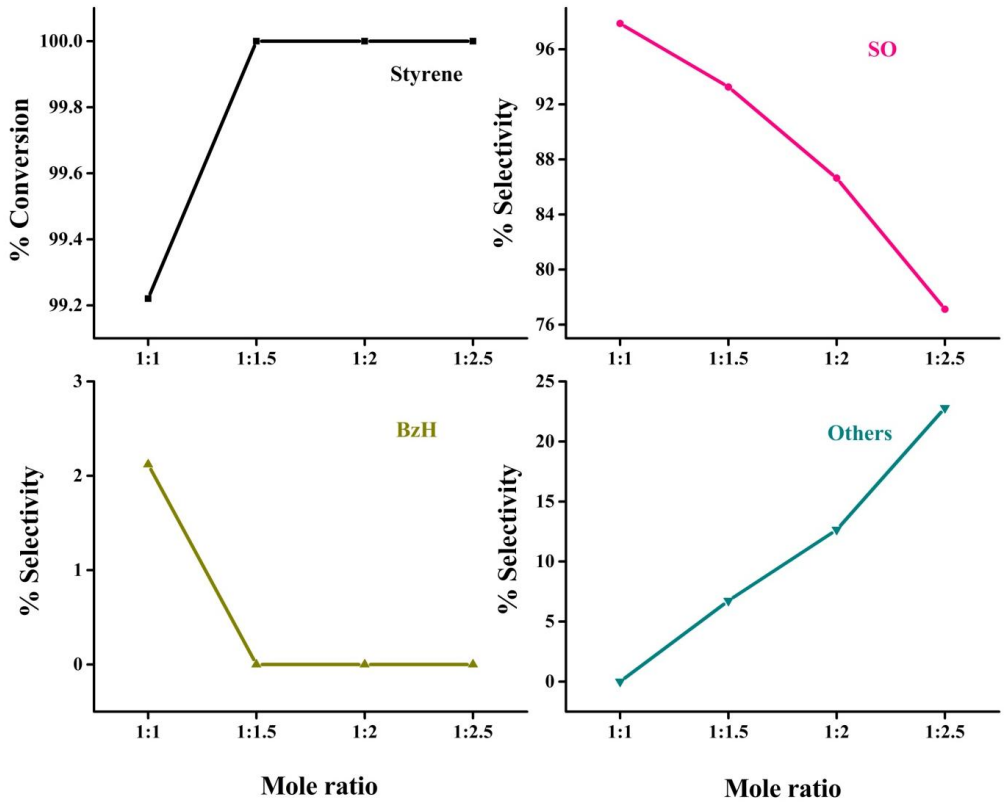

Fig. 4.14. Impact of varying mole ratio on the epoxidation of styrene.
Reaction condition: styrene (40 mmol), 30% H_2O_2 (mmol), VOL-*f*-GO (10 mg), 80°C, ethylene glycol (5 mL), 3h.

4.2.4. Impact of amount of catalyst

To assess the catalyst on a commercial degree, the potential of the quantity of as-synthesized catalyst on the respective transformation is rather a vital parameter. Hence, three concentrations viz. 10, 20 and 30 mg of catalyst is inspected for the epoxidation of styrene over 30% H_2O_2 as an oxidant using ethylene glycol as a potent hygroscopic solvent. The result of the reaction is depicted in Fig. 4.15. At lower concentration of catalyst, higher conversin of styrene is observed and vice-versa. This dissimilarity observed in the styrene conversion with the increasing concentration of catalyst is anomalous. The higher styrene conversion at lower concentration is thought to be due to the high rate of epoxidation of styrene. However, on increasing catalyst concentration to 20 mg, styrene conversion declined to 67.45% with 19.6% SO selectivity; while on employing 30 mg of catalysts amount, styrene conversion further decreases to 61.31% with 31.74% SO selectivity.

Therefore, we have chosen 10 mg as preferred catalyst concentration for further investigation of the other experimental variables.

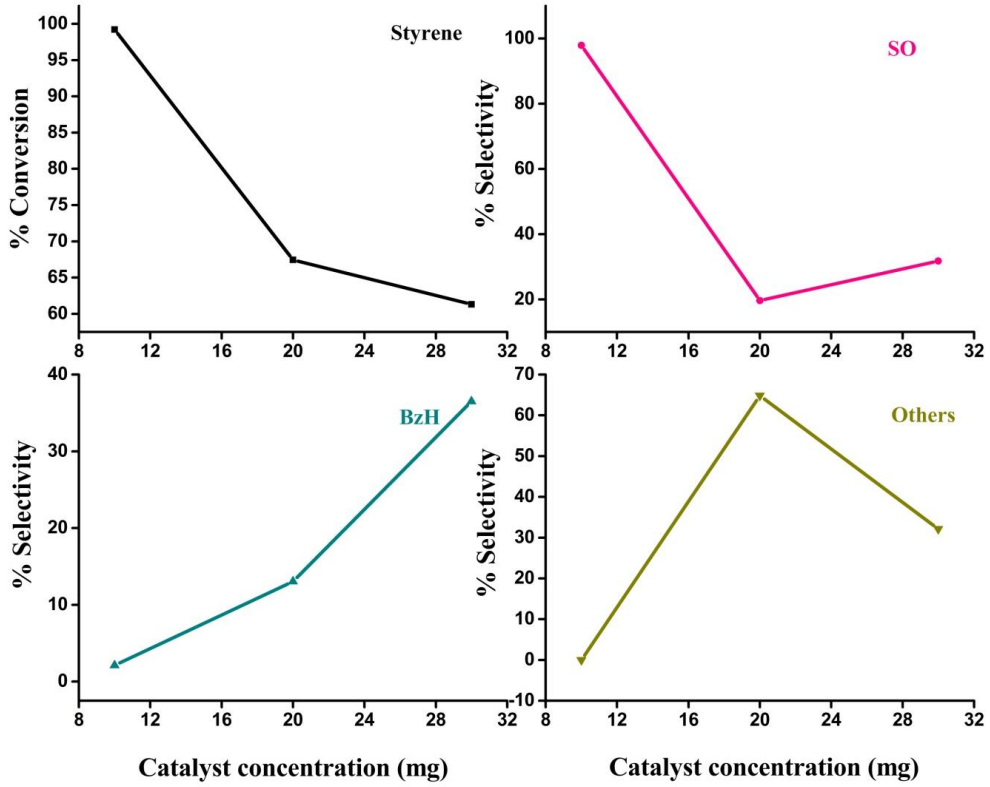

Fig. 4.15. Impact of varying amount of catalyst on the epoxidation of styrene. Reaction condition: styrene (40 mmol), 30% H_2O_2 (40 mmol), VOL-*f*-GO (mg), 80 °C, ethylene glycol (5 mL), 3h.

4.2.5. Impact of solvent amount

Next to desired results obtained using ethylene glycol as a solvent, we have examined the effect of amount of solvent on the epoxidation of styrene. From Fig. 4.16, while employing 2 mL of solvent, very poor or negligible conversion of 1.17% is observed which might be due to insufficient amount of solvent for dissolution of substrate molecule. On increasing amount of solvent from 2 to 5 mL, this transformation is switched to expected high conversion and selectivity of SO. The conversion is increased up to 99.22% while highest selectivity obtained for SO is 97.88%. This result increases our keenness to study more effect of solvent amount. Subsequently, moving ahead with catalytic epoxidation reaction of styrene by employing further excessive amount of solvent (10 mL), we inspected astonishing results that by increasing solvent amount, absolute conversion (100%) is achieved with 99.50% SO

selectivity. Here, conversion and selectivity of SO both increases with increasing solvent amount, but with 10 mL, formation of undesirable by-products (0.5%) is seen. Hence, for this epoxidation reaction, 5 mL is chosen as preferred solvent amount for further investigation of other experimental variables.

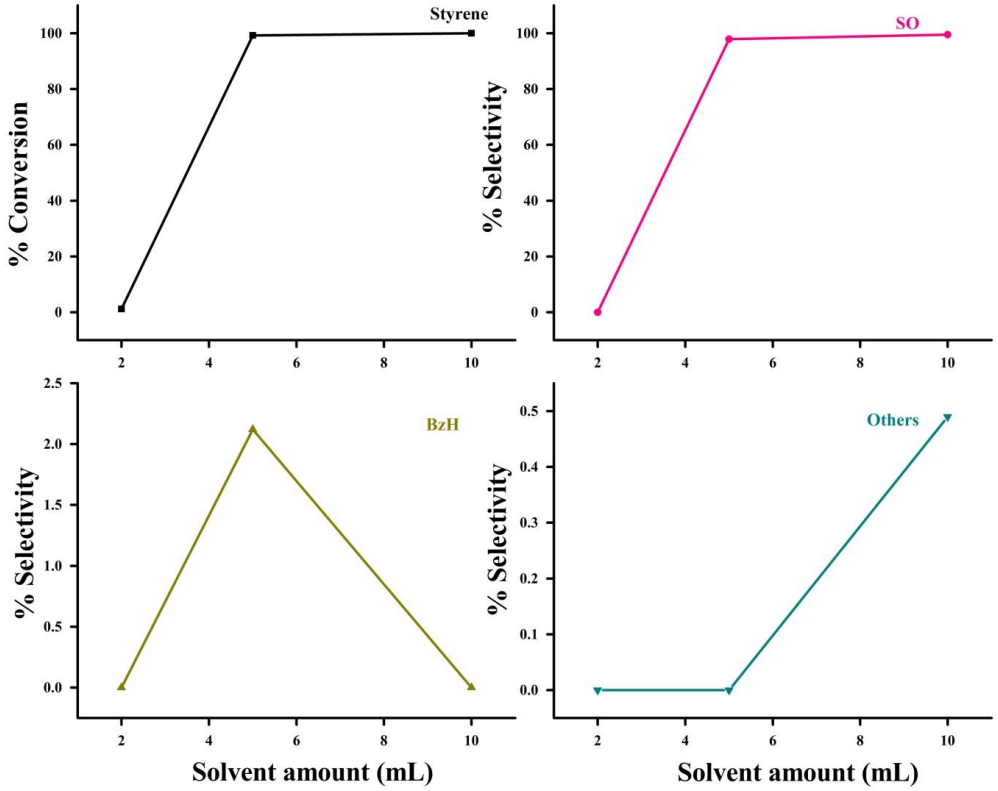

Fig. 4.16. Impact of varying amounf of solvent on the epoxidation of styrene. Reaction condition: styrene (40 mmol), 30% H_2O_2 (40 mmol), VOL-*f*-GO (10 mg), 80 °C, ethylene glycol (mL), 3 h.

4.2.6. Impact of time

With the aim of studying the impact of time on the conversion of styrene and product distribution, the epoxidation reaction has been conducted up to 12 h by keeping other parameters fixed. The conversion of styrene as a function of time is depicted in Fig. 4.17. At 1 h styrene conversion is very poor (3.33%); while with increasing time to 2 h, 64.78% conversion of styrene with 71.74% SO selectivity is obtained. However, 99.22% styrene conversion with 97.88% SO selectivity is achieved at 3 h. Whereas, after 3 h it shows the almost steady trend in the conversion of styrene with time but the investigation

of product distribution and selectivity come up with more thought-provoking statistics. At 6 and 12 h, the observed SO selectivity is 9.89% and 7.5%, respectively. While, BzH and by-products selectivity is 35.67% and 54.44% at 6 h and 26% and 66.5% at 12 h, respectively. The trend to SO and BzH selectivity is seen to be inconsistent to each other as the time goes on. The selectivity of SO reached maximum at 3 h and then declined markedly. This observable alteration in the SO selectivity is due to side reaction or over oxidation of styrene which resulted in improved selectivity of BzH. Quite the opposite to SO, the noteworthy upsurge is shown in the selectivity of BzH as the reaction continues and attained maximum at 6 h. After 6 h, a shortfall analyzed may relate to the secondary reactions. Undoubtedly, the reaction mixture is not hold up only SO and BzH, but also carry by-products like BA and PAC up to some extent by the further oxidation of BzH. At the same time, when the selectivity of BzH commences to decline after 6 h, the selectivity of by-products started to rise. As a result, we have chosen 3 h as the preferred time for further investigation of other experimental variables.

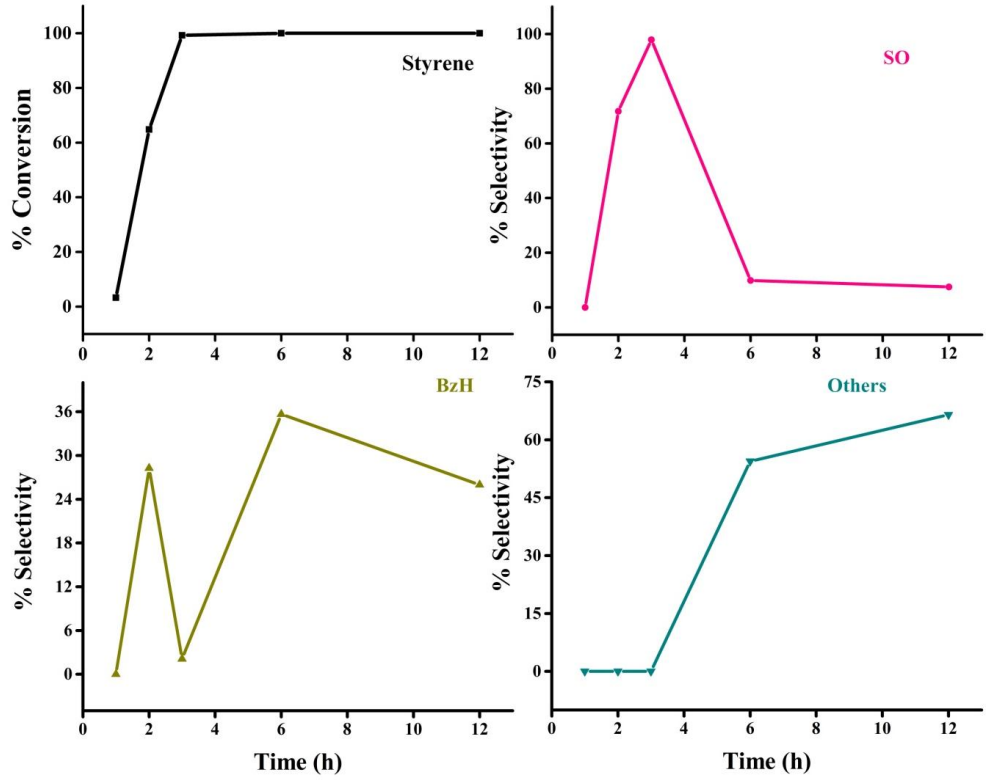

Fig. 4.17. Impact of varying time on the epoxidation of styrene.
Reaction condition: styrene (40 mmol), 30% H_2O_2 (40 mmol), VOL-*f*-GO (10 mg), 80 °C, ethylene glycol (5 mL), time (h).

4.2.7. Impact of oxidant

In order to achieve the greener approach, it is decided to examine the effect of oxidant on styrene conversion. 70% TBHP is decided to examine as an oxidant besides H_2O_2. Fig. 4.18 has been illustrating the result of this transformation. TBHP, having diminutive effect on conversion of styrene (97.55%), product distribution along with selectivity of the key product SO (0.5%), is proved to be unfavourable as an oxidant. It shows a reverse effect on the propensity to SO and BzH selectivity which has been switched each other. Selectivity of SO is found to be declining, whereas, selectivity of BzH is seen to be increasing with same rate. Even though, the formation of by-product is not noticed with TBHP, this reaction is aimed with mainly a sole key product SO, we have preferred H_2O_2 as a greener and environmentally benign oxidant as it give almost as a single product SO (97.88%). Besides these, H_2O_2 is quite inexpensive, easy to handle and produced only water as by-product.

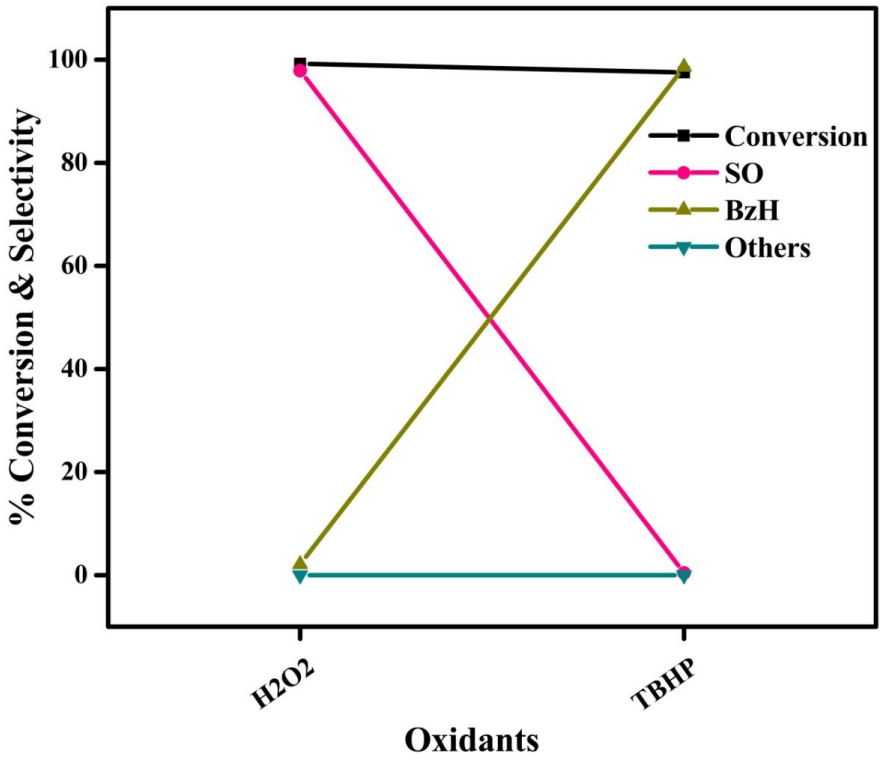

Fig. 4.18. Impact of oxidants on the epoxidation of styrene.

Reaction condition: styrene (40 mmol), oxidant (40 mmol), VOL-*f*-GO (10 mg), 80 °C, ethylene glycol (5 mL), 3h.

4.2.8. Impact of temperature

Effect of reaction temperature on epoxidation of styrene is demonstrated in Fig. 4.19. It is clear from the figure that 59.38% conversion of styrene is attained with 100% SO selectivity at 70 °C. On rising the temperature to 80 °C, utmost conversion of 99.22% of styrene is monitored with 97.88% SO selectivity. Moreover, on further increasing the temperature (90 °C), a gel type formation is seen after 1 h that might be due to polymerization of styrene in addition to concurrent rapid decomposition of H_2O_2, lowers the conversion to 43.05% and selectivity of SO to 23.65%. Accordingly, we have chosen 80 °C as preferred reaction temperature for further investigation.

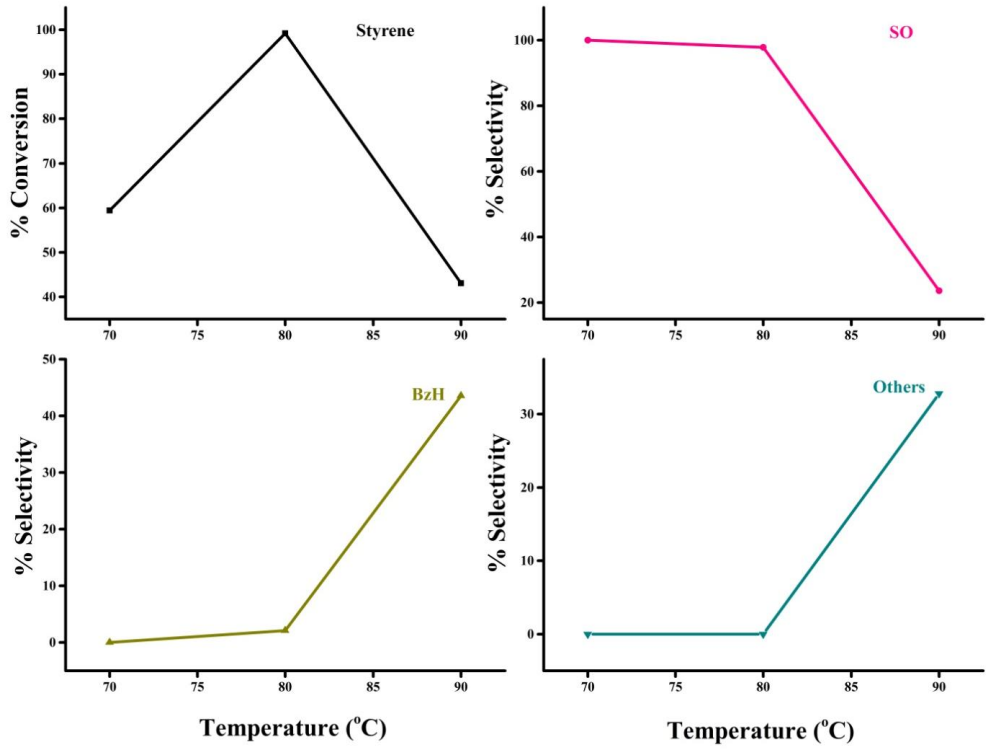

Fig. 4.19. Impact of varying temperature on the epoxidation of styrene.
Reaction condition: styrene (40 mmol), 30% H_2O_2 (40 mmol), VOL-*f*-GO (10 mg), temperature (°C), ethylene glycol (5 mL), 3h.

4.2.9. Leaching and recyclability test

VOL-*f*-GO undergo for the leaching test using styrene as a substrate under the experimentally acquired optimized reaction conditions to verify the truly heterogeneous nature of the catalyst. To execute this experiment, the reaction is sustained for 2 h and then catalyst is removed from the reaction mixture by simple filtration. The reaction is further continued with filtrate for another one hour as the maximum conversion achieved at 3 h. The reaction mixture is then analyzed by GC and noted the small increase of ~18% in the conversion, thought to be due to oxidant. The result of this experiment is depicted in Fig. 4.20.

We have also corroborated the effect of oxidant on this transformation by performing a blank experiment. A blank oxidation reaction is conducted with no use of catalyst under the experimentally acquired optimized reaction conditions to have a perception of the role of H_2O_2 in the epoxidation of styrene. This reaction is resulted in very less 11.2% styrene conversion without catalyst. No metal leaching is detected during the experiment.

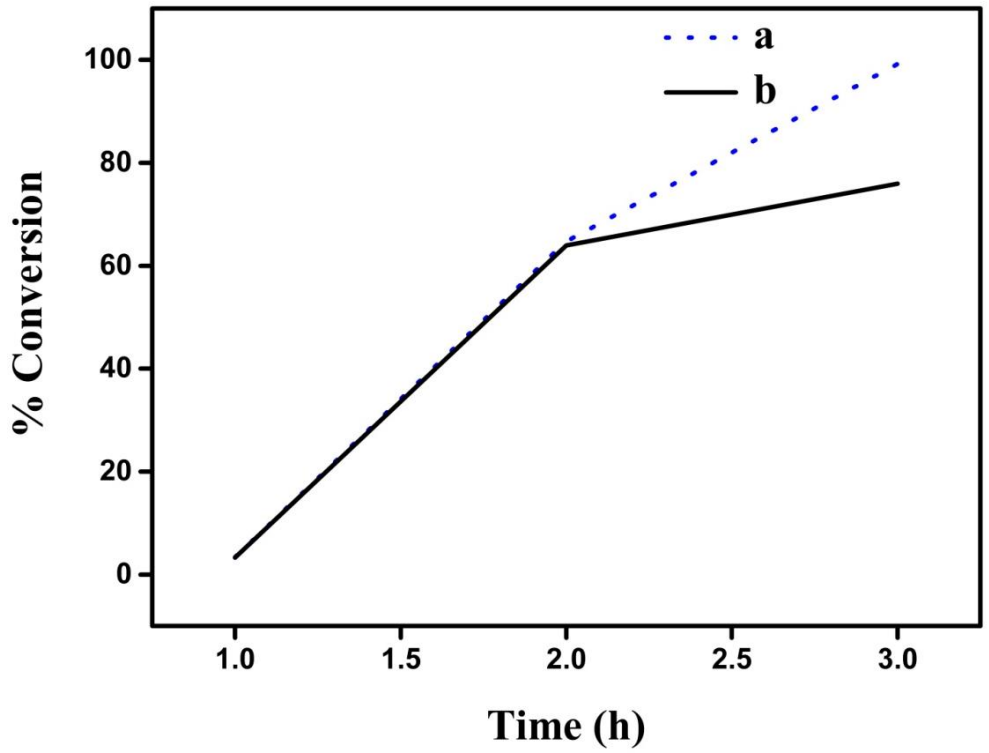

Fig. 4.20. Leaching test of VOL-*f*-GO for epoxidation of styrene under optimized conditions, a) presence of catalyst and b) after removal of catalyst.

Peroxide, in particular, H_2O_2 is recognized as useful oxidant and hence, it is quite imperative to know its expenditure during catalytic reaction. Therefore, we have carried out the redox titration of the pure 30% H_2O_2 before and after completion of the reaction. We have titrated pure 30% H_2O_2 against the known normality of $KMnO_4$ before employed. A relative amount of aqueous H_2O_2 decreases as a result of disproportionation and thermal decomposition. So the consumption of H_2O_2 during reaction mixture is calculated by titrating the reaction mixture after completion of the reaction with same normality of $KMnO_4$ used to measure the weight % of the pure H_2O_2. The calculated result confirms 96.2 weight % consumption of the H_2O_2 during the epoxidation reaction.

To study the recyclability of the as-prepared heterogeneous catalyst for this transformation, the catalyst is recovered by filtration from the reaction mixture and washed with solvent followed by oven drying prior to employing for further catalytic test.The reaction mixture of each catalytic experiment is analyzed by GC under the same conditions. The results of each recycle test are portrayed in Fig. 4.21 and it can be observed that catalyst gives its best performance up to three cycles with no significant loss of activity. The conversion in first to three recycle is 97.99%, 96.61%, 93.28% and selectivity of SO is 95.27%, 93.1% and 89.18%, respectively. Leaching and recyclability test confirmed the truly heterogeneous nature of VOL-*f*-GO catalyst and this is believed to be due to reciprocal action of metal-support interaction.

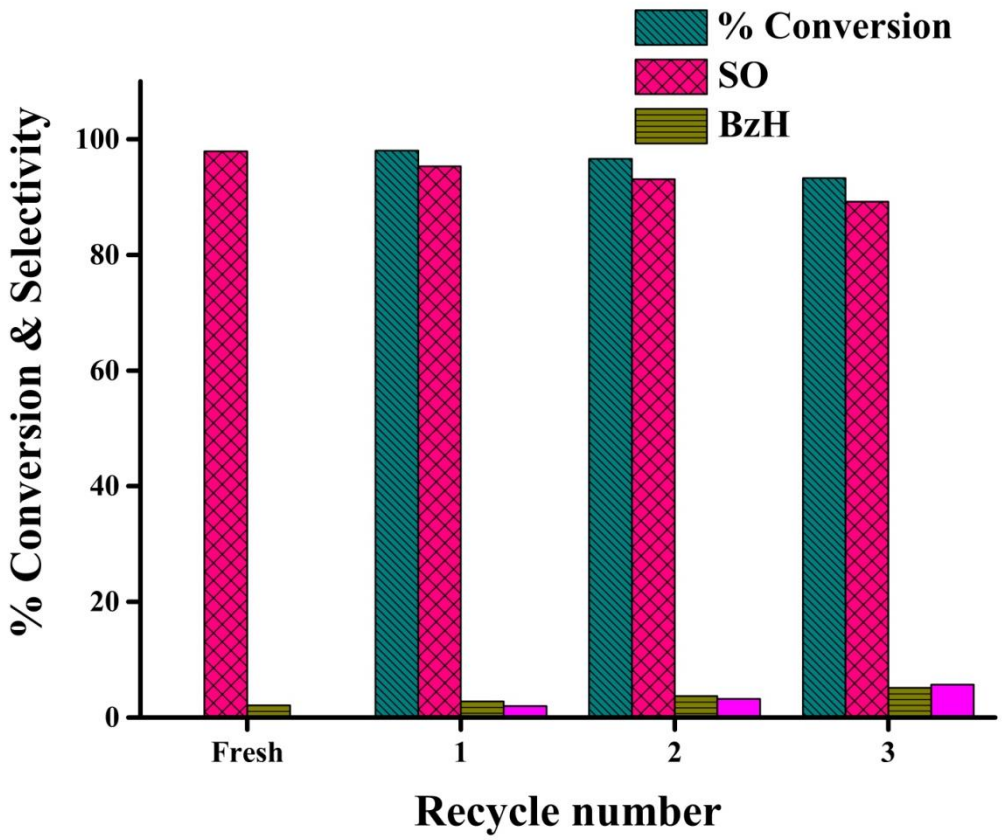

Fig. 4.21. Recyclability test of VOL-*f*-GO on epoxidation of styrene.
Reaction condition: styrene (40 mmol), 30% H_2O_2 (40 mmol), VOL-*f*-GO (10 mg), 80 °C, ethylene glycol (5 mL), 3h.

4.2.10. DFT Study

To distinctively check the effect of H_2O_2 on structural properties, binding mechanism and electronic properties of VOL-*f*-GO catalyst and styrene, density functional theory (DFT) is carried out. All the computations are performed in Gaussian09 program package[59] using well-adapted hybrid functional namely Becke three parameters with Lee-Yang-Perdew correlation functionals (B3LYP) which is the merger of Hartree-Fock (HF) exchange and DFT exchange-correlation functional[60,61]. The spin-unrestricted DFT method is employed for VOL-*f*-GO catalyst because of the spin-polarized nature of this transition metal[62]. The basis set "LANL2DZ" was used for H_2O_2 over VOL-*f*-GO catalyst. Conversely, for H_2O_2 over styrene, 6-31G(d,p) basis set is used owing to the existence of hydrogen and carbon atoms. The molecular orbitals are made visible using GaussView (version 5) through the results of DFT calculations[63]. Additionally, all considered systems have been re-

optimized to obtain the precision at the same level of theory. The adsorption energy (E_{ad}) of H_2O_2 over VOL-*f*-GO and styrene is computed using the following equations:

$$E_{ad} = E_{H_2O_2+VO-Catalyst} - (E_{H_2O_2} + E_{VO-Catalyst}) \quad (1)$$

$$E_{ad} = E_{H_2O_2+styrene} - (E_{H_2O_2} + E_{styrene}) \quad (2)$$

Where $E_{H_2O_2+VO-Catalyst}$ and $E_{H_2O_2+styrene}$ is the optimized total energy of the system in which H_2O_2 was adsorbed on VOL-*f*-GO and styrene, respectively. $E_{H_2O_2}$ is the optimized energy of H_2O_2, $E_{VO-Catalyst}$ is the optimized energy of catalysts and $E_{styrene}$ is the optimized total energy of styrene. By definition, a negative value of E_{ad} shows a stable adsorption complex on the catalyst and styrene. We have also examined their chemical reactivity to investigate the effect of H_2O_2 on electronic properties of styrene and VOL-*f*-GO catalyst. The chemical reactivity of H_2O_2 on styrene and VOL-*f*-GO catalyst is expressed by global electronic reactivity descriptors. According to Koopman's theorem[64], the diverse global reactivity descriptors, i.e., electronegativity (χ), chemical potential (μ), global hardness (η), global electrophilicity index (ω) and global softness (S) are explored using the energies of frontier molecular orbitals ϵ_{LUMO}, ϵ_{HOMO} and are given by[65, 66];

$$\chi = -\frac{1}{2}(\epsilon_{HOMO} + \epsilon_{LUMO}) \quad (3)$$

$$\mu = -\chi = \frac{1}{2}(\epsilon_{HOMO} + \epsilon_{LUMO}) \quad (4)$$

$$\eta = \frac{1}{2}(\epsilon_{LUMO} - \epsilon_{HOMO}) \quad (5)$$

$$S = \frac{1}{2\eta} \quad (6)$$

$$\omega = \frac{\mu^2}{2\eta} \quad (7)$$

$$\Delta N_{max} = -\frac{\mu}{\eta} \quad (8)$$

The energies ω, μ, χ, η, S, ϵ_{LUMO}, ϵ_{HOMO} and energy bandgap ($\epsilon_{LUMO} - \epsilon_{HOMO}$) for all considered systems are presented in Table 4.3. The electron

affinity (EA) of all considered systems was articulated by LUMO orbital energies obtained using Gaussian09 package[59] as EA = -LUMO.

Table 4.3

Calculated electron affinity (EA), electronegativity (χ), chemical potential (μ), global hardness (η) and softness (S), global electrophilicity index (ω), additional electronic charge (ΔN_{max}) of all considered systems.

System	EA (eV)	χ (eV)	μ (eV)	η (eV)	S (1/eV)	ω (eV)	ΔN_{max} (eV)
Styrene	-1.12	2.64	-2.64	3.76	0.13	0.92	0.70
VOL-*f*-GO	2.91	3.40	-3.40	0.49	1.02	11.79	6.93
Styrene+H_2O_2	1.06	3.65	-3.65	2.59	0.19	2.57	1.41
VOL-*f*-GO +H_2O_2	3.25	4.0	-4.0	0.75	0.66	10.66	5.33

To acquire the intuition of H_2O_2 over styrene and VOL-*f*-GO catalyst, the structural properties are inspected in the presence and absence of H_2O_2 molecule. Fig. 4.22 represents the initial structure of H_2O_2 over styrene and VOL-*f*-GO catalyst with top and side view in the case of styrene (Fig. 4.22(a)). The H_2O_2 molecule is situated parallel at a distance of 2.7 Å (C-C) and 2.2 Å (C-H) on styrene. On the other hand, in the case of VOL-*f*-GO, H_2O_2 is placed between two wings like shape to have better approach. Fig. 4.23 exhibits the optimized structures of H_2O_2 over all considered systems. For H_2O_2 over styrene, subsequent to the optimization, H_2O_2 molecule is reoriented at the edges of styrene which can be attributed to the presence of hydrogen (Fig. 4.23(a)). Moreover, in VOL-*f*-GO catalyst, the presence of H_2O_2 absolutely alters the structure that made it slight planer contrast to its initial structure (Fig. 4.23(b-d)). This alteration in the structural properties has an effect on its electronic properties. With the purpose of understanding the binding mechanism of H_2O_2 to styrene and to VOL-*f*-GO catalyst, we have computed the adsorption energy of all considered systems and are presented in Table 4.4.

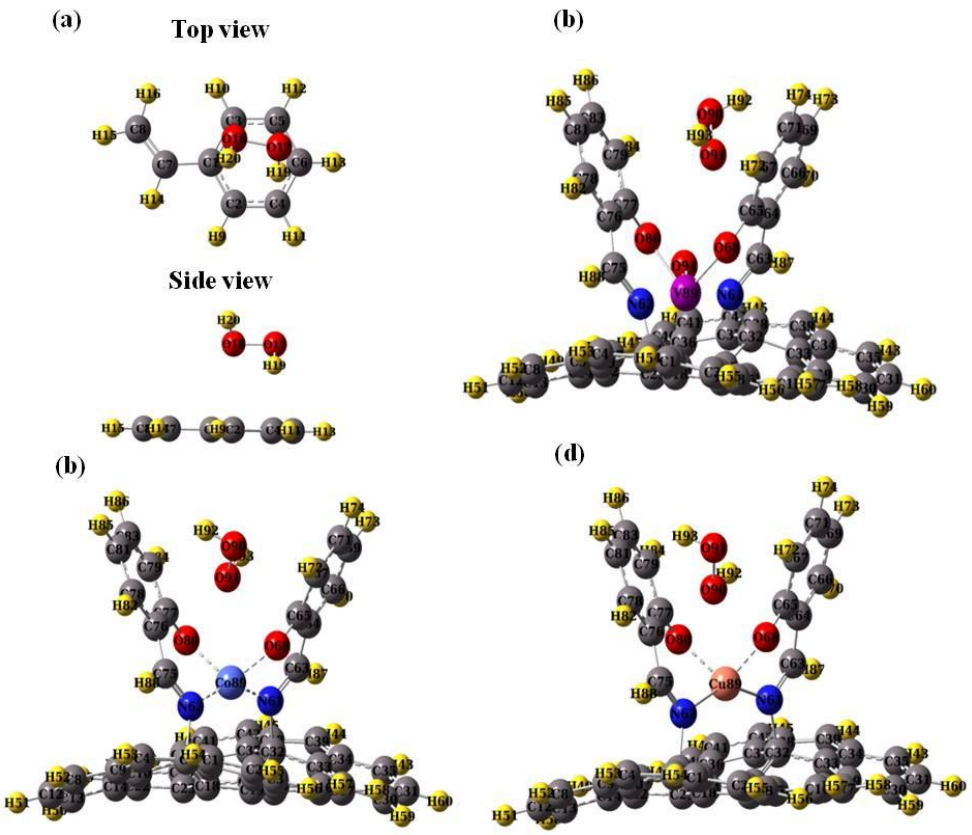

Fig. 4.22. Initial structures of H_2O_2 over (a) styrene (b) VOL-*f*-GO (c) CoL-*f*-GO and (d) CuL-*f*-GO.

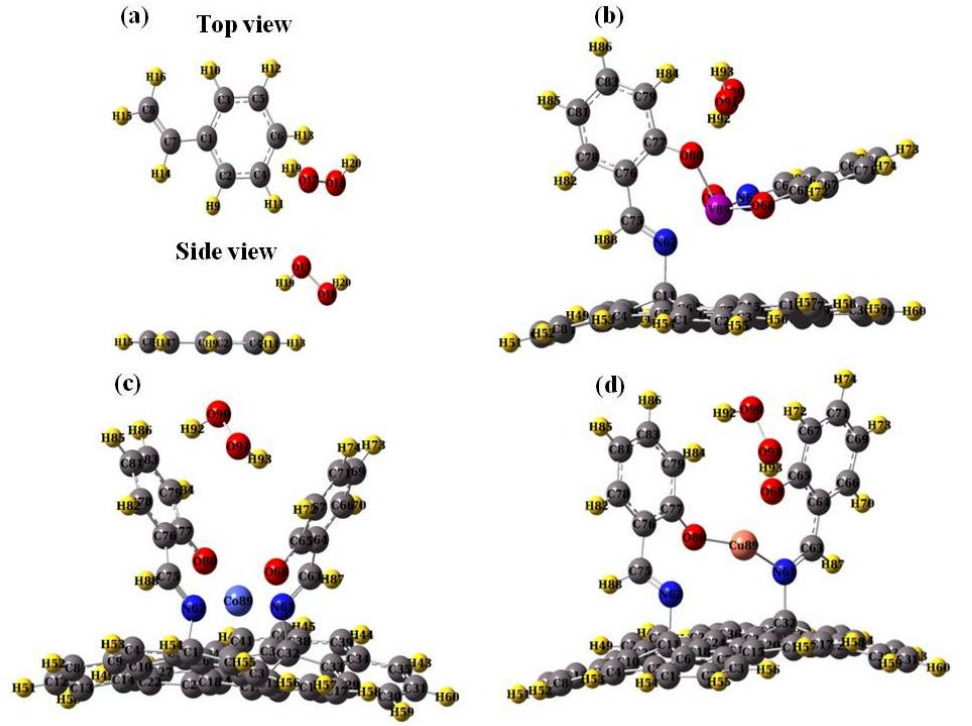

Fig. 4.23. Optimized structures of H_2O_2 over (a) styrene (b) VOL-*f*-GO (c) CoL-*f*-GO and (d) CuL-*f*-GO.

Table 4.4

Calculated electron affinity (EA), electronegativity (χ), chemical potential (μ), global hardness (η) and softness (S), global electrophilicity index (ω), additional electronic charge (ΔN_{max}) of all considered systems.

Systems	EA (eV)	χ (eV)	μ (eV)	η (eV)	S (1/eV)	ω (eV)	ΔN_{max} (eV)
Styrene	-1.12	2.64	-2.64	3.76	0.13	0.92	0.70
VOL-*f*-GO	2.91	3.40	-3.40	0.49	1.02	11.79	6.93
CoL-*f*-GO	2.98	3.92	-3.92	0.94	0.53	8.17	4.17
CuL-*f*-GO	3.05	3.91	-3.91	0.86	0.58	8.88	4.54
Styrene + H_2O_2	1.06	3.65	-3.65	2.59	0.19	2.57	1.41
VOL-*f*-GO + H_2O_2	3.25	4.0	-4.0	0.75	0.66	10.66	5.33
CoL-*f*-GO + H_2O_2	3.08	4.06	-4.06	0.98	0.51	8.40	4.14
CuL-*f*-GO + H_2O_2	3.16	4.02	-4.02	0.86	0.58	9.39	4.67

The adsorption energy of H_2O_2 over styrene and VOL-*f*-GO catalyst is in the ascending order of -0.159 eV< -3.102 eV. The high adsorption energy of VOL-*f*-GO catalyst represents its high activity. The investigation of calculated adsorption energy using DFT is in good accordance with our experimental results. Fig. 4.24 illustrates the highest occupied molecular orbitals (HOMO) and lowest unoccupied molecular orbitals (LUMO) for all considered systems. The HOMO and LUMO which corresponds to the electronic nature of materials play a crucial role in its chemical stability[67]. The ability to give away an electron is portrayed by HOMO while the potential to gain an electron is represented by LUMO. The energy gap determined through HOMO and LUMO reveals the chemical reactivity, polarizability and global descriptors like hardness-softness of any material[68]. Fig. 4.24 demonstrates HOMO-LUMO plots of H_2O_2 adsorption over styrene and VOL-*f*-GO catalyst.

The red and green color in the plots exhibits the positive and negative phase of all systems. It is clearly visible from Fig. 4.25 that the HOMO-LUMO levels are proliferated utterly all over styrene leaving H_2O_2 molecule which was attributed to the low adsorption energy of H_2O_2 resulted in low charge transfer. On the other hand, in the case of VOL-*f*-GO catalyst, the HOMO proliferated nearly on the entire catalyst whereas LUMO merely resides on the catalyst part.

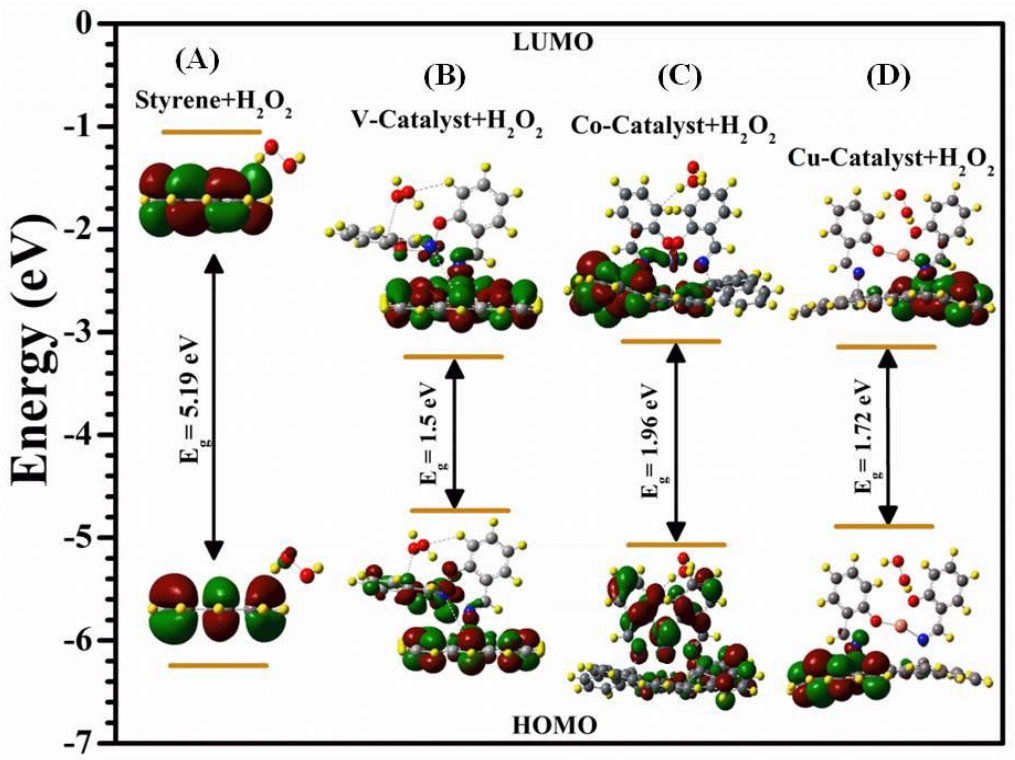

Fig. 4.24. HOMO-LUMO plots of H_2O_2 over (a) styrene (b) VOL-*f*-GO (c) CoL-*f*-GO and (d) CuL-*f*-GO.

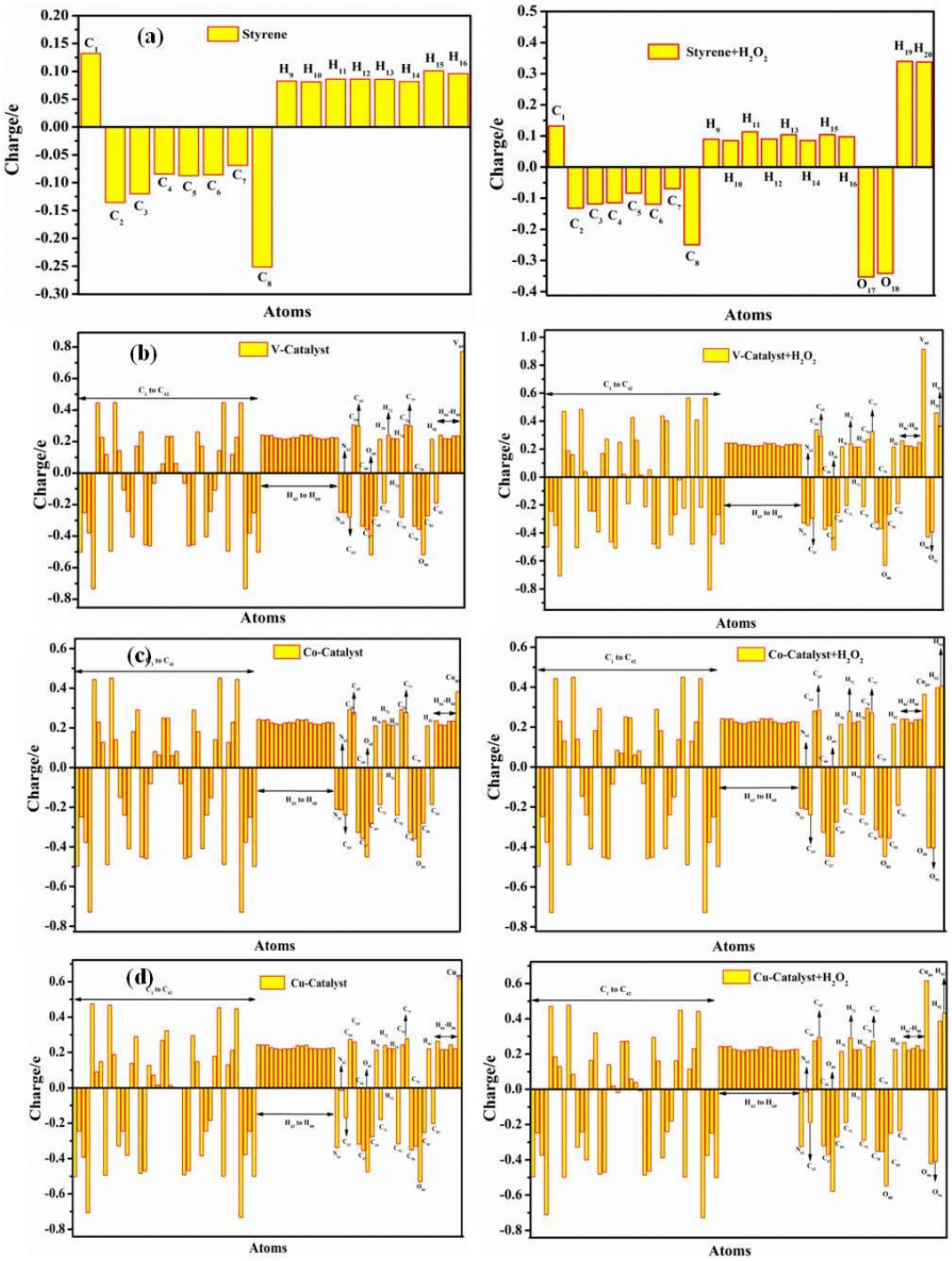

Fig. 4.25. Mulliken charge transfer plots of pristine (left panel) and H_2O_2 over (a) styrene (b) VOL-*f*-GO (c) CoL-*f*-GO and (d) CuL-*f*-GO (right panel).

The energy gap is calculated using the equation, $E_g = E_{LUMO} - E_{HOMO}$. The band gap enhancement is shown in VOL-*f*-GO catalyst after the adsorption of the H_2O_2 molecule. Conversely, the band gap reduces for styrene is from 7.53eV to 5.19eV. To understand this, we have further inspected the atomic charge distribution of H_2O_2 over styrene and VOL-*f*-GO catalyst via

Mulliken population analysis (MPA) at the same level of theory and depicted in Fig. 4.25. It is clearly seen from the figure that the positive and negative charge contribution of carbon and oxygen while hydrogen, vanadium consist of positive charge only. After the insertion of H_2O_2 in VOL-*f*-GO catalyst, the charge of vanadium increases to 0.91e from 0.77e, demonstrating the charge transfer of vanadium to H_2O_2.

The electrophilic and nucleophilic nature of any system can be estimated with the help of global electronic descriptors. Hence, in order to explore the chemical reactivity and site selectivity of styrene and VOL-*f*-GO catalyst over H_2O_2, with the help of Koopman's theorem, global hardness (η), softness (S) values, electrophilicity index (ω), chemical potential (μ), additional electronic charge (ΔN) from the neighbouring atoms are calculated and tabulated in Table 4.4. A system as a good electrophile is illustrated through greater values of ω; whereas lower values of ω represents a system as a good nucleophile. From the calculated values, it can be clearly seen that VOL-*f*-GO catalyst with or without H_2O_2 represents higher values of electrophilicity index leading to the higher binding energies with H_2O_2. As stated by maximum hardness principle, the most stable structure includes maximum hardness. Table 4.4 shows that styrene with interaction of H_2O_2 comprises maximum global hardness value indicating H_2O_2 as the most stable structure. Global electrophilicity index (ω) also appraises the stabilization in energy once a system attains an additional electronic charge from its neighbours. The high value of ω in case of H_2O_2 over VOL-*f*-GO catalyst shows that it is acting as a strong electrophile compared to styrene. The track of charge transfer as an electrophile was systematically explained through μ of the system. Subsequently, μ must be negative and the higher values make them more efficient in connection with electron transfer reaction.

Electronic affinity (EA) is the fundamental parameter in forecasting the electron accepting ability of a particular system (associated with any redox processes) to gain approaching of proton transport mechanisms establishing in gas phase or in condensed phase[69]. EA is also of immense importance in developing structure reactivity to contribute in designing new materials. The EA of H_2O_2 over the considered catalyst and styrene is in the order of: VOL-*f*-GO+H_2O_2 (3.25 eV) > Styrene+H_2O_2 (1.06 eV). The EA of VOL-*f*-GO+H_2O_2

is highest exhibiting its high electron accepting nature leading to highest binding energy between H_2O_2 and VOL-*f*-GO catalyst. All theoretical results are in good accordance with our experimental works.

4.2.11. Plausible reaction pathway of peroxidative epoxidation of styrene over VOL-*f*-GO

Based on DFT computations, the adsorption energy of H_2O_2 is highest towards VOL-*f*-GO rather than styrene; this signifies the generation of metal-peroxo species. On the basis of what has been discussed heretofore, we have proposed a catalytic reaction mechanism for the production of SO and BzH (Scheme 4.2).

In the first step, an electrophilic attack of H_2O_2 activates the VO^{IV} (catalyst) leading to the generation of quite unstable $HOOV^{IV}OH$ intermediary species in the second step[70-72]. This intermediary species then experiences displacement of hydrogen in the next step followed by a loosening of water molecule generating metal-peroxo species (step - 3). This is the most important and determining step approaching the forward movement of the reaction. The generation of $VOO^{\bullet}$ was also substantiated by UV/Vis and Raman analysis. This peroxo-vanadium formation is reflected in the UV/Vis spectra of catalyst + H_2O_2 (Fig. 4.26(b)) and in the resonance Raman spectra of the reaction mixture as an additional peak at around 997 cm^{-1} (Fig. 4.27). Introduction of the styrene in the fourth step, change the prospective of the reaction pathway. This inserted styrene molecule make a π bond with metal-peroxo species that constructs 3-membered cyclic ring. Subsequential reductive elimination step authenticates the exactitude of the synthesized catalyst in the context of exquisite quality.

The relationship among the hydrogen to be abstracted and the abstracting species is of enormous importance for any catalyst. High selectivity of the desired product may be acquired by weakening of C-H bond in styrene molecule which resulted in the cleavage of C=C bond and forming BzH. Owing to strong bonding constitution, if C-H bond cannot be weaken then it provides greater protection to the conservation C=C bond in styrene which proceed the yielding of SO. At the end of the cycle, products were

isolated from the intermediate species and regenerated VOL-*f*-GO catalyst back.

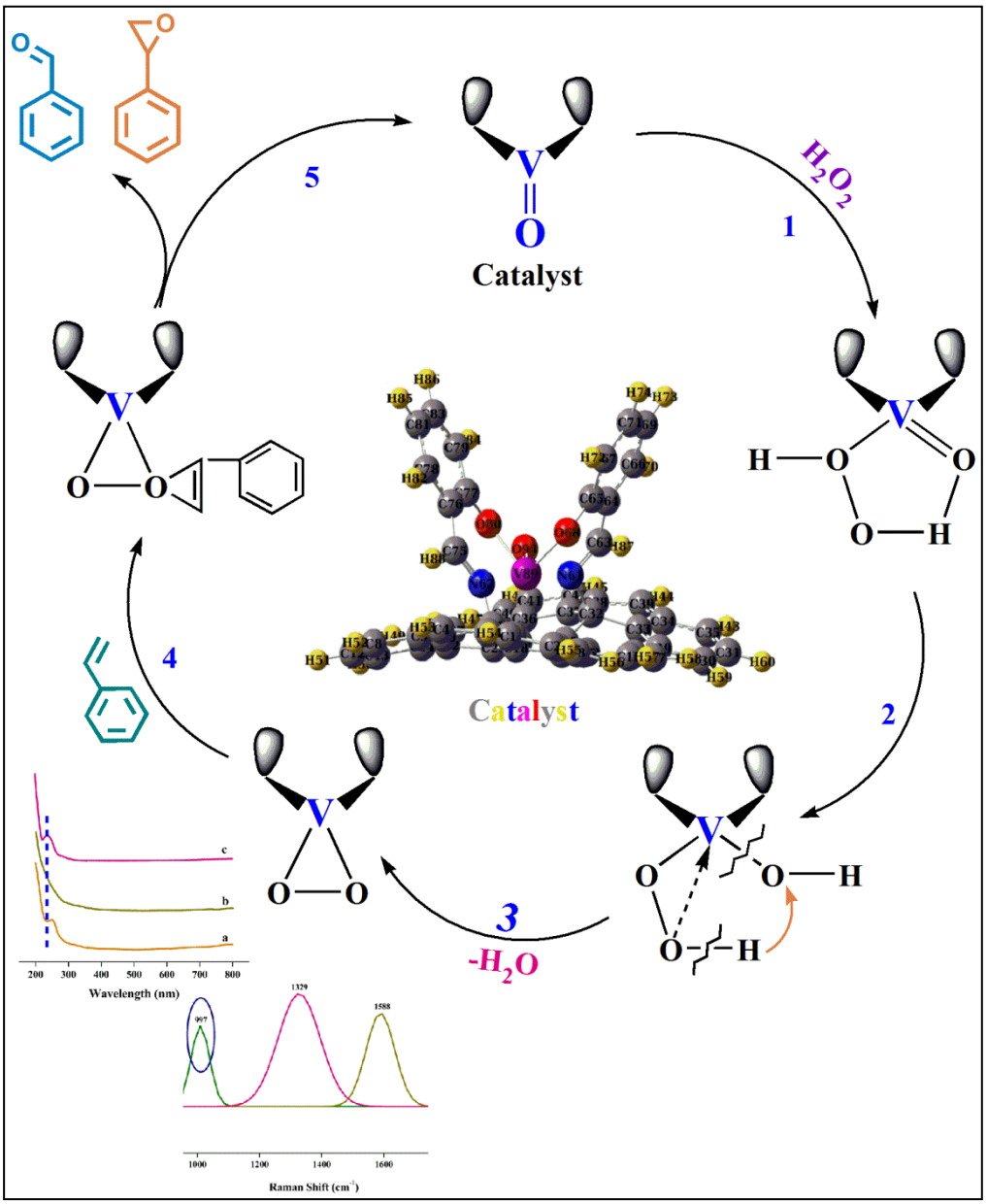

Scheme 4.2. Plausible reaction pathway for epoxidation of styrene over VOL-*f*-GO.

4.2.12. Corroboration of the formation of peroxo-vanadium species

It is identified from theoretical (DFT) computations that inserted H_2O_2 unites with the catalyst forming metal-peroxo species which changes the metal ion environment (i.e. the geometry of a metal-ion, ligating site, co-valency of metal-ligand bond). These changes (in the metal ion surrounding) could also

be endorsed by the spectroscopic tools like UV/Vis and resonance Raman analysis of the reaction mixture extracted periodically as discussed below.

4.2.12.1.UV/Vis. spectroscopy

Three sets of the sample are prepared: catalyst suspension in deionized water, catalyst and H_2O_2 mixture and reaction mixture collected after 2.5 h and analyzed by UV/Vis spectroscopy. A suspension of catalyst (VOL-*f*-GO) in deionized water exhibited a typical band in the near-UV region at around 250 nm (Fig. 4.26(a)) which is attributed to π type LMCT transition. However, a distortion in the shape is observed on adduct of H_2O_2 to the catalyst (second sample, Fig. 4.26(b)), indicating an alterations in the environment of metal ion. This change in the central metal ion is thought to be due to transfer of H atom from H_2O_2 to oxo-vanadium species. Peroxo species generated in this way demonstrates strong molar absorptivity than those of metal-centred *d-d* transition. As a result of strong absorbance of the incident wavelength, it shows higher stretching frequency which points towards the structural alterations. Typically, metal-oxo bonds are appreciably deteriorated in the LMCT excited state because of inferior vibrational energy of the metal-peroxo species in the excited state. Additionally, metal-oxo species exhibit a band as a result of electron transfer from O^{2-} to d^1 orbital of V^{IV}, however, on the generation of peroxo-vanadium species, V^{IV} ion oxidized to V^{V} (step - 4 in Scheme 4.2) with no electron in *d*-orbital and not expected to be evidence for such a band. According to this structural alteration, a different pattern is observed on adduct of H_2O_2.

Quite the opposite to this, on adduct of styrene molecule to this mixture, the peroxo species are expected to oxidize the styrene molecule and get reduced to V^{IV} showing a blue shift at around 236 nm contrast to the aqueous suspension of catalyst. As the product molecules depart from the surface, the reactant molecules adsorbed at the same time might be responsible for this blue shift.

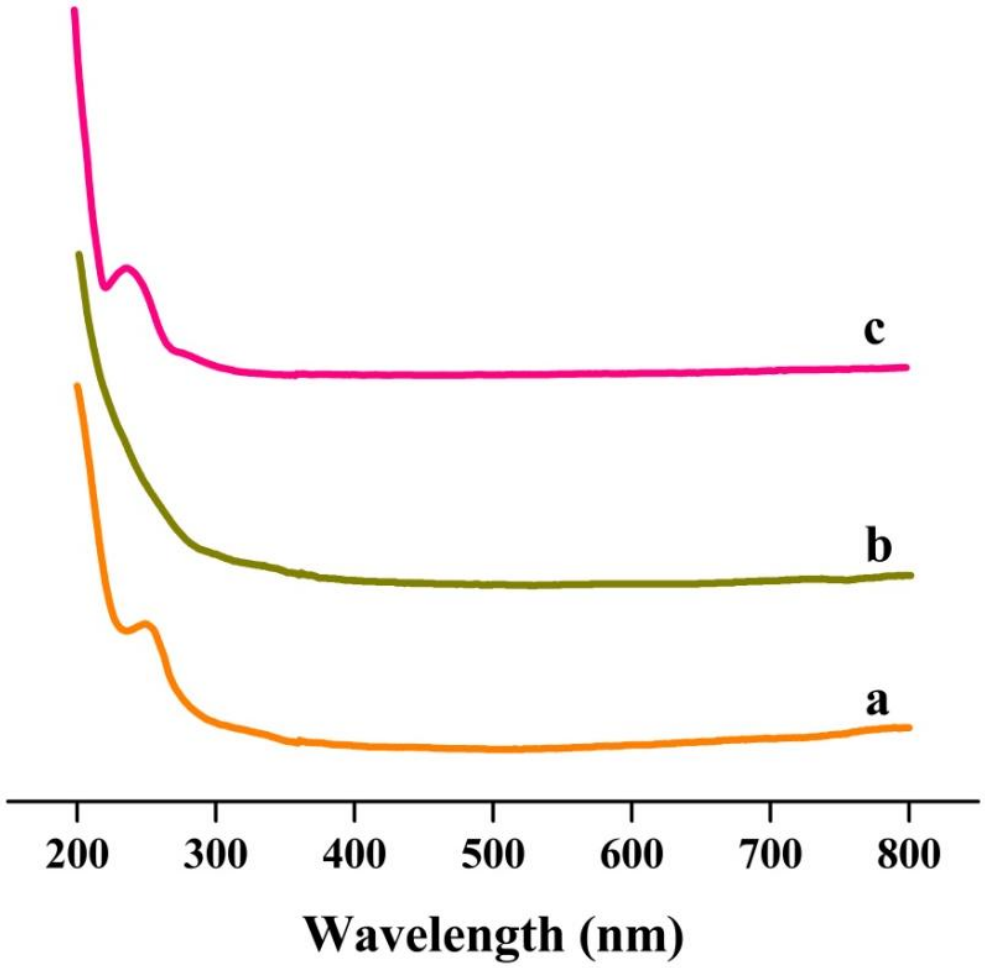

Fig. 4.26. UV/Vis spectra of catalyst (VOL-*f*-GO) in deionized water (a), catalyst + H_2O_2 (b) and reaction mixture at 2.5 h (c).

4.2.12.2.Raman Spectroscopy

Usually, complex MO_2 species remain as a cis or trans component (Scheme 4.3). However, VO_2 groups in d^0 configuration would be expected to be as cis species[73]. Two modes, metal-oxygen stretching and deformation mode are get-at-able for such species. All these three vibrations are Raman active.

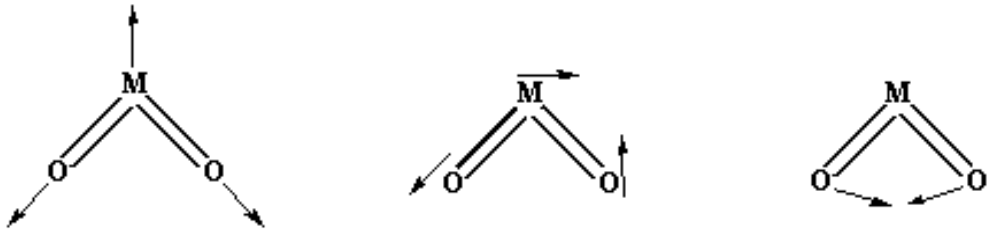

Scheme 4.3. Vibrations of MO_2 species

We have inspected the reaction mixture drawn after 2.5 h through resonance Raman analysis too (Fig. 4.27). The Raman spectra of solid catalyst demonstrates a characteristic D and G bands at 1334 and 1578 cm^{-1}, on the other hand, the resonance Raman spectra of the reaction mixture shows one additional band at 997 cm^{-1} in addition to these two characteristic D and G bands at 1329 and 1588 cm^{-1}. This additional band ascribes to the the stretching frequency of oxovanadium species[74]. Consequently, the generation of $VOO^{\bullet}$ species is also corroborated by Raman analysis which is considered as the plinth of step - 4 in Scheme 2. By confirming with theoretical study and spectroscopic tools like UV/Vis and Raman analysis, we asserts with the assurance that epoxidation of styrene over VOL-*f*-GO using 30% H_2O_2 as an oxidant proceed through peroxo radical species.

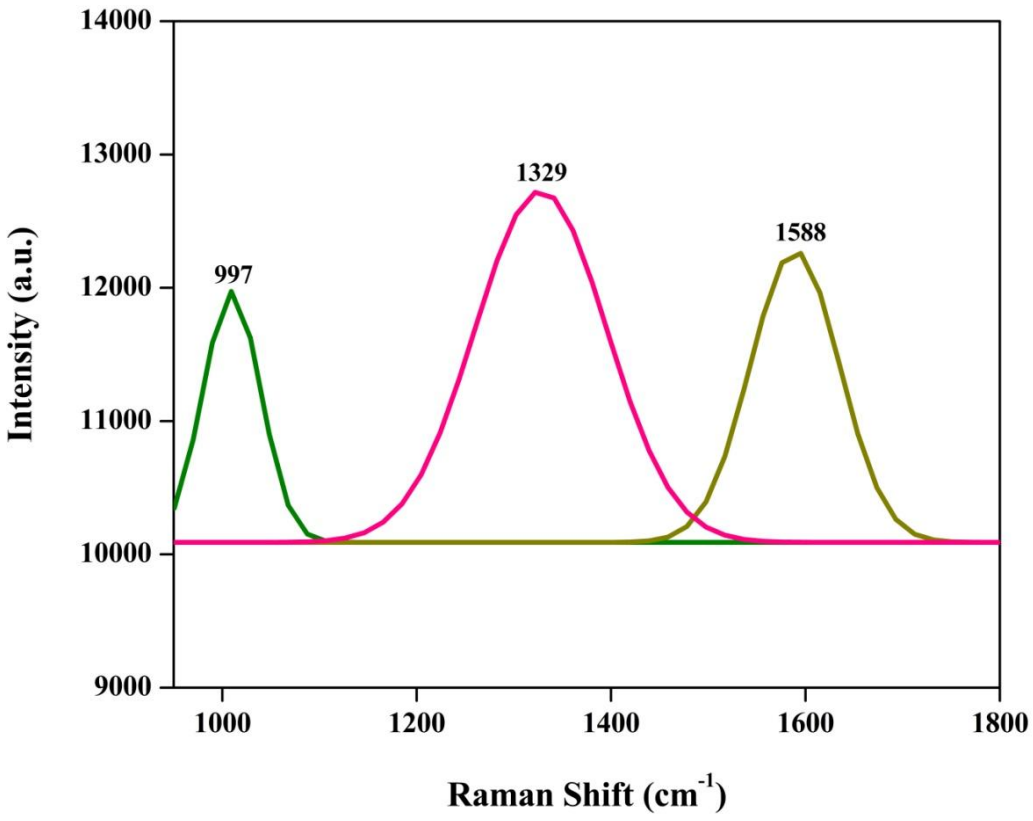

Fig. 4.27. Resonance Raman spectra of reaction mixture at 2.5 h

4.2.13. Conclusion

VOL-*f*-GO catalyst exhibits a superior catalytic activity for this transformation in assistance with ethylene glycol as a high boiling and potent hygroscopic solvent to avoid the adverse effect of water generated during reaction by the decomposition of H_2O_2. The vanadium ion in the catalyst plays a vital role as an active site and demonstrates an outstanding 99.22% conversion of styrene to SO with greater selectivity of 97.88%.

In assistance with DFT studies, we have computed the affinity of H_2O_2 to styrene and to each catalyst which illustrates the utmost affinity of H_2O_2 to VOL-*f*-GO signifying to prefer this catalyst for this transformation which is also in good accordance with experimental results. Based on binding energy computations, we have given a plausible reaction mechanism for this epoxidation of styrene explaining the formation of key products SO and BzH on cleavage of C-H and C=C bond.

The influences of distinct parameters like diverse catalysts, mole ratio of H_2O_2 to substrate, temperature, time, catalyst concentration, solvents, solvent amount and oxidant have also been examined and the results apparently implied that styrene conversion together with product distribution and selectivity are extensively affected by the reaction variables. For example, TBHP favoured the production of BzH as a key product, however, if we seek for SO as the key product then 30% H_2O_2 is to be chosen as a selective greener oxidant. Likewise, to evade the undesirable effect of generated water due to the decomposition of H_2O_2 and to avert the acid formation, ethylene glycol is preferred high boiling and potent hygroscopic product selective solvent. This catalyst recycles three times without significant loss activity and this excellent performance of the catalyst is believed to be due to the GO support and dynamic immobilization approach.

4.3. Selective epoxidation of norbornene

More or less in all kinds of chemical industries, catalytic oxidation is becoming more important as it is conducting on a large scale for the remedy of pollutants, production of energy and valuable chemicals[75]. A numerous efforts had been made in the earlier period for the oxidation reactions using stoichiometric amounts of strong reagents and oxidants. However, these chemicals are toxic, corrosive to reaction vessel, unstable at atmospheric conditions, product non-specific and produced many detrimental by-products. Purification of this product is very costly and also causing environmental pollution[76-78]. Besides these, this traditional techniques are time consuming and non-recyclable as well[79].

For the execution of green chemistry, use of the chemicals should be minimized to a level that meets the health and environmental safeties determined[80]. Bearing this in mind, for any chemical transformation, dealing with catalytic reaction might think to be green as it reduces toxic waste and production cost as well by completing a reaction in shorter period of time with little amount of catalyst[81]. A lot of research has been carried out and drawn the attention towards transition metal complex with Schiff base ligand grafted on solid support due to its inertness, non-volatility and recyclability[82,83]. H. P. Mungse et al.[84] have prepared graphene-bound oxo-vanadium Schiff base catalysts and employed for the oxidation of various alcohols to carbonyl compounds using tert-butylhydroperoxide (TBHP) as an oxidant. This catalyst is easily recoverable and reused several times. M. A. Nasseri et al.[85] have synthesized a chiral Mn(III) complex supported on modified graphene oxide by a covalent grafting method using 3-chloropropyltrimethoxysilane as a reactive surface modifier. The as-prepared catalyst was tested over the epoxidation of olefins and showed higher catalytic activity and product selectivity with 5 times reusability. S. Rayati and co-workers[86] immobilized copper(II) Schiff base complex onto reduced graphene oxide (RGO) via covalent bonding. The potential catalytic activity of RGO-CuL as heterogeneous catalyst for oxidation of alkenes was examined using H_2O_2 as a green oxidant in ethanol and reused multiple consecutive times for oxidation of cyclooctene without any significant loss of activity or selectivity. RGO-CuL was also exhibited higher TON of 47000 in the epoxidation of styrene.

Ali Allahresani[87] synthesized Ni-Schiff base complex by the reaction of nickel acetate tetrahydrate with N,N'-bis(2,4-di-hydroxybenzaldehyde)-1,2-cyclohexanediamine and supported on modified graphene oxide nano-sheets using 3-chloropropyltrimethoxysilane as a reactive surface modifier. This catalyst was used for the epoxidation of alkenes using tert-butyl hydroperoxide as an oxidant and gave excellent conversions and selectivity. This catalyst was reused five times without any significant decrease in reactivity. A. Zarnegaryan et al.[88] have prepared the Cu(II) Schiff base complex immobilized onto graphene oxide and used for the epoxidation of various alkenes using *tert*-butyl hydroperoxide as an oxidant. The main advantage of this catalytic system is that it shows high yields, excellent selectivity and reusability.

Form the ancient time, strong stoichiometric oxidants such as chromium (IV) reagents, permanganates, tert-butyl hydroperoxide (TBHP), selenium oxide (SeO_2), ruthenium (VIII) oxide, hydrogen peroxide, nitric acid, and oxygen are being used for the oxidation reactions[89-91]. Amongst them, H_2O_2 is becoming increasingly a choice of oxidant due to enhancing the removal of organic matter. Epoxidation of alkenes is one of the most vital chemical transformations in organic synthesis since these compounds are the useful intermediates for the fabrication of wide variety of valuable compounds[92,93]. Epoxides are the potent class of intermediates for the synthesis of various oxygenated industrial chemicals both in industries and academia. Herein, this sub-chapter involves the epoxidation of norbornene over $M(L)_n$-*f*-GO ($M = Cu^{2+}$, Co^{2+} and VO^{4+}) using 30% H_2O_2 as an oxidant.

The catalytic epoxidation of norbornene over the transition metal grafted via ligand spacer onto the GO support as heterogeneous catalysts is carried out in a 50 mL two-necked round-bottom-flask equipped with a water condenser in an oil bath with a magnetic stirrer. To obtain the best-suited catalyst for the epoxidation of norbornene, a typical reaction is carried out using 10 mg of catalyst in acetonitrile as a solvent and 30% H_2O_2 as an oxidant at 80°C for 3 h. The influence of the various parameters, for instance, mole ratio of substrate to oxidant, temperature, oxidants, catalytic amount, solvent, solvent amount and time are also inspected in order to acquire the optimized reaction condition.

Typically, reaction flask is feed with 10 mmol of norbornene, 10 mmol of 30% H_2O_2, 5 mL of acetonitrile as a solvent and 10 mg of catalyst, such as, graphite, GO, A-*f*-GO and $M(L)_n$-*f*-GO and equilibrated at 80 °C for 3 h. As a result of heterogeneous epoxidation of nornornene, in addition to the formation of 2,3-epoxy norbornane as a major product along with exo/endo norborneols with 2-norbornanone as by-products are also identified in little amount.

4.3.1. Impact of catalysts

We have incorporated selectivity of norbornene epoxide with % conversion to make the absolute comparison between diverse catalysts more propitious (Table 4.5). The result divulges that under the identical conditions, enormously little or no conversion is obtain with pristine graphite (1.55%), GO (3.67%) and A-*f*-GO (4.30%). On employing CoL-*f*-GO and CuL-*f*-GO ~7% conversion of norbornene is obtained and such conversion does not hold sense in academia and industry both. As is observed, VOL-*f*-GO is able to offer 29.08% conversion of norbornene with 39.58% epoxide selectivity. However, lower selectivity can be increased with conversion through an appropriate modus operandi at hand. Our main centre of interest is on the materialistic products (epoxide) that should be commercially acquisitive and hence, we have preferred VOL-*f*-GO as the representative catalyst for further investigation of the influence of other experimental variables.

Table 4.5

Impact of varying catalysts on epoxidation of norbornene.

Systems	Norbornene conversion (%)	Epoxide Selectivity (%)	Other Selectivity (%)	TOF[a] (h^{-1})
Graphite	1.55	-	-	-
GO	3.67	-	-	-
A-*f*-GO	4.30	-	-	-
CoL-*f*-GO	6.89	-	-	30.37
CuL-*f*-GO	7.50	-	-	14.80
VOL-*f*-GO	29.08	39.58	60.42	21.46

Reaction condition: norbornene (10 mmol), 30% H_2O_2 (10 mmol), catalyst (10 mg), 80 °C, acetonitrile (5 mL), 3 h.

[a]TOF: Moles of norbornene converted per mole of metal per hour.

4.3.2. Impact of mole ratio

Another important aspect comprises the authentic experimental results rather than theoretical and conceptional hypothesis for this oxidation reaction is mole ratio of norbornene to H_2O_2. Data of this experiment is depicted in Fig. 4.28. Norbornene conversion exhibits the trend of descending order with ascending order of H_2O_2. After experiencing the result of 1:1 mole ratio, we have employed 1:1.5 mole ratio to this transformation and we get 9.68% norbornene conversion with 49.69% epoxide selectivity. On further increasing the mole ratio to 1:2, norbornene conversion again decrease to 9.11%, however, highest mole ratio (1:2.5) offers 22.75% norbornene conversion with 38.59% epoxide selectivity. If we look for the product selectivity, it is found to be greatly affected with changing the mole ratio of H_2O_2. The key product epoxy norbornane initially increases and achieves highest with 1:2 mole ratio. On further increasing the mole ratio, it experiences drastic decline. This is believed to be due to over oxidation. Conversely, with highest selectivity at 1:2 mole ratio, the conversion is lessened almost thrice and it is not wise to choose the mole ratio only for higher selectivity at the cost of conversion. Therefore, we have chosen 1:1 mole ratio for further investigation.

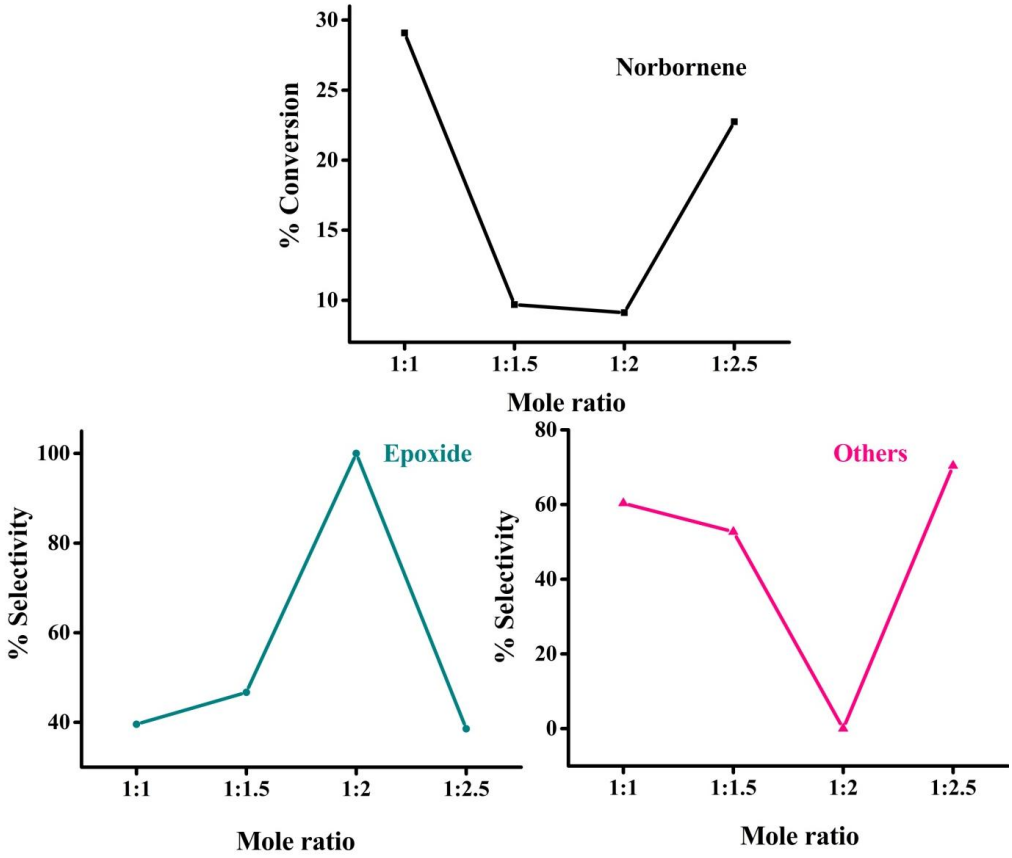

Fig. 4.28. Impact of varying mole ratio on the epoxidation of norbornene. Reaction condition: norbornene (10 mmol), 30% H_2O_2 (mmol), VOL-*f*-GO (10 mg), 80 °C, acetonitrile (5 mL), 3 h.

4.3.3. Impact of amount of catalyst

Three different concentrations viz. 10, 20 and 30 mg of representative catalyst is inspected for the epoxidation of norbornene over 30% H_2O_2 as an oxidant using acetonitrile as a solvent. The result of the reaction is depicted in Fig. 4.29. Higher norbornene conversion (29.08%) is observed at lower concentration of catalyst (10 mg) with 39.58% epoxide selectivity and opposite to this, higher concentration shows a conflicting trend. With 20 and 30 mg catalyst amount, 17.44% and 12.79% norbornene conversion with 100% and 33.82% epoxide selectivity, respectively is observed. This anomalous behaviour of higher norbornene conversion at lower concentration is believed to be due to much faster decomposition of H_2O_2 at higher concentration of the catalyst and residual amount of H_2O_2 is not sufficient for higher norbornene conversion. Epoxidation starts to happen as soon as H_2O_2 decomposes and hence rate of decomposition of H_2O_2 affects the product

distribution and selectivity as well. As we achieve higher norbornene conversion with superior product selectivity with 10 mg of catalyst, we have chosen this amount as preferred catalyst concentration.

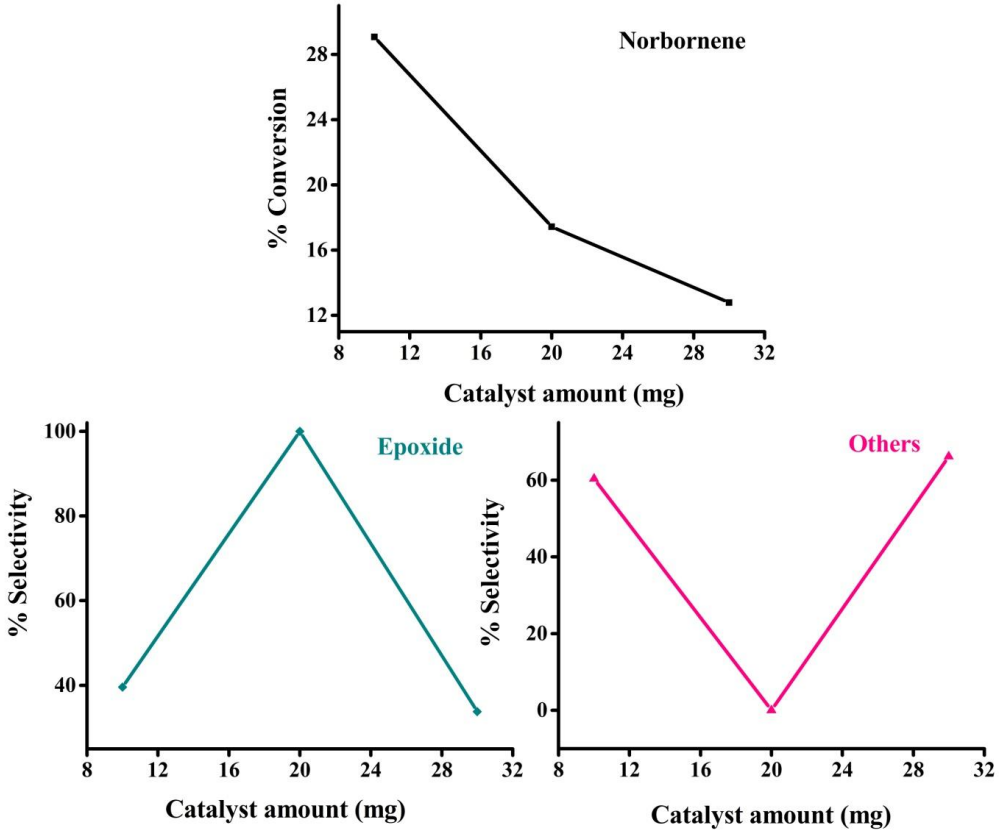

Fig. 4.29. Impact of amount of catalyst on the epoxidation of norbornene. Reaction condition: norbornene (10 mmol), 30% H_2O_2 (10 mmol), VOL-*f*-GO (mg), 80 °C, acetonitrile (5 mL), 3 h.

4.3.4. Impact of solvent

Solvent properties like polarity, dielectric constant, basicity and protocity strongly affect the catalytic process, therefore determining the correct solvent for a catalytic reaction, is very crucial[94]. Hence, we have conducted the experiment to examine the effect of various solvents, i.e., toluene, DMF, acetonitrile, 1,4-dioxane, methanol and ethylene glycol on the epoxidation of norbornene (Fig. 4.30). This study is intended to reduce the by-product and to enhance the key product formation. With toluene and DMF no conversion is observed, however, acetonitrile exhibited 29.08% conversion

with 39.58% selectivity of epoxide. While using 1,4-dioxane, healthy rise in the conversion is seen i.e. 97.45%, however, the selectivity for epoxide is found to be very petite (26.22%). Herein, conversion obtain with 1,4-dioxane is rather satisfactory but the aim of the study is absolute utilization of substrate molecule with higher selectivity of solely key product. Hence, in order to increase % selectivity of key product, we thought of moving the reaction exercising methanol as a solvent. Methanol is being proved as a good solvent in achieving almost comparable conversion (97.92%) to 1,4-dioxane, it is nevertheless eventuated in the lesser selectivity (1.22%) of key product. Reaction is then performed with ethylene glycol and due to its high dielectric constant; higher selectivity of key product is achieved (96.51%) with 97.17% conversion of norbornene. Consequently, ethylene glycol is chosen as the preferred solvent for further investigation.

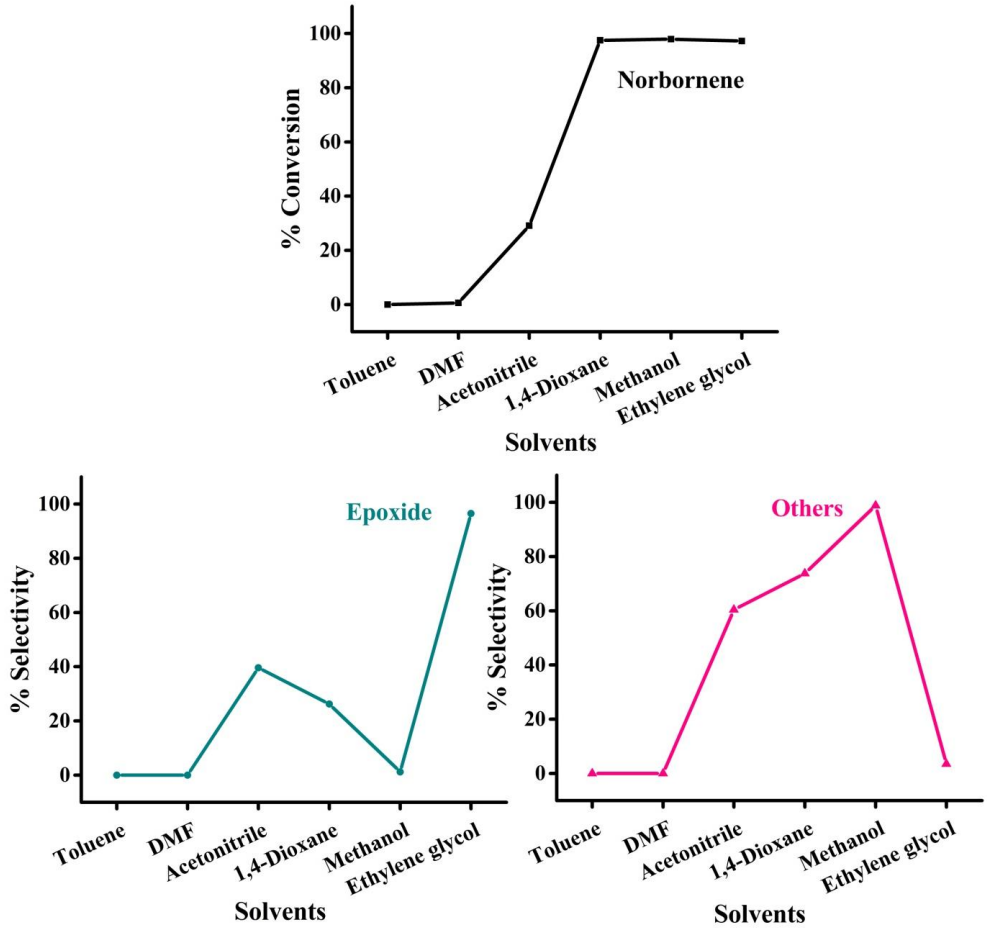

Fig. 4.30. Impact of varying solvents on the epoxidation of norbornene. Reaction condition: norbornene (10 mmol), 30% H_2O_2 (10 mmol), VOL-*f*-GO (10 mg), 80 °C, solvent (5 mL), 3 h.

4.3.5. Impact of solvent amount

After succeeding in achieving the desire outcome on employing ethylene glycol as a solvent, it is further decided to explore the effect of one more parameter, amount of solvent, on the epoxidation of norbornene. Vindicating our expectations, solvent amount markedly demonstrated a vital effect on the conversion. It is perceptible from Fig. 4.31 that 2 mL solvent amount is found to be inapt in achieving the desire conversion and selectivity of key product. It gives 3.1% norbornene conversion. It might be due to inadequate quantity of the solvent to dissolve the substance completely. However, further increase the amount of solvent, 5 mL is found to be ideal for this transformation as it provides the higher conversion of norbornene (97.2%) with the desire product selectivity of 96.51%. On exploration of the influence of further rise in the solvent amount to 10 mL, the result obtain is identical (0.94%) with the result obtained with 2 mL of solvent amount. This observed downward move in the conversion and selectivity of the key product is might be due to the exceed amount of solvent dilutes the reaction mixture to a large extent. Hence, for this epoxidation reaction, 5 mL is chosen as a preferred amount of the solvent.

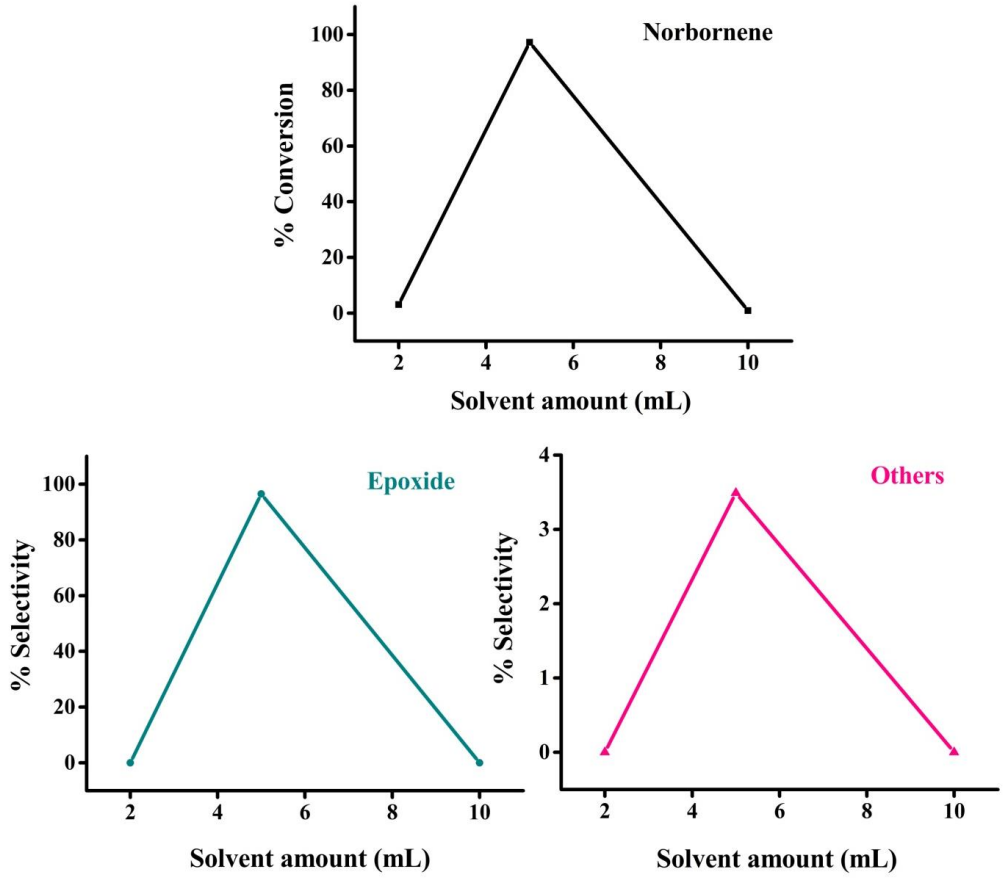

Fig. 4.31. Impact of varying solvent amount on the epoxidation of norbornene. Reaction condition: norbornene (10 mmol), 30% H_2O_2 (10 mmol), VOL-*f*-GO (10 mg), 80 °C, ethylene glycol (mL), 3 h.

4.3.6. Impact of time

As chemical reactions are governed by the time and exceeding of this factor may lead to problems, it is quite important to determine the correct time for any chemical transformation. Consequently, with the intent to decide the right time for this epoxidation reaction, we have conducted this experiment at three different time viz. 0.5, 1 and 2 h by keeping other parameters fixed. The conversion of norbornene as a function of time is depicted in Fig. 4.32. It can be seen from the figure that initially at 0.5 h, 70% norbornene conversion is achieved with epoxide selectivity of 18.54%. However, on continuing the reaction with time, conversion also upholds the increasing trend and achieved maximum (97.17%) at 1 h with the epoxide selectivity of 96.51%. If the reaction still continued to 2 h, utmost conversion of 100% is achieved but the selectivity of key product showed a slight reduction (95.31%) along with little

rise in the selectivity of by-products (4.69%) compared to 1 h. As a result, we have chosen 1 h as the preferred time for further investigation of other experimental variables.

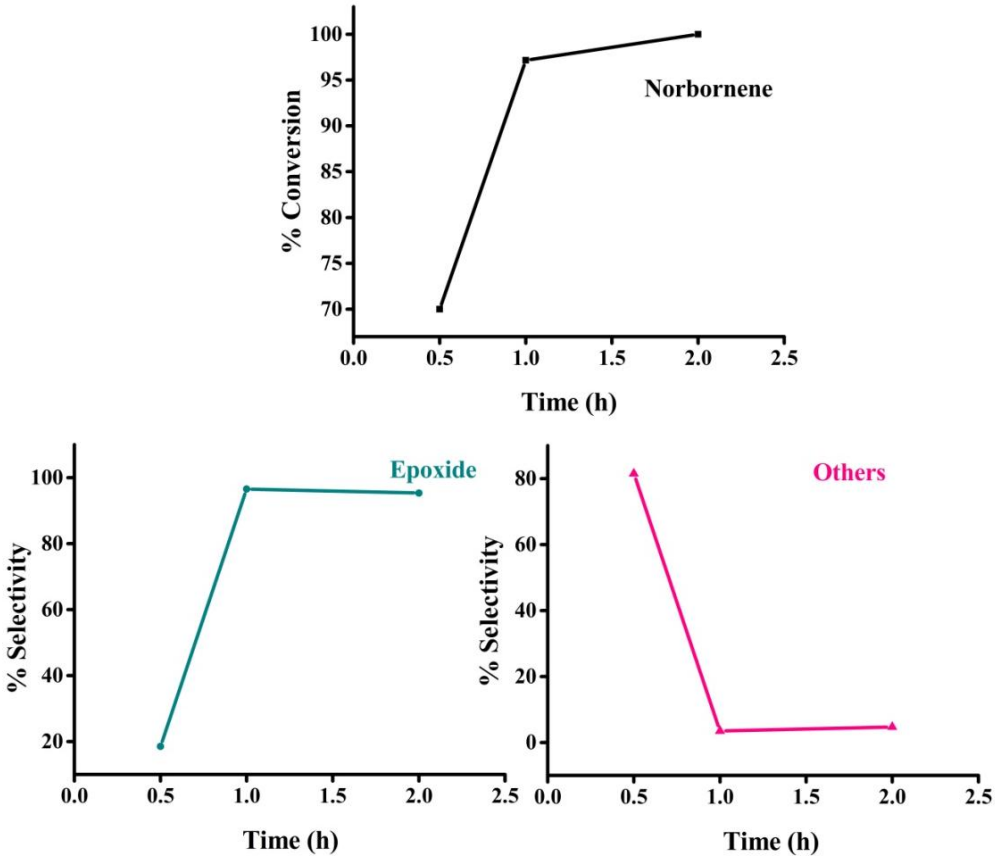

Fig. 4.32. Impact of varying time on the epoxidation of norbornene.
Reaction condition: norbornene (10 mmol), 30% H_2O_2 (10 mmol), VOL-*f*-GO (10 mg), 80 °C, ethylene glycol (5 mL), time (h).

4.3.7. Impact of oxidant

For the purpose that at least one of principles of green chemistry may be justified, it is decided to inspect this transformation using 70% TBHP as an oxidant besides 30% H_2O_2 and the data obtained from this study is screened in Fig. 4.33. It has been observed form the figure that conversion of norbornene increases linearly with TBHP and the maximum conversion achieved is 93.4% which is lower than the results achieved with H_2O_2 (97.17%). Product distribution along with selectivity of the key product is also affected. Higher epoxide selectivity (96.51%) is obtained with H_2O_2 while TBHP shows

93.13%. However, contrast to this, the ratio of by-product formation is higher 6.73% in TBHP while in H_2O_2 it limits to 3.49%. Hence, reverse trend in the selectivity of key product and by-product is seen and the propensity to epoxide and by-product has been switched over in TBHP. Therefore, we have chosen 30% H_2O_2 as an oxidant.

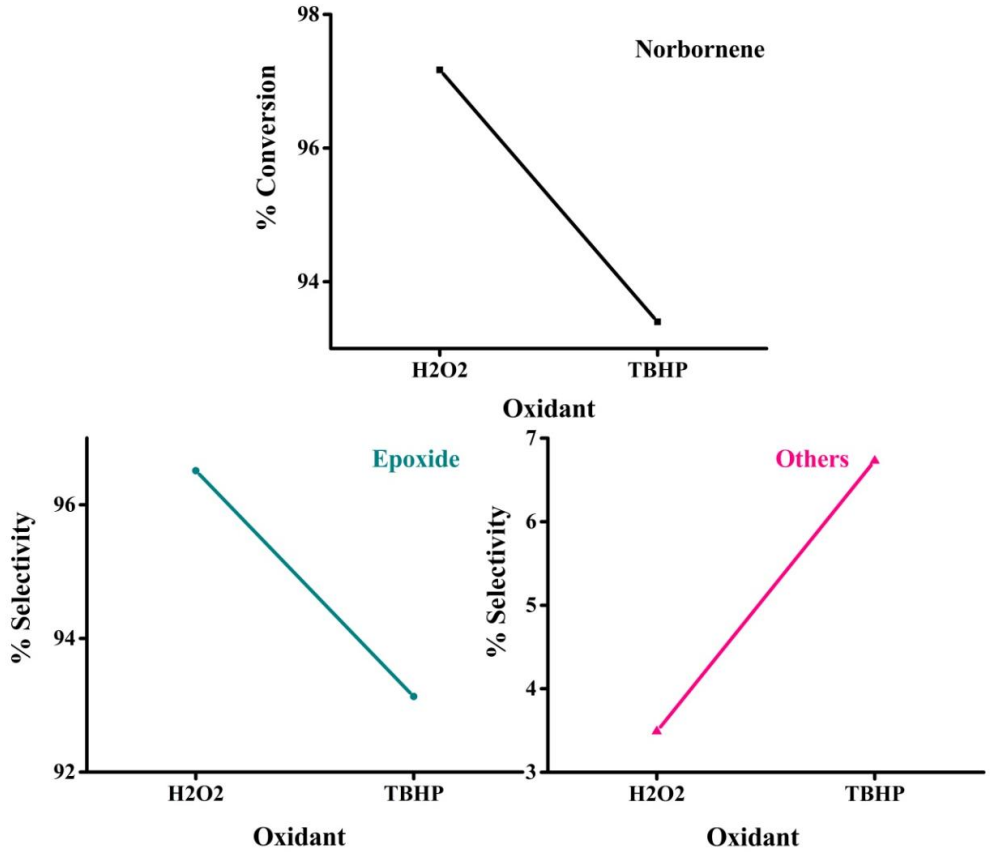

Fig. 4.33. Impact of oxidant on the epoxidation of norbornene.
Reaction condition: norbornene (10 mmol), oxidant (10 mmol), VOL-*f*-GO (10 mg), 80 °C, ethylene glycol (5 mL), 1h.

4.3.8. Impact of temperature

Effect of three different reaction temperatures such as 50, 60 and 70 °C on the epoxidation of norbornene is demonstrated in Fig. 4.34. It is visible from the figure that negligible (0.5%) conversion of norbornene is achieved at 50 °C. When temperature rises to 60 °C, maximum conversion of 97.17% of norbornene is monitored together with 96.51% epoxide selectivity. Moreover, on further increasing the temperature up to 70 °C, conversion drop downed to 8.15%. Subsequently, 60 °C is chosen as representative temperature.

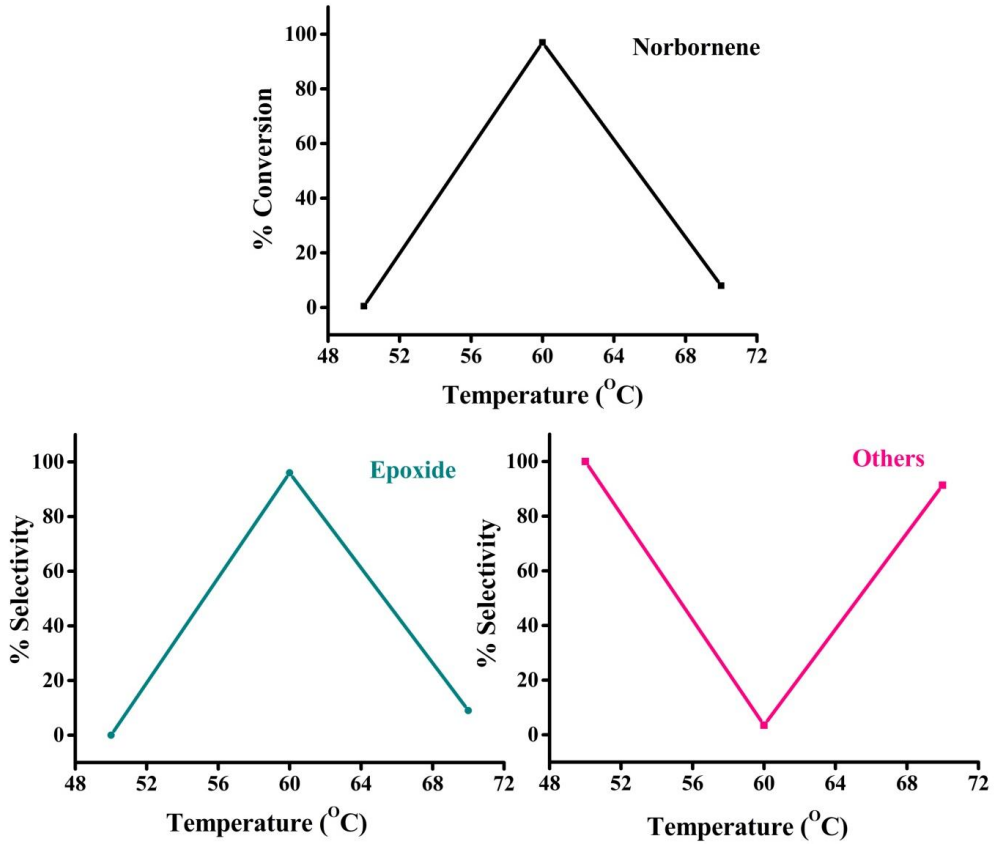

Fig. 4.34. Impact of varying temperature on the epoxidation of norbornene. Reaction condition: norbornene (10 mmol), 30% H_2O_2 (10 mmol), VOL-*f*-GO (10 mg), temperature (°C), ethylene glycol (5 mL), 1h.

4.3.9. Recyclability test

To examine the recyclability of the as-prepared heterogeneous catalyst for this transformation, the catalyst is recovered by filtration from the reaction mixture and washed with solvent followed by oven drying prior to employing for further catalytic test.The reaction mixture of each catalytic experiment has been analyzed by GC under the same condition as used for the previous catalytic tests. The results of each recycle test are represented in Fig. 4.35 and it is evidently seen that catalyst give its best performance up to three cycles with no significant loss of activity. The conversion in first to 3rd recycle is 96.89%, 94.35%, 91.51% and selectivity is of epoxide 95.12%, 93.01% and 90.79%, respectively.

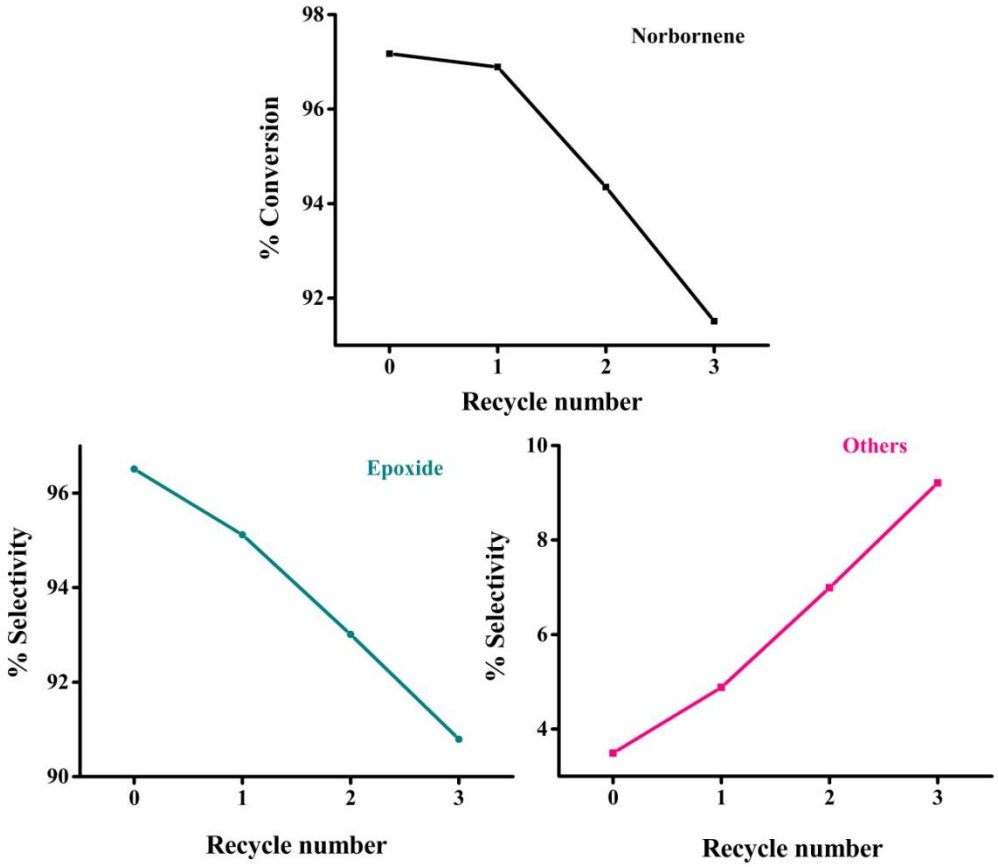

Fig. 4.35. Recyclability test on the epoxidation of norbornene.
Reaction condition: norbornene (10 mmol), 30% H_2O_2 (10 mmol), VOL-*f*-GO (10 mg), 60 °C, ethylene glycol (5 mL), 1h.

4.3.10. Conclusion

In the oxidation of norbornene VOL-*f*-GO exhibits a superior catalytic activity with 97.17% of norbornene conversion and 96.51% epoxide selectivity using 30% H_2O_2 as an oxidant and ethylene glycol as a solvent which is being helpful to selectively oxidized the norbornene to its epoxide product owing to its high dielectric constant. It is also clear from the discussion so far that the selectivity of the products depends on the solvent and temperature used for reaction conditions. The influences of distinct parameters like diverse catalysts, mole ratio, temperature, time, catalyst concentration, solvents, solvent amount and oxidant have also been inspected and the results strongly suggest that norbornene conversion along with product distribution and selectivity is broadly affected by the reaction variables. This catalyst is recycled three times without significant loss activity.

4.4. Selective oxidation of glucose

The conversion of biomass is ignious and sustainable modus operandi for the green manufacture of commercial organic compounds[95-97]. Glucose is one of the plentiful and renewable raw materials for the production of platform chemicals[99-102]. However, there is a main disadvantage of using glucose is presence of various functional groups which lowers the selectivity[103-105]. Hence, during the oxidation of glucose various acids along with keto acids are typically seen[106]. Conventional methods for glucose oxidation involve harsh conditions, for instance, high temperature, strong acids and toxic promoters[106,107]. It increases the use of biochemical processes for the production of glucose, but it was also laborious from separation of product, waste removal, formation of by-products and low yield[108].

Hence, there is a need to develop an alternative route for the oxidation of glucose. In recent years, metal based catalytic systems have been developed, however, monometallic catalysts did not provide adequate due to lower activities and sensitivities[109-115]. In order to improve the selectivity of the oxidative products, bi-metallic catalysts were also employed for this transformation[116-124]. However, owing to high-priced, sustainability, reusability and selectivity reason, highly active heterogeneous catalysts have been developed in recent years. M. Wenkin et al.[125] have prepared Bi-promoted Pd/C catalyst by deposition and used for the selective oxidation of glucose to gluconic acid by O_2. They studied the effect of Bi leaching on the catalyst lifetime as significant amount of Bi was leached during the reaction. Y. Cao et al.[126] have prepared Au/TiO_2 catalysts by different methods and explore its effect on the base-free aqueous phase oxidation of glucose to gluconic acid. They found that their sol-immobilization method was more favourable in achieving high catalytic activity. After examining, they came to the conclusion that Au particle size and pre-treatment of catalysts has a considerable influence on the catalytic activity.

Gluconic acid produced, has wide applications in various fields such as food industry, flavouring agent, reducing fat absorbent in doughnuts[127]. It is also key element in the production of various chemicals and pharmaceutical industries and cosmetics[106, 127,128]. Owing to significant wide applications, industrial production of gluconic acid involves the bio-catalysts[129]. However,

the use of these enzymes is restricted by these labile natural catalysts, for instance, pH, O_2 pressure and recovery of the catalyst[105]. Hence, an alternative route for the green synthesis, the use of H_2O_2 together with supported metal heterogeneous catalysts has attracted tremendous attention. This H_2O_2 decomposes into water during the oxidation reaction and this water is the serve as a basis for both –OH group of carboxylic acid and the proton, an origin of the molecular hydrogen[105]. A vital role of the water in the conversion of alcohols and aldehydes to carboxylic acids is narrated in the literature[130-138].

In this sub-chapter, as-fabricated heterogeneous catalysts have been employed for the selective oxidation of glucose to gluconic acid using H_2O_2 as a greener oxidant and we have also probed the effect of water as an environment friendly solvent in this transformation. The catalytic oxidation of glucose over the as-synthesized catalysts is carried out in a 50 mL two-necked round-bottom-flask furnished with water condenser in an oil bath with a magnetic stirrer. In a standard reaction condition to find out the best-suited catalyst for the oxidation of glucose, a typical reaction is carried out with arbitrary catalyst concentration (10 mg), temperature (80°C), ethylene glycol as a solvent and 30% H_2O_2 as an oxidant for 3 h. Various reaction parameters such as impact of the varying mole ratio of substrate to oxidant, temperature, oxidant, amount of catalyst, solvent, solvent amount and time are inspected to acquire the optimized reaction condition.

First, the catalyst was dispersed in ethylene glycol and stirred for 10 min. followed by the addition of substrate molecule and allows stirring again for 10 min. In the next step, drop-wise addition of oxidant was executed. This final reaction mixture is then stirred for an experimentally pre-decided time to achieve the maximum conversion and selectivity. Formation of the product was analyzed by GC analysis of aliquots of the reaction mixture drawn at diverse time intervals.

For the pilot reaction, 6 mmol of glucose, 6 mmol of 30% H_2O_2, 5 mL ethylene glycol and 10 mg of catalyst (graphite, GO, A-*f*-GO, CuL-*f*-GO, CoL-*f*-GO and VOL-*f*-GO) is feed to a reaction container and equilibrated at 80 °C for 3 h. As a result of heterogeneous oxidation, gluconic acid (GA) is found to be the main product.

4.4.1. Impact of catalysts

The assessment of effects of assorted heterogeneous catalysts on the glucose conversion and product selectivity are tabulated in Table 4.6. As can be seen, little or no conversion is achieved with pristine graphite (0.3%), GO (0.4%) and A-*f*-GO (0.34%). However, almost comparable conversion is observed with CoL-*f*-GO, VOL-*f*-GO and CuL-*f*-GO. Co-*f*-GO offers 93.8% conversion with 100% selectivity, VO-*f*-GO gives 96.0% conversion with 100% selectivity and Cu-*f*-GO exhibited 97.0% conversion of glucose with 100% selectivity of GA. Higher conversion of glucose is observed with Cu-*f*-GO, hence, we have chosen it as preferred catalyst for the optimization of other reaction parameters.

Table 4.6

Impact of varying catalysts on the oxidation of glucose.

Systems	Glucose Conversion (%)	GA Selectivity (%)	Others Selectivity (%)	TOF[a] (h^{-1})
Graphite	0.3	0	0	-
GO	0.4	0	0	-
A-*f*-GO	0.34	0	0	-
CoL-*f*-GO	93.8	100	0	248.11
VOL-*f*-GO	96.01	100	0	42.51
CuL-*f*-GO	97.10	100	0	114.83

Reaction condition: glucose (6 mmol), 30% H_2O_2 (6 mmol), catalyst (10 mg), 80 °C, ethylene glycol (5 mL), 3 h.

[a]TOF: Moles of glucose converted per mole of metal per hour.

4.4.2. Impact of mole ratio

Varying mole ratios of a substrate to the oxidant such as 1:1, 1:1.5, 1:2, 1:2.5 are employed to examine their effect on the oxidation of glucose with keeping all other parameters fixed. A key role of H_2O_2 is clearly noticeable from Fig. 4.36. Highest conversion of glucose of 98.12% and 99.68% selectivity of GA is obtained with 1:1 mole ratio, while on further increasing

mole ratio reverse trend is observed. 1.5 moles of H_2O_2 convert 97.59% glucose with 99.47% GA selectivity, however, higher concentration of oxidant has resulted in decrease of conversion to 97.45% along with 97.78% GA selectivity. Higher ratio of glucose to H_2O_2 (1:2.5) has resulted in further lowering of conversion of glucose to 96.47% with 100% selectivity of GA. Conflicting trend is seen in the conversion and selectivity with increasing mole ratio of glucose to H_2O_2, however, rise in selectivity is negligible (0.32%); while significant decrease in conversion is noticed that is 1.65%. Hence, 1:1 is chosen as preferred mole ratio for the investigations.

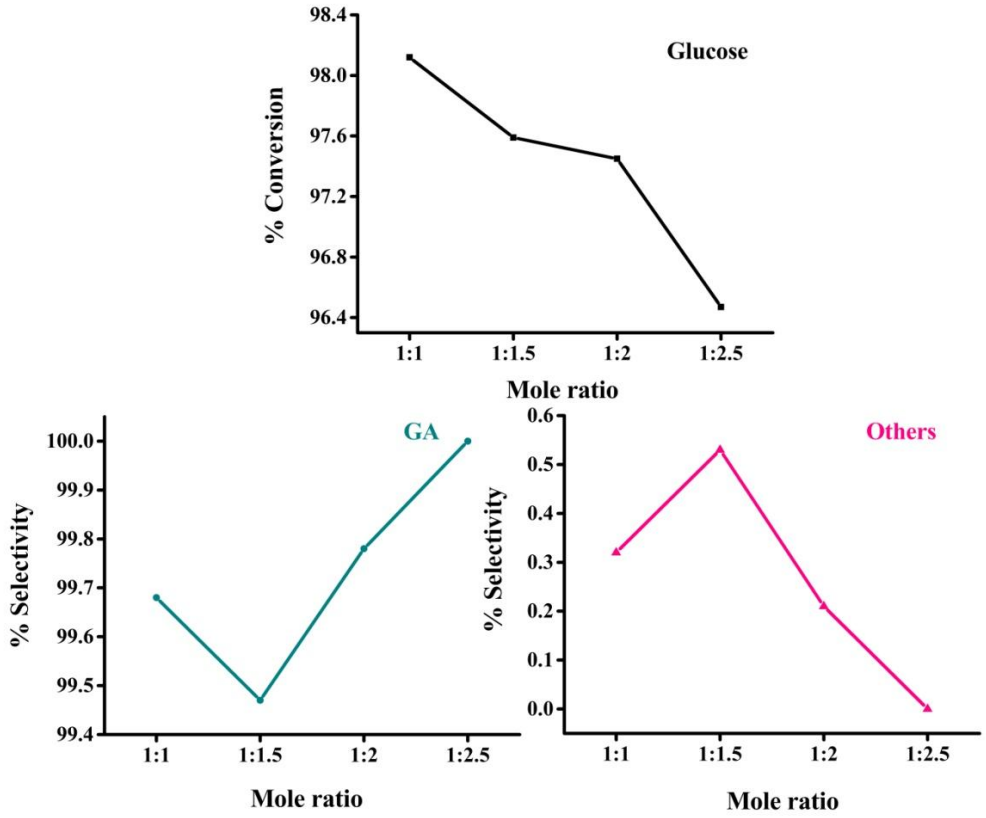

Fig. 4.36. Impact of varying mole ratio on the oxidation of glucose.
Reaction condition: glucose (6 mmol), 30% H_2O_2 (mmol), CuL-*f*-GO (10 mg), 80 °C, ethylene glycol (5 mL), 3 h.

4.4.3. Impact of time

To obtain the precise yield with high selectivity, it is of quite important to terminate the reaction at correct time. This study is aiming to determine the correct time for this heterogeneous oxidation of glucose. For this intend, we

have implemented three different time, for instance, 1, 2 and 3 h (Fig. 4.37). In 1 h, 99.3% conversion of glucose is achieved with 100% selectivity of GA. However, if we continue the reaction for 2 h, conversion is seen to be decreased (98.37%) with identical selectivity. At this point higher conversion obtained is with 1 h and it shows the decreasing propensity with time. To confirm this down trend nature of the reaction with time, the reaction mixture is analyzed at 3 h and the similar trend is found. After 3 h, conversion and selectivity both falls to 98.12% and 99.68%, respectively. The probable reason for this reduction in conversion with time may be due to reversible nature of the reaction. For this reason, we have decided to set the reaction time 1 h for further exploration of other parameters.

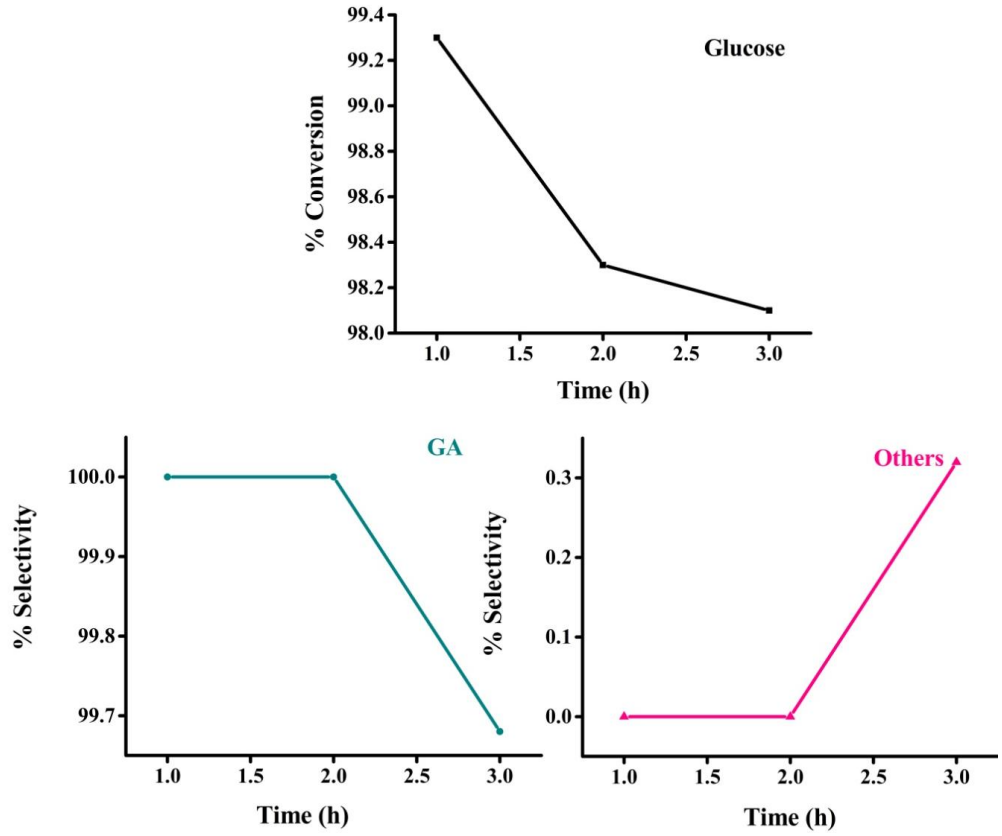

Fig. 4.37. Impact of varying time on the oxidation of glucose.

Reaction condition: glucose (6 mmol), 30% H_2O_2 (6 mmol), CuL-*f*-GO (10 mg), 80 °C, ethylene glycol (5 mL), time (h).

4.4.4. Impact of solvent

As it is well known that solvent may have an effect on the conversion, stability and selectivity of the desired product[94], this study is aimed to examine the practicality of solvent effect on the oxidation of glucose. As glucose is soluble in water, N,N- dimethylformamide (DMF) and ethylene glycol, these solvents are chosen to inspect their effect on the glucose conversion and the selectivity of GA. As shown in Fig. 4.38, DMF offers very petite conversion of glucose (0.17%); while with water 87.16% conversion of glucose and 47.37% selectivity of GA is observed. In order to further increase the conversion, ethylene glycol is studied for this transformation. It is proved to be a model solvent for this transformation by giving 99.30% conversion of glucose with 100% selectivity of GA. As a result, ethylene glycol is chosen as the preferred solvent for this transformation.

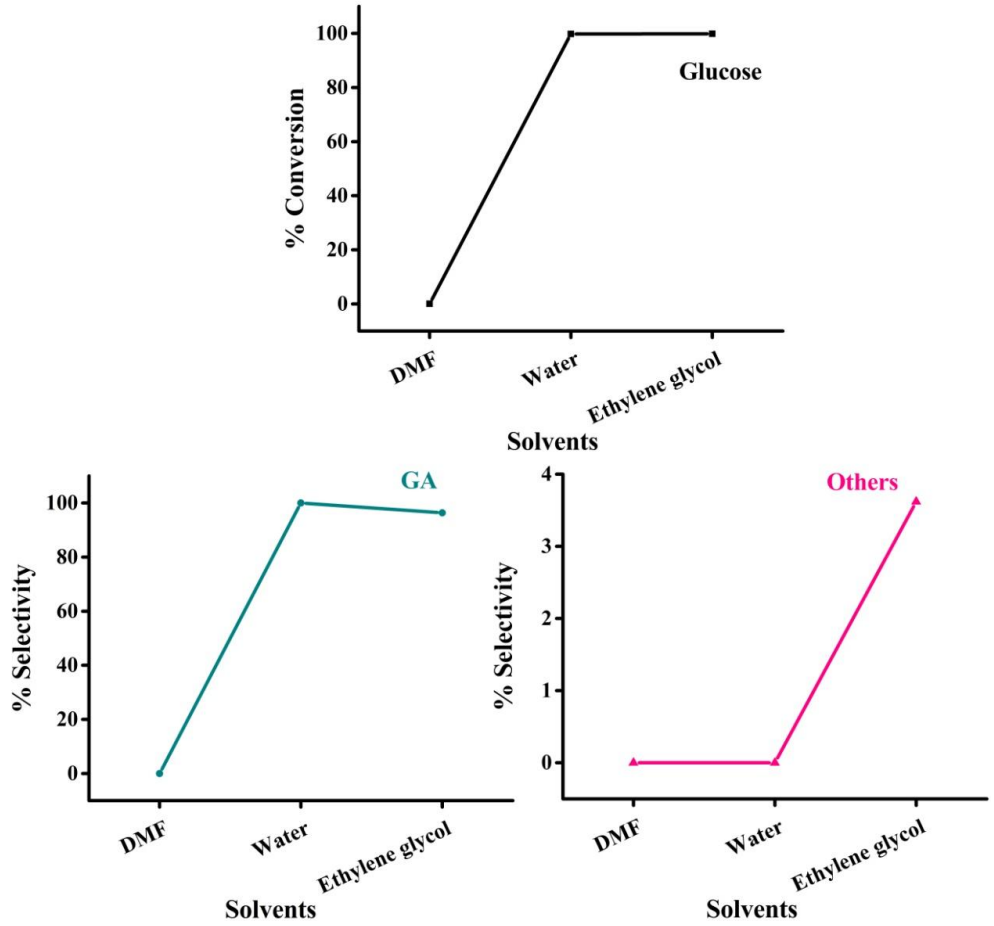

Fig. 4.38. Impact of varying solvents on the oxidation of glucose.
Reaction condition: glucose (6 mmol), 30% H_2O_2 (6 mmol), CuL-*f*-GO (10 mg), 80 °C, solvent (5 mL), 1 h.

4.4.5. Impact of solvent amount

Diverse solvent amount like 2, 5 and 10 mL is taken to examine its effect on the conversion of glucose and selectivity of GA. As can be seen from Fig. 4.39, petite conversion of glucose is observed with 2 mL quantity of solvent with sole product formation GA. This may be explaining as lower amount of solvent is not sufficient to dissolve the reaction mixture. However, dissolving the reactant in 5 mL of solvent proved to be an adequate amount providing 99.30% conversion of glucose and 100% selectivity of GA. On further increasing the solvent amount to 10 mL, absolute conversion is observed, but selectivity experiences reverse trend (97.94%). One can conquer, no significant conversion is observed with higher solvent amount but decrease in selectivity (2.06%) is noteworthy. Therefore, we have chosen 5 mL as the preferred solvent amount for further optimization of reaction parameters.

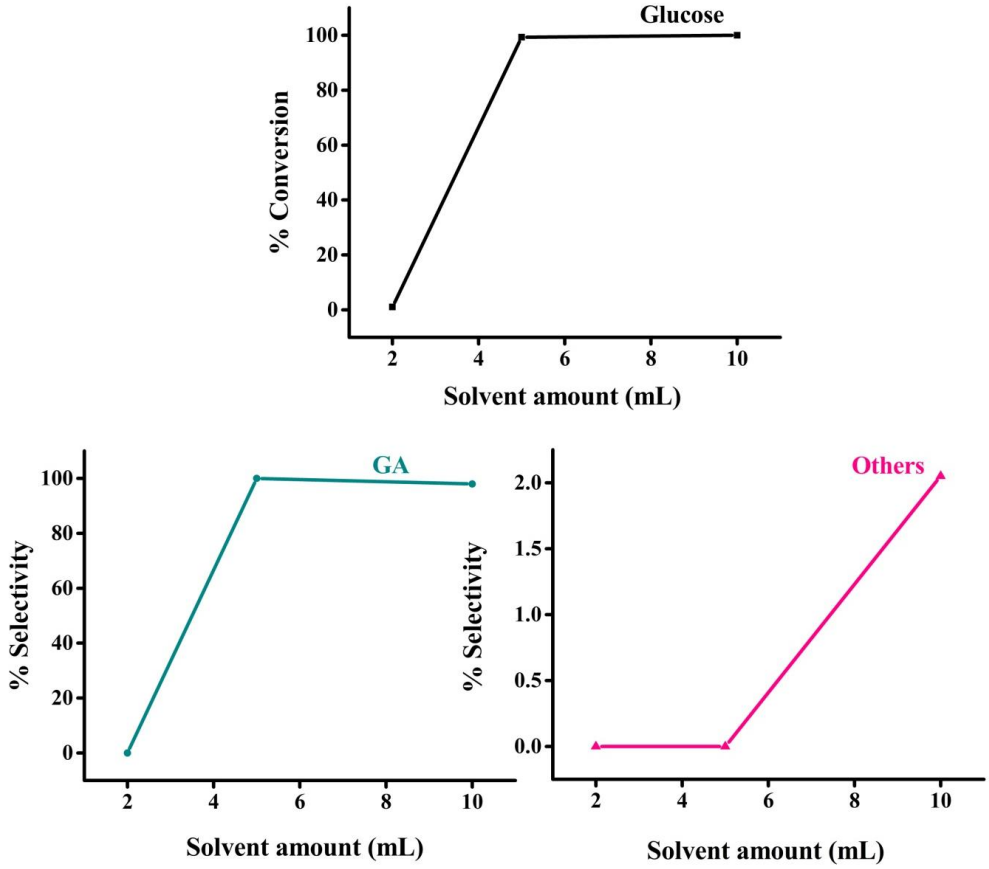

Fig. 4.39. Impact of varying solvent amount on the oxidation of glucose. Reaction condition: glucose (6 mmol), 30% H_2O_2 (6 mmol), CuL-*f*-GO (10 mg), 80 °C, ethylene glycol (mL), 1 h.

4.4.6. Impact of oxidant

In addition to 30% H_2O_2, another oxidant 70% TBHP is used to explore the effect of other oxidant on this transformation under an experimentally obtained reaction parameters. The results of this analysis are depicted in Fig. 4.40. The data reveals that TBHP is not suitable for this transformation. Looking forward to figures, 98.69% conversion is achieved with TBHP; while with 30% H_2O_2, 99.3% conversion is obtained. However, selectivity found to be similar in both the cases. If we consider this difference in conversion to be small or insignificant, we cannot ignore the other benefits of 30% H_2O_2 over TBHP. It is quite economical, easy handling, more resourceful and greener oxidant as yielded only water as the by-product. Subsequently, 30% H_2O_2 is chosen as preferred oxidant for further the catalytic investigation.

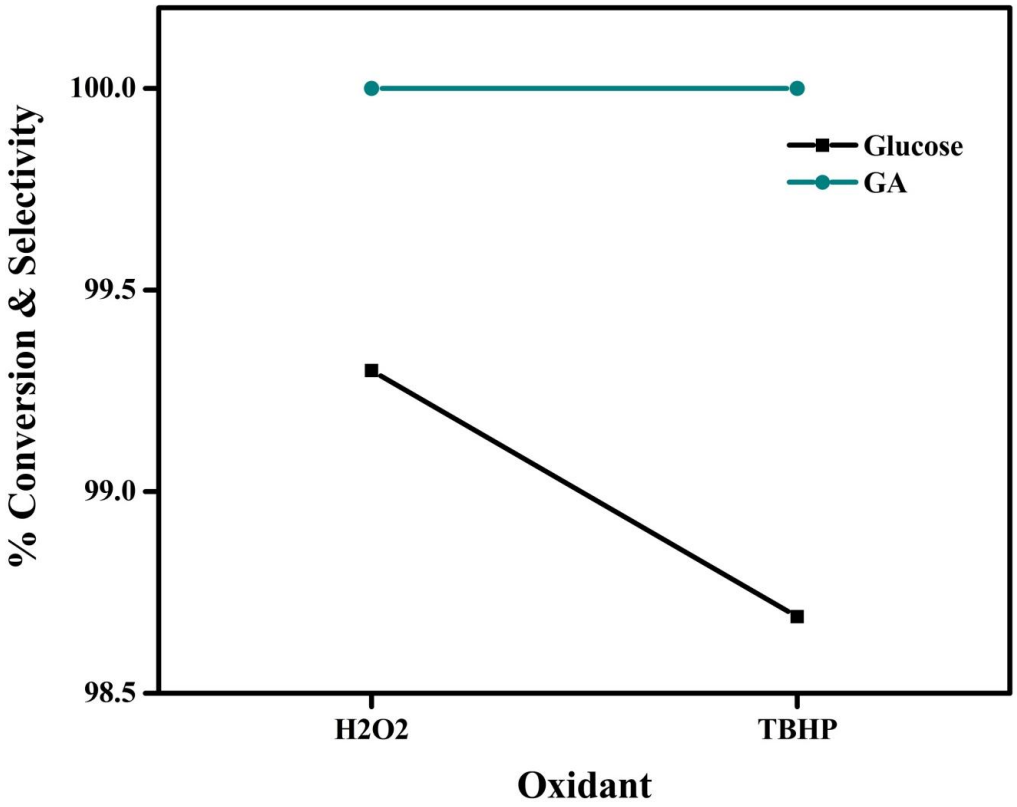

Fig. 4.40. Impact of oxidant on the oxidation of glucose.

Reaction condition: glucose (6 mmol), oxidant (6 mmol), CuL-*f*-GO (10 mg), 80 °C, ethylene glycol (5 mL), 1 h.

4.4.7. Impact of amount of catalyst

In this selective oxidation of glucose, we have also studied the effect of three different amounts of catalyst i.e. 10, 20 and 30 mg (Fig. 4.41). After achieving 98.12% conversion of glucose and 99.68% GA selectivity with 10 mg catalyst, the amount of catalyst is increased to 20 mg. It is clearly visible from the figure that this alteration shows positive results; conversion is seen to be increased to 98.51% with sole product GA. Here, conversion is found to be increased with increase in catalyst amount, but the augmentation is not as per hope. Hence, in order to obtain absolute conversion, we have further increase the catalyst amount to 30 mg and conversion shows an increase as expected. Highest glucose conversion of 99.24% with 100% GA selectivity is achieved with 30 mg of catalyst. The reason for this increasing trend may given as on increasing the catalyst amount, metal loading per gram of catalyst is also increased and achieve adequate at 30 mg. For this reason, we have chosen 30 mg as preferred catalyst amount for further investigation of other parameters.

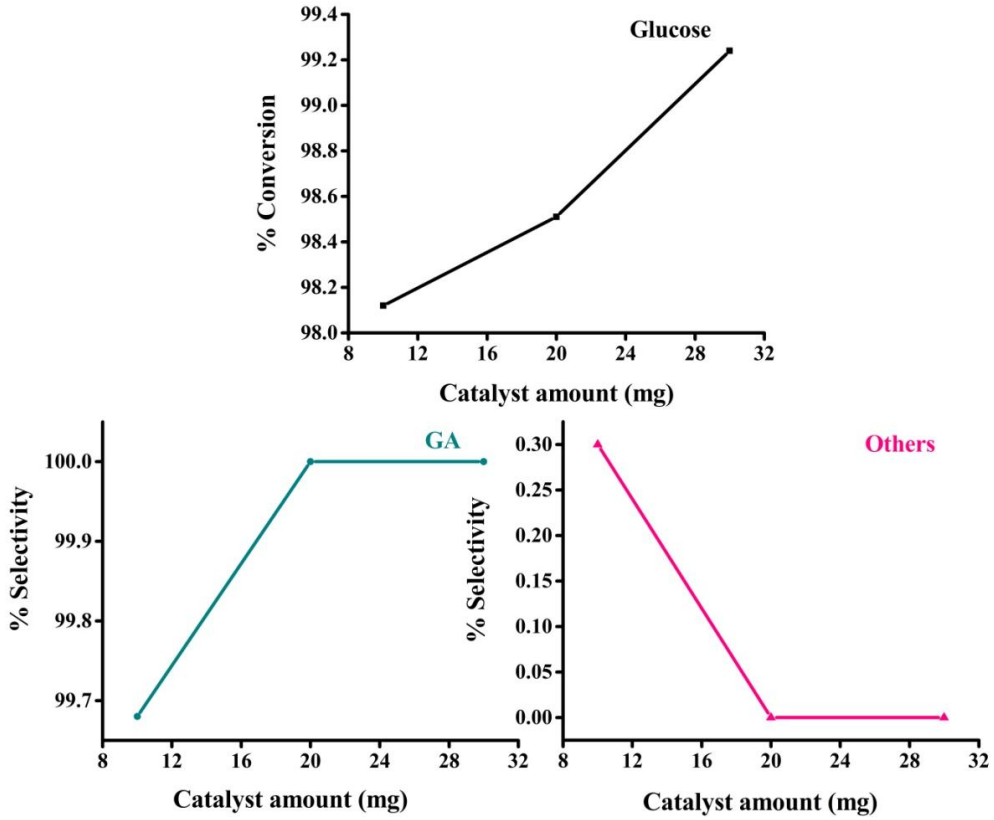

Fig. 4.41. Impact of varying amount of catalyst on the oxidation of glucose. Reaction condition: glucose (6 mmol), 30% H_2O_2 (6 mmol), CuL-*f*-GO (mg), 80 °C, ethylene glycol (5 mL), 1 h.

4.4.8. Impact of temperature

Effect of three diverse reaction temperatures (viz. 70, 80 and 90 °C) on oxidation of glucose is demonstrated in Fig. 4.42. It is obvious from the figure that 99.67% conversion of glucose is achieved with 100% GA selectivity at 70 °C. On increasing the temperature, inverse trend of conversion is found. When temperature rised to 80 °C, a reduced conversion is observed (99.3%). Further increasing the temperature to 90 °C, major short-fall of 3.24% is experienced in the conversion of glucose and the obtained conversion is 96.43%. The possible reason for this reduction in conversion is may be the faster catalytic decomposition of H_2O_2 at higher temperature. As a result, 70 °C is chosen as preferred reaction temperature.

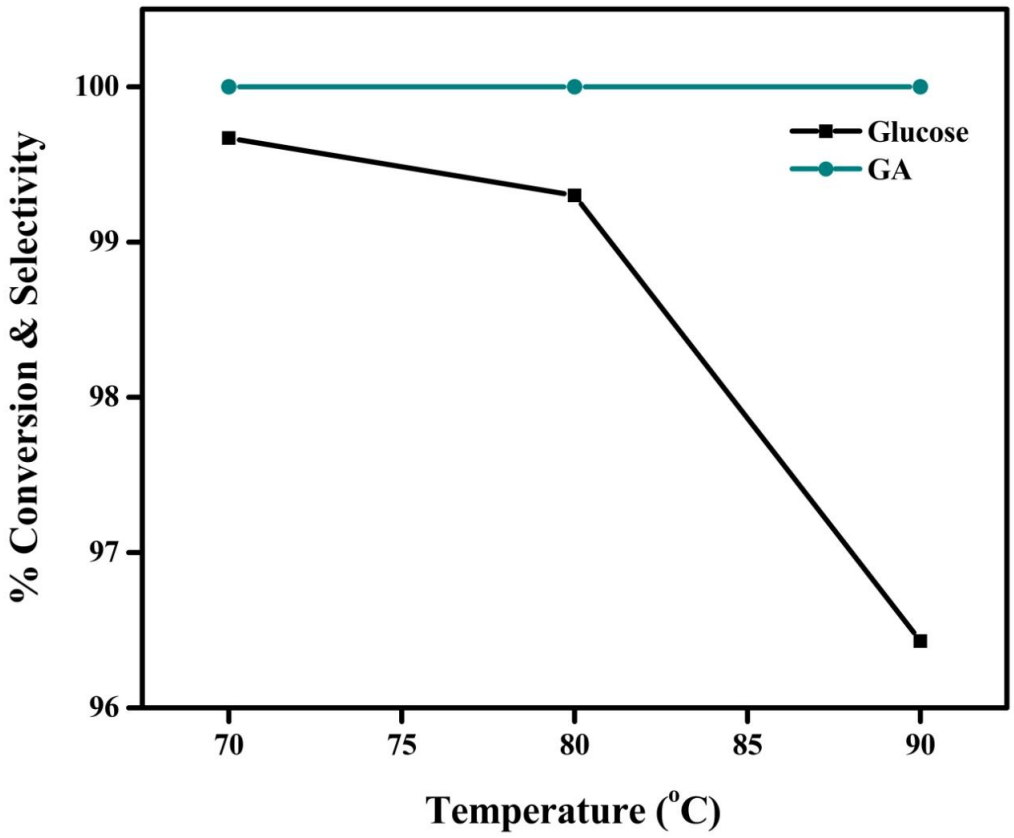

Fig. 4.42. Impact of varying temperature on the oxidation of glucose. Reaction condition: glucose (6 mmol), 30% H_2O_2 (6 mmol), CuL-*f*-GO (30 mg), temperature (°C), ethylene glycol (5 mL), 1 h.

4.4.9. Recyclability test

To inspect the recyclability of the as-prepared heterogeneous catalyst for this transformation, the catalyst is recovered by filtration from the reaction mixture and washed with solvent followed by oven drying prior to employing for further catalytic test.The results of each recycle test are represented in Fig. 4.43 and it is evidently seen that catalyst give its best performance up to four cycles with no significant loss of activity. The conversion in first to fourth recycle is 99.10%, 98.78%, 98.15%, 97.56% and selectivity is 100%, repectively.

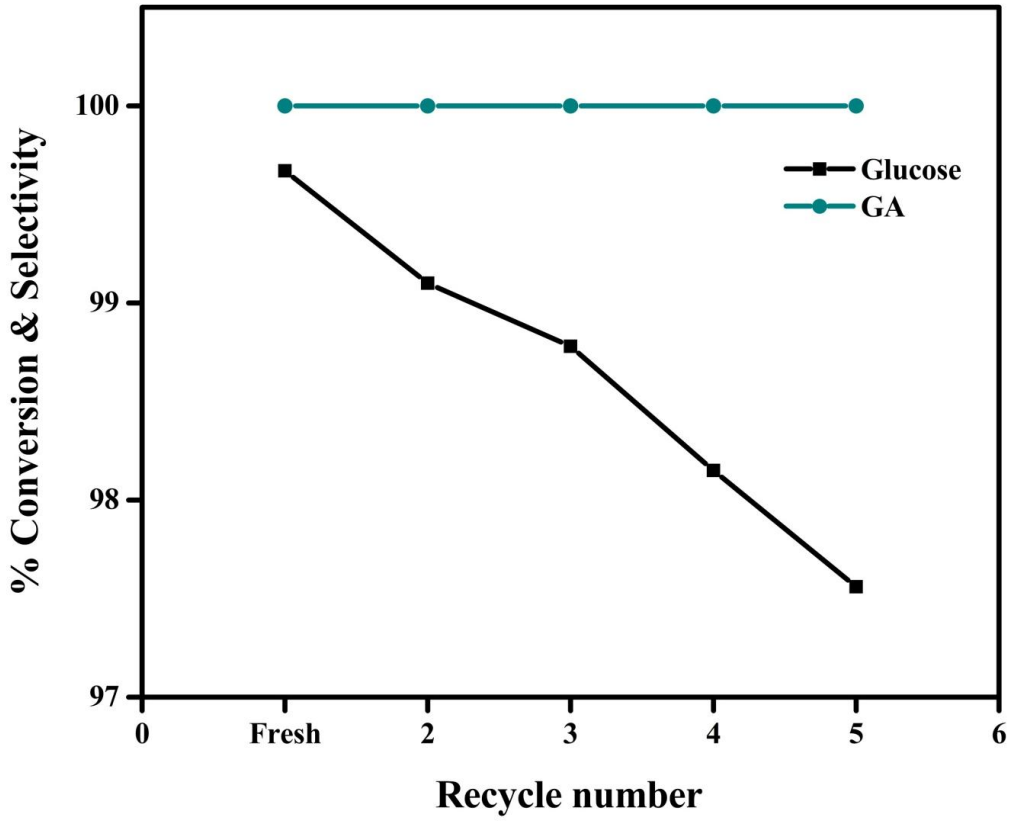

Fig. 4.43. Recyclability test on the oxidation of glucose.
Reaction condition: glucose (6 mmol), 30% H_2O_2 (6 mmol), CuL-*f*-GO (30 mg), 70 °C, ethylene glycol (5 mL), 1 h.

4.4.10. Conclusion

In the oxidation of glucose, CuL-*f*-GO exhibits a superior catalytic activity with 99.67% glucose conversion and 100% GA selectivity using 30% H_2O_2 as an oxidant and ethylene glycol as a solvent. The influences of distinct parameters like diverse catalysts, mole ratio, temperature, time, catalyst concentration, solvents, solvent amount and oxidant have also been inspected and the results suggest that glucose conversion is strongly affected by the reaction variables. This catalyst is recycled four times without significant loss activity.

4.5. References

1. M. D. Argyle, C. H. Bartholomew, *Catalysts*, 2015, **5**, 145-269.
2. J. L. Figueiredo, 'Carbon formation and gasification on nickel' in *Progress in Catalyst Deactivation*; (NATO Advanced Study Institute Series E, No. 54); Springer, Netherlands, 1982, pp. 45-63. DOI: 10.1007/978-94-009-7597-2.
3. J. R. Hughes, Deactivation of catalysts; Academic Press, London, UK, 1984.
4. J. Oudar, H. Wise, and M. Dekker, Deactivation and poisoning of catalysts, New York, NY, USA, 1985.
5. J. B. Butt and E. E. Petersen, Activation, Deactivation, and poisoning of catalysts, Academic Press, San Diego, CA, USA, 1988.
6. P. J. Denny and M. V. Twigg, 'Factors determining the life of industrial heterogeneous catalysts', in B. Delmon, G. F. Froment, *Catalyst deactivation*, Elsevier, Amsterdam, The Netherlands, 1980, **6**, pp. 577-599.
7. C. H. Bartholomew, *Chem. Eng.*, 1984, **91**, 96-112.
8. J. B. Butt, 'Catalyst deactivation and regeneration' in J. R. Anderson and M. Boudart, *Catalysis-Science and Technology*, Springer-Verlag, New York, USA, 1984, **6**, pp. 1-63.
9. C. H. Bartholomew and R. J. Farrauto, Fundamentals of Industrial Catalytic Processes, 2nd ed., Wiley-Interscience: Hoboken, NJ, USA, 2006.
10. B. Delmon and G. F. Froment, Catalyst Deactivation, Elsevier, Amsterdam, The Netherlands, 1980, **6**.
11. B. Delmon and G. F. Froment, Catalyst Deactivation, Elsevier, Amsterdam, The Netherlands, 1987, **34**.
12. C. H. Bartholomew and J. B. Butt, Catalyst Deactivation, Elsevier, Amsterdam, The Netherlands, 1991, **68**.
13. B. Delmon and G.F. Froment, Catalyst Deactivation, Elsevier, Amsterdam, The Netherlands, 1994, **88**.
14. C. H. Bartholomew and G. A. Fuentes, Catalyst Deactivation, Elsevier, Amsterdam, The Netherlands, 1997, **111**.

15. B. Delmon and G. F. Froment, Catalyst Deactivation, Elsevier, Amsterdam, The Netherlands, 1999, **126**.
16. C. H. Bartholomew and R. J. Farrauto, Fundamentals of industrial catalytic processes, 2nd ed., Wiley-Interscience, Hoboken, NJ, USA, 2006.
17. K. Suwannakarn, E. Lotero, J. G. Goodwin Jr. and C. Lu, *J. Catal*., 2008, **255**, 279-286.
18. K. Suwannakarn, E. Lotero and J. G. Goodwin Jr., *Catal. Lett*. , 2007, **114**, 3-4.
19. X. Fan, G. Zhang and F. Zhang, *Chem. Soc. Rev.*, 2015, **44**, 3023-3035.
20. N. M. Julkapli and S. Bagheri, *Int. J. Hydrogen Energy*, 2015, **40(2)**, 948-979.
21. M. D. Stoller, S. J. Park, Y. W. Zhu and R. S. Ruoff, *Nano Lett*., 2008, **8(10)**, 3498-3502.
22. J. K. Nam, M. J. Choi, D. H. Cho, J. K. Suh and S. B. Kim, *J. Mol. Catal. A: Chem*., 2013, **370**, 7-13.
23. Z. Li, S. Wu, H. Ding, D. Zheng, J. Hu, X. Wang, Q. Huo, J. Guan and Q. Kan, *New J. Chem.*, 2013, **37(5)**, 1561-1568.
24. H. P. Mungse, S. Verma, N. Kumar, B. Sain and O. P. Khatri, *J. Mater. Chem*., 2012, **22**, 5427-5433.
25. S. Sabater, J. A. Mata and E. Peris, *ACS Catal*., 2014, **4(6)**, 2038-2047.
26. J. J. Bozell and G. R. Petersen, *Green Chem.*, 2010, **12(4)**, 539-554.
27. T. Werpy and G. R. Petersen, Top value added chemicals from biomass, Volume I - Results of Screening for Potential Candidates from Sugars and Synthesis Gas, USA, 2004. DOI: 10.2172/15008859.
28. S. E. Davis, M. S. Ide and R. J. Davis, *Green Chem*., 2013, **15(1)**, 17-45.
29. J. R. Monnier, *Appl. Catal. A.*, 2001, **221(1-2)**, 73-91.
30. N. Lingaiah, K. M. Reddy, N. Seshu Babu, K. N. Rao, I. Suryanarayana and P. S. Sai Prasad, *Catal. Commun*., 2006, **7(4)**, 245-250.
31. R. Vithalani, D. Patel, C. K. Modi, N. N. Som, P. K. Jha and S. R. Kane, *Diamond & Related Materials*, 2018, **90**, 154-165.
32. C. Reichardt and T. Welton, 4th Ed. Wiley-VCH, Weinheim 2010.
33. W. Zhang, V. Carravetta, Z. Li, Y. Luo, J. Yang, *J. Chem. Phys*., 2009, **131(24)**, 244505-6.

34. A.K. Manna and K.S. Pati, *Chem. Asian J.*, 2009, **4**, 855-860.
35. I. Erden, 'Three-membered rings, with all fused systems containing three-membered rings' in A.R. Katritzky, C.W. Rees, E. F. V. Scriven and A. Padwa, *Comprehensive Heterocyclic Chemistry II* , Pergamon, New York, 1996, **1A**, pp 97-144.
36. M. Dusi, T. Mallat and A. Baiker, *Catal. Rev. Sci. Eng.* 2000, **42(1 & 2)**, 213-278.
37. N. T. Thao, D. V. Long, D. M. Hoan, *Vietnam J. Sci. Tech.*, 2017, **55(4)**, 403-410.
38. S. Enomoto, M. Inoue, O. Ohura, T. Kamiyama and H. Nitoh, US Pat. 5041569, August 20, 1991.
39. Q. Tang, Q. Zhang, H. Wu and Y. Wang, *J. Catal.* 2005, **230**, 384-397.
40. B. Tyagi, U. Sharma and R. V. Jasra, *Appl. Catal. A*, 2011, **408**, 171-177.
41. W. Zhu, Q. Zhang and Y. Wang, *J. Phys. Chem. C*, 2008, **112**, 7731-7734.
42. N. T. Thao and L. T. K. Huyen, *Chem. Eng. J.*, 2015, **279**, 840-850.
43. N. T. Thao and H. H. Trung, *Catal. Commun.*, 2014**, 45,** 153-157.
44. I. Kirm, F. Medina, X. Rodriguez, Y. Cesteros, P. Salagre and J. Sueiras, *Appl. Catal. A*, 2004, **272**, 175-185.
45. L. Espinal, S. L. Suib and J. F. Rusling, *J. Am. Chem. Soc.*, 2004, **126**, 7676-7682.
46. S. Sharma, S. Sinha and S. Chand, *Ind. Eng. Chem. Res.*, 2012, **51**, 8806-8814.
47. V. R. Choudhary, R. Jha, N. K. Chaudhari and P. Jana, *Catal. Commun.*, 2007, **8**, 1556-1560.
48. S. C. Laha and R. Kumar, *J. Catal.*, 2001, **204**, 64-70.
49. H. J. Zhan, Q. H. Xia, X. H. Lu, Q. Zhang, H. X. Yuan, K. X. Su and X. T. Ma, *Catal. Commun.*, 2007, **8**, 1472-1478.
50. R. Manktala, R. S. Dhillon and B. R. Chhabra, *Indian J. Chem.*, 2006, **45B**, 1591-1594.
51. M. Nemanashi and R. Meijboom, *Catal. Lett.*, 2013, **143**, 324-332.
52. L. Nie, K. K. Xin, W. S. Li and X. P. Zhou, *Catal. Commun.*, 2007, **8**, 488-492.
53. I. W. C. E. Arends and R. A. Sheldon, *Appl. Catal. A: Gen.*, 2001, **212**, 175-187.

54. I. W. Davies, L. Matty, D. L. Hughes and P. J. Reider, *J. Am. Chem. Soc.*, 2001, **123**, 10139-10140.
55. H. Nur, S. Ikeda and B. Ohtani, *J. Catal.*, 2001, **204**, 402-408.
56. H. Salavati and N. Rasouli, *Mater. Res. Bull.*, 2011, **46**, 1853-1859.
57. J. Carroll, Natural Gas Hydrates, A Guide for Engineers, 3rd ed., Chap-5, 2014, pp. 135-173.
58. S. N. Rao, K. N. Munshi and N. N. Rao, *J. Mol. Catal. A*, 2000, **156**, 205-211.
59. M. J. Frisch et al. GAUSSIAN 09 (Revision C.01), Gaussian, Inc., Wallingford, CT, 2010.
60. A. D. Becke, *Phys. Rev. A*, 1988, **38**, 3098-3100.
61. C. Lee, W. Yang and R. G. Parr, *Phys. Rev. B*, 1988, **37**, 785-789.
62. C. J. Cramer, D. G. Truhlar, *Phys. Chem. Chem. Phys.*, 2009, **11**, 10757-10816.
63. R. Dennington and T. Keith, J. Millam, GaussView, version 5, Semichem Inc. Shawnee Mission, KS, 2009.
64. R. G. Parr, W. Yang, Density- functional theory of atoms and molecules, Oxford University Press, New York, 1989, pp. 101.
65. R. G. Pearson, *J. Org. Chem.*, 1989, **54**, 1423-1430.
66. R. G. Parr and R. G. Pearson, *J. Am. Chem. Soc.*, 1983, **105**, 7512-7516.
67. S. Gunasekaran, R. A. Balaji, S. Kumaresan, G. Anand and S. Srinivasan, *Can. J. Anal. Sci. Spectrosc.*, 2008, **53**, 149-162.
68. B. Kosar and C. Albayrak, *Spectrochim. Acta. A*, 2011, **78**, 160-167.
69. K. Khistyaev, K. B. Bravaya, E. Kamarchik, O. Kostko, M. Ahmed and A. I Krylov, *Faraday Discuss.* 2011, **150**, 313-330; (b) S. Yokojima, N. Yoshiki, W. Yanoi and A. Okada, *J. Phys. Chem. B*, 2009, **113**, 16384-16392.
70. A. Butler, M. J. Clague and G. E. Meister, *Chem. Rev.*, 1994, **94**, 625-638.
71. H. Mimoun, L. Saussine, E. Daire, M. Postel, J. Fischer and R. Weiss, *J. Am. Chem. Soc.*, 1983, **105**, 3101-3110.
72. S. Parihar, S. Pathan, R. N. Jadeja, A. Patel and V. K. Gupta, *Inorg. Chem.*, 2012, **51**, 1152-1161.
73. W. P. Griffith, *J. Chem. Soc. A*, 1969, 211-218.

74. P. Schwendt and M. Pisarcik, *Spectrochim. Acta. A*, 1990, **46A (3)**, 397-399.
75. G. Franz and R. A. Sheldon, "Oxidation" in Ullmann's Encyclopedia of Industrial Chemistry, Wiley-VCH, Weinheim, 2000. Doi:10.1002/14356007.a18_261.
76. I. Kani and M. Kurtça, *Turk. J. Chem.*, 2012, **36(6)**, 827-840.
77. P. Gallezot, *Catal. Today*, 1997, **37(4)**, 405-418.
78. K. George and S. Sugunan, *Catal. Commun.*, 2008, **9(13)**, 2149-2153.
79. S. Devika, M. Palanichamy and V. Murugesan, *Chinese J. Catal.*, 2012, **33(7-8)**, 1086-1094.
80. G. Centi and S. Perathoner, *Catal. Today*, 2003, **77(4)**, 287-297.
81. J. H. Clark and D. J. Macquarrie, *Organic Process Research & Development*, 1997, **1(2)**, pp. 149-162.
82. M. Yoon, R. Srirambalaji and K. Kim, *Chem. Rev.*, 2012, **112(2)**, 1196-1231.
83. K. C. Gupta, A. K. Sutar, and C. C. Lin, *Coord. Chem. Rev.*, 2009, **253(13-14)**, 1926-1946.
84. H. P. Mungse, S. Verma, N. Kumar, B. Sain and O. P. Khatri, *J. Mater. Chem*., 2012, **22**, 5427–5433.
85. M. A. Nasseri, A. Allahresani and H. Raissi, *RSC Adv*., 2014, **4**, 26087-26093.
86. S. Rayati, E. Khodaei, S. Shokoohi, M. Jafarian, B. Elmi and A. Wojtczak, *Inorganica Chimica Acta*, 2017, **466**, 520-528.
87. Ali Allahresani, *J. Iran. Chem. Soc.*, 2017, **14**, 1051-1057.
88. A. Zarnegaryan, Z. Pahlevanneshan, M. Moghadam, S. Tangestaninejad, V. Mirkhani and I. M. Baltork, *J. Iran Chem. Soc.*, 2019, **16**, 747-756.
89. I. Kani and M. Kurtca, *Turk. J. Chem.*, 2012, **36 (6)**, 827-840.
90. P. Gallezot, *Catal. Today*, 1997, **37(4),** 405-418.
91. K. George and S. Sugunan, *Catal. Commun.*, 2008, **9 (13)**, 2149-2153.
92. R. A. Sheldon and J. K. Kochi, Metal-Catalysed Oxidations of Organic Compounds, Academic Press, New York, 1981.
93. Q. H. Xia, H. Q. Ge, C. P. Ye, Z. M. Liu and K. X. Su, *Chem. Rev*., 2005, **105**, 1603-1662.
94. P. J. Dyson and P. G. Jessop, *Catal. Sci. Technol*., 2016, **6**, 3302-3316.

95. A. Corma, S. Iborra and A. Velty, *Chem. Rev*., 2007, **107**, 2411-2502.
96. M. Besson, P. Gallezot and C. Pinel, *Chem. Rev*., 2014, **114**, 1827-1870.
97. R. A. Sheldon, *Green Chem*., 2014, **16**, 950-963.
98. L. T. Mika, E. Cséfalvay and A. Nemeth, *Chem. Rev*., 2018, **118**, 505-613.
99. M. J. Climent, A. Corma and S. Iborra, *Green Chem*., 2011, **13**, 520-540.
100. M. J. Climent, A. Corma and S. Iborra, *Chem. Rev*., 2011, **111**, 1072-1133.
101. P. Gallezot, *Chem. Soc. Rev*., 2012, **41**, 1538-1558.
102. B. C. E. Makhubela and J. Darkwa, *Johns. Matthey Technol. Rev*., 2018, **62**, 4-31.
103. P. Gallezot, *ChemSusChem*, 2008, **1**, 734-737.
104. F. M. A. Geilen, B. Engendahl, A. Harwardt, W. Marquardt, J. Klankermayer and W. Leitner, *Angew. Chem., Int. Ed*., 2010, **49**, 5510-5514.
105. P. Borja, C. Vicent, M. Baya, H. Garcia and J. A. Mata, *Green Chem*., 2018, **20**, 4094-4101.
106. N. A. Samoilova, M. A. Krayukhina, T. P. Klimova, T. A. Babushkina, O. V. Vyshivannaya, I. V. Blagodatskikh and I. A. Yamskov, *Russ. Chem. Bull., Int. Ed.*, 2014, **63(4)**, 1009-1016.
107. I. Witonska, M. Frajtak and S. Karski, *Appl. Catal. A*, 2011, **401**, 73-82.
108. I. Nikov and K. Paev, *Catal. Today*, 1995, **24**, 41-47.
109. J. W. M. Jacobs and D. Schryvers, *J. Catal*., 1987, **103**, 436-449.
110. P. A. Legare, L. Hilaire and G. Maire, *Surf. Sci*., 1984, **141**, 604-616.
111. A. Abbadi and H. van Bekkum, *J. Mol. Catal. A: Chem*., 1995, **97**, 111-118.
112. Z. Gogova and J. Hanika, *Chem. Pap.*, 2009, **63**, 520-526.
113. J. M. H. Dirkx and H. S. van der Baan, *J. Catal*., 1981, **67**, 1-13.
114. M. Comotti, C. D. Pina, E. Falletta and M. Rossi, *Adv. Synth. Catal*., 2006, **348**, 313- 316.
115. S. Karski and I. Witonska, *J. Mol. Catal. A: Chem*., 2003, **191**(1), 87-92.
116. S. Karski, T. Paryjczak, J. Rynkowski and I. Witonska, *J. Pol. Technol.*, 2000, **2**, 10-13.

117. A. Abbadi and H. Van Bekkum, *J. Mol. Catal.*, 1995, **97**, 111-118.
118. M. Besson, F. Lahmer, P. Gallezot, P. Fuertes and G. Fleche, *J. Catal.*, 1995, **152**, 116-121.
119. M. Wenkin, R. Touillaux, P. Ruiz, B. Delmon and M. Devillers, *Appl. Catal. A*, 1996, **148**, 181-199.
120. A. Abbadi and H. Van Bekkum, *Appl. Catal. A*, 1995, **124(2)**, 409-417.
121. P. Gallezot, *Catal. Today*, 1997, **37(4)**, 405-418.
122. S. Karski and I. Witonska, *Chem. Environm. Res.*, 2001, **10(3-4)**, 283-293.
123. S. Karski and I. Witonska, *Przem. Chem.*, 2002, **81(11)**, 713-715.
124. M. Wenkin, C. Renard, P. Ruiz, B. Delmon and M. Devillers, 3rd World Congress on Oxidation Catalysis, Elsevier Science B.V., 1997, **110**, pp 517-526.
125. Y. Cao, X. Liu, S. Iqbal, P. J. Miedziak, J. K. Edwards, R. D. Armstrong, D. J. Morgan, J. Wang and G. J. Hutchings, *Catal. Sci. Technol*., 2016, **6**, 107-117.
126. S. Ramachandran, P. Fontanille, A. Pandey and C. Larroche, *Lett. Appl. Microbiol.*, 2007, **44**, 155-160.
127. P. Gallezot, *Green Chem*., 2007, **9**, 295-302.
128. M. Bohnet, Ullmann's Encyclopedia of Industrial Chemistry, 6th ed., **15**, Wiley-VCH, Weinheim, 2003.
129. H. Hustede, H. J. Haberstroh and E. Schinzig, Ullmann's Encyclopedia of Industrial Chemistry, Wiley-VCH Verlag, 2000.
130. E. Balaraman, E. Khaskin, G. Leitus and D. Milstein, *Nat. Chem*., 2013, **5**, 122-125.
131. T. Zweifel, J. V. Naubron and H. Grützmacher, *Angew. Chem., Int. Ed*., 2009, **48**, 559-563.
132. K. Fujita, R. Tamura, Y. Tanaka, M. Yoshida, M. Onoda and R. Yamaguchi, *ACS Catal*., 2017, **7**, 7226-7230.
133. T. P. Brewster, W. C. Ou, J. C. Tran, K. I. Goldberg, S. K. Hanson, T. R. Cundari and D. M. Heinekey, *ACS Catal*., 2014, **4**, 3034-3038.
134. G. E. Dobereiner, J. Yuan, R. R. Schrock, A. S. Goldman and J. D. Hackenberg, *J. Am. Chem. Soc.*, 2013, **135**, 12572-12575.

135. J. Choi, A. H. R. MacArthur, M. Brookhart and A. S. Goldman, *Chem. Rev*., 2011, **111**, 1761-1779.
136. C. Wang and J. Xiao, *Chem. Commun*., 2017, **53**, 3399-3411.
137. X. Wang, C. Wang, Y. Liu and J. Xiao, *Green Chem*., 2016, **18**, 4605-4610.
138. Y. Sawama, K. Morita, T. Yamada, S. Nagata, Y. Yabe, Y. Monguchi and H. Sajiki, *Green Chem*., 2014, **16**, 3439-3443.